ABSTRACT

MIAO, GUOFANG. A Multi-scale Study on Respiratory Processes in a Lower Coastal Plain Forested Wetland in the Southeastern United States. (Under the direction of Dr. John S. King and Dr. Asko Noormets).

Carbon cycling in wetlands is an important component of the carbon budget in terrestrial ecosystems. Environmental change and land conversion for agricultural use have been affecting wetlands in recent decades and might change their role from carbon sinks to sources. However, carbon dynamics in wetlands are less-well investigated than in upland systems and still absent in most regional- or global-scale studies. This research, as a part of a comprehensive study on carbon dynamics of a lower coastal plain forested wetland in the Southeastern USA, focused on respiration - a key determinant affecting the role of an ecosystem as carbon source or sink.

Ecosystem respiration, soil respiration and decomposition of coarse woody debris were investigated by quantifying CO_2 emissions of each in response to temperature and water table fluctuation. Soil respiration was intensively measured with an automated system to obtain high-frequency (30 minutes) temporal data as well as a survey system to characterize spatial variation. Stable isotope composition (^{13}C) of soil-respired CO_2 was also studied to understand the components of soil respiration. Ecosystem respiration was measured by an automated eddy-covariance flux system. Decomposition of coarse woody debris was measured monthly across the same survey area as soil respiration. To account for effects of microtopography on respiration and decrease up-scaling uncertainties, an ancillary study on microtopographic variation was also conducted.

Respiratory components under non-flooded conditions responded similarly to

temperature between this forested wetland and upland ecosystems in an exponential pattern and with comparable temperature sensitivities. Hydrology had additional effects on soil respiration and ecosystem respiration, with the relationship resembling a saturating pattern of Michaelis-Menten reaction; that is, the rate increased with the water table drawdown and was nearly constant at deeper water table depths. Soil respiration responded rapidly to flooding and decreased significantly, whereas ecosystem respiration responded slowly because the plants were tolerant to flooding.

Based on the exponential pattern of response to temperature and Michaelis-Menten pattern of response to water table depth, models were developed to estimate soil respiration and ecosystem respiration. Ecosystem respiration was estimated at 1331 to 1731 g CO_2-C m^{-2} yr^{-1}, and soil respiration ranged 593 to 1082 g CO_2-C m^{-2} yr^{-1} during the study period (2009-2011). The contribution of soil respiration to ecosystem respiration increased with the water table drawdown, with an annual average relative contribution of 0.67±0.11 (mean±SD) during non-flooded periods and 0.24±0.06 when flooded. Decomposition of coarse woody debris contributed much less to ecosystem respiration, but with large uncertainty related to biomass estimation.

^{13}C composition of soil-respired CO_2 ($\delta^{13}C_{Rs}$) varied seasonally and exhibited a significant relationship with hydrology and microtopography. The $\delta^{13}C_{Rs}$ at mound microsites was depleted during summer and enriched in spring and autumn, whereas the $\delta^{13}C_{Rs}$ at low-lying microsites exhibited the opposite pattern (i.e. enriched during summer and depleted in spring). This suggests that under warmer and drier conditions the relative contribution of root respiration to soil respiration increased at mound microsites, but soil organic carbon decomposition had a higher relative contribution at low-lying microsites.

Accounting for microtopographic difference and hydrologic effects will improve methods partitioning soil respiration and differentiating fast and slow turnover carbon pools.

A Multi-scale Study on Respiratory Processes in a Lower Coastal Plain Forested Wetland in the Southeastern United States

by
Guofang Miao

A dissertation submitted to the Graduate Faculty of
North Carolina State University
in partial fulfillment of the
requirements for the Degree of
Doctor of Philosophy

Forestry and Environmental Resources

Raleigh, North Carolina

2013

APPROVED BY:

Dr. John S. King Co-Chair of Advisory Committee	Dr. Asko Noormets Co-Chair of Advisory Committee
Dr. Montserrat Fuentes	Dr. David Genereux
Dr. Carl C. Trettin	

DEDICATION

TO

My parents

My grandparents

&

Young Mono

BIOGRAPHY

Guofang grew up in a small town in southeastern China before starting her undergraduate study in Beijing. She graduated from Beijing Normal University in 1998 with a B.S. in chemistry. She entered an M.S. program in Environmental Science at Peking University in 1999, where she selected a project about the influence of air pollution on the ocean for her master thesis. This experience helped her get a research assistant position in China National Marine Environmental Forecasting Center. She learned meteorology and oceanography there and worked for algal bloom forecasting for four years. She left this job in 2006 and went to Stockholm, Sweden for another master program in Environmental Engineering and Sustainable Infrastructure at Royal Institute of Technology (Kungliga Tekniska Högskolan). This period of study was a short break in her pursuit of science and to satisfy her curiosity on engineering. She then chose a project about carbon cycle in an African rainforest for her thesis, and started the study on forest ecology. In 2008, she moved to U.S. for her doctoral study in forestry in North Carolina State University.

Guofang plans to continue research in forest ecology, and hopes to work on ecological education in developing countries. She likes to read, photograph wildflower, and travel around the world. She would not mind to be a volunteer if humans will grow Earth plants on Mars.

ACKNOWLEDGEMENTS

First of all, I would like to say thanks to my doctoral project for those expected and unexpected challenges and surprises in the swamp. As I expected for changing major to forest ecology, walking in the woods has more fun than floating on the ocean, but it also comes with pains. The pain was so real at my last trip of regular field measurements that I forgot to cheer for the accomplishment as planned, when I tripped over a big tree root, fell bang on the ground and tasted some soils that I had been measuring for years. Thanks to those moments in hot summer, hurricane season, tornado day and freezing winter days, fighting with mosquitoes, flies, wind and flooding, which made me realize that being an ecologist in the field is not as simple as hiking in the wilderness. These experiences have almost made myself believe that I can survive anywhere, and will become fun memories.

I would like to express sincere appreciation to my advisors, Dr. John S. King and Dr. Asko Noormets, who gave me tremendous freedom to do research. Thanks for their patience when I misunderstood or made confusions again and again during our meetings. Thank them for sharing their own stories in academia and encouraging me all the time. Thank Asko for teaching me patiently and carefully the technical details in the field, although sometimes I felt that he might have forgotten the 50-cm difference between his height and mine. Also, I would like to thank John for those barbecue parties and delicious food and thank Asko for the Estonian chocolates.

Sincere thanks to other committee members, Dr. Montserrat Fuentes, Dr. David Genereux and Dr. Carl Trettin, for the guidance during my study in the U.S. Those interesting questions for my qualify exam did inspire some ideas for future research. Thank

Carl for inviting me to the Center for Forested Wetlands Research to learn wetland modeling. I loved that quiet place in the middle of a large area of forests. I also want to apologize that I changed the dissertation structure, and could not finish and combine the modeling work into my dissertation. Specially, I must express my sincere appreciation to Dr. Ge Sun, for his kindness and willingness to work as a substitute for Dr. Genereux in my defense.

Thanks to the Southeast Climate Science Center for supporting my last two years of study. Thank Dr. Gerard McMahon, Dr. Damian Shea, and Aranzazu Lascurain for organizing the monthly seminars, which provided the opportunity to communicate with other researchers from different backgrounds. Those seminars refreshed me when I felt frustrated and boring during my dissertation writing.

I also want to thank Siyao for three years of collaboration. Thank her for all the hard work she did for this project. The nights in the first year that we got lost on the way back to campus from the field might have been scary and exhausting, but I hope they could be fun when becoming memories. My best wishes to you and your little girl, Siyao.

Thanks to our lab manager, Aletta Davis, for helping planning the lab and field work. It was fun to listen to her describing the feeling of tasting chicken feet. Thanks to other lab members, Andrew Radecki, David Zietlow, Wen Lin, Eric Wards, Alexia Kelley and Janine Albaugh. Thanks for all their comments and suggestions to my manuscripts and presentations. It was nice to work with them and share experiences in research and anything else. Thanks to Joseph Bradley and all other undergraduate students who had helped me for the field work.

Thanks to the Hunt Library, a nice surprise during the final period of my PhD study, and thanks to those library technicians who gave me the smiling faces every day in my last few

months of writing. For a long time, the words I spoke every day were only *hello* and *good night* to them.

Thanks to all my friends in China, U.S. and other countries. It appeared that I have been moving around the world like a nomad, but I never feel alone with them always being somewhere to accompany, comfort and encourage me.

Finally, warm thanks to my dear parents, my brother and his family for the unconditional love and supports. You always make me feel I am one of the luckiest daughters and sisters in the world. Apologies for my absence from those days that family should be together.

There is simply no way to thank everyone enough. Working hard and living sincerely and passionately are all that I can do to return to the supports and favors I received. No matter how fast time flies and how far we are away from each other, these words will never change in my heart.

Guofang Miao

Sep. 2013 @ Raleigh, NC

TABLE OF CONTENTS

LIST OF TABLES

CHAPTER 2

CHAPTER 3

CHAPTER 4

APPENDICES

LIST OF FIGURES

CHAPTER 1

CHAPTER 2

CHAPTER 4

CHAPTER 5

APPENDICES

CHAPTER 1. INTRODUCTION

Carbon storage in vegetation and soil, and carbon flow between pools in terrestrial ecosystems, have fundamental impacts on regional and global climate. Dynamic feedbacks in terrestrial ecosystems are one of the major uncertainties for balancing the carbon budget between anthropogenic emissions and increase in the atmosphere [*Beer et al.*, 2010; *Ciais et al.*, 1995; *Schimel*, 1995]. During recent decades, many studies have been conducted in different types of terrestrial ecosystems to quantify carbon stocks and fluxes and investigate the controlling mechanisms regulating potential feedback to climate. The difference in carbon dynamics among ecosystems is enormous due to geographic location, vegetation type, and associated interactions between ecological processes and physical environment [*GLOBALVIEW-CO2*, 2012].

While interest in wetlands carbon budgets is increasing [*Aselmann and Crutzen*, 1989; *Bridgham et al.*, 2006; *Brinson et al.*, 2002; *Chmura et al.*, 2003; *Erwin*, 2009; *Junk et al.*, 2013; *Keller*, 2011; *P D Moore*, 2002], studies on characterizing and parameterizing carbon dynamics in wetlands are still rare compared with upland ecosystems. Due to data scarcity, wetlands are absent in most regional- or global-scale research [*Battin et al.*, 2009; *Davidson*, 2010; *Luyssaert et al.*, 2007; *Mahecha et al.*, 2010]. In existing global research networks, the proportion of wetlands represented is also small. For example, there were 25 wetland sites in the 545 sites in global FLUXNET networks (including the 'permanent wetlands' defined by IGBP-Land-Use and the results searched with words 'wetland', 'peatland', 'mire', 'bog', 'fen', and 'marsh'). Eight sites were defined as forested, 5 shrub lands, 4 woody savannas and the rest were grassland, cropland or barren (information updated to Apr. 2013, Figure 1-

1). In the global soil respiration database (SRDB, version 20100517), there were only 135 data records for wetlands among a total of 3821 records.

1. Brief literature review on wetlands

A wetland is defined as an ecosystem that "depends on constant or recurrent, shallow inundation or saturation at or near the surface of the substrate", with "the common diagnostic features of hydric soils and hydrophytic vegetation" [*NRC*, 1995]. Due to the slow decomposition rate and long-term accumulation resulting from the permanent or intermittent flooding, wetlands store large amounts of carbon in soil, which also causes wetlands to be one of the most sensitive ecosystems to climate change [*Ise et al.*, 2008]. It has been estimated that wetland soils store 18-30% of the 1550 Pg (1 m deep) of total global soil organic carbon while covering only a small proportion of the total land area, recently estimated at 7 to 10 million km^2 globally [*Mitsch and Gosselink*, 2007; *Trettin and Jurgensen*, 2003].

1.1 Carbon storage and fluxes in wetlands

Generally, wetlands store more carbon in soils than in vegetation compared with upland ecosystems, although carbon allocation between vegetation and soils in wetlands is variable globally. In northern regions, early studies estimated 580 Mg C ha^{-1} (1 m deep) was stored in peat, whereas the carbon stored in vegetation ranged from 3.4 Mg C ha^{-1} in relatively open peat lands to 62 Mg C ha^{-1} in dense forested wetlands [*Gorham*, 1991]. This implies that almost 98.5% of total peat land carbon is stored in peat and only 1.5% in the vegetation [*Gorham*, 1991]. Previous studies specifically on forested wetlands estimated 65-280 Mg C

ha^{-1} (assuming carbon content of 50% in dry biomass) stored in vegetation [*Lugo et al.*, 1990]. Soil carbon pools in forested wetlands varies with soil type and has been estimated at 180 to 500 Mg C ha^{-1} from wet mineral soil to peat [*Trettin and Jurgensen*, 2003].

Net primary production was estimated at 350 to 800 g C m^{-2} yr^{-1} for global natural wetlands [*Aselmann and Crutzen*, 1989], and at 300 to 650 g C m^{-2} yr^{-1} for some forested wetlands [*Lugo et al.*, 1990]. It was also estimated in early studies that the average soil CO_2 efflux is 94±16 (mean±SD) g C m^{-2} yr^{-1} in northern bogs and mires, and 200 g C m^{-2} yr^{-1} in swamps and marshes [*Raich and Schlesinger*, 1992]. From the global SRDB, an average soil CO_2 efflux from wetlands was 344±278 g C m^{-2} yr^{-1} as compared to an average 816±516 g C m^{-2} yr^{-1} in upland ecosystems [*Bond-Lamberty and Thomson*, 2010]. Individual studies indicate that wetlands have the potential of releasing an amount of CO_2 to the atmosphere comparable to upland ecosystems of similar climate zones, with rates of soil CO_2 efflux up to 1200 g C m^{-2} yr^{-1} [*Chimner*, 2004; *Raich and Schlesinger*, 1992].

While there are still many uncertainties in estimating total CO_2 emission from wetlands on a global scale, another uncertainty in carbon budgets of wetlands is methane (CH_4) emission from anaerobic respiration. Matthews and Fung [1987] estimated global wetland CH_4 emission at 16 g C m^{-2} yr^{-1}, with northern peat-rich bogs from 50°-70°N contributing 60% and tropical/subtropical peat-poor swamps from 20°N-30°S contributing ~25%. The greenhouse effect of this amount of CH_4 is equivalent to the effect of 350 g C m^{-2} yr^{-1} of CO_2 emissions, calculated with the global warming potential of 21.8 mole CH_4/mole CO_2 [*Lelieveld et al.*, 1998].

This comparison between carbon input and output implies a net accumulation of carbon in wetlands. A recent estimate on sequestration in global wetland soils was 0.14 Pg C yr^{-1} with the estimated area of 6 million km^2 [*Bridgham et al.*, 2006]. For comparison, the recent estimates on CO_2 emissions were 8.7 Pg C yr^{-1} from fossil fuel combustion and 1.2 Pg C yr^{-1} from land use change in 2008 [*Le Quere et al.*, 2009]. The annual carbon sequestration of global wetlands was equivalent to 1.4% of the annual anthropogenic CO_2 emissions. The mean residence time of soil organic carbon in wetlands was estimated about 500 years, much greater than a mean residence time of 32 years for global pool of soil organic carbon [*Raich and Schlesinger*, 1992]. Carbon accumulation and long residence time demonstrate the importance of wetlands in mitigating climate change.

1.2 Wetlands under climate change and land use change

The impacts of climate change, however, may alter the carbon dynamics of wetlands and offset their role as carbon sinks. Major changes in climate will exert different impacts on wetlands in different areas. The increase in temperature at high latitudes may cause greater evapotranspiration rate or a decrease in precipitation could result in less-frequent flooding or decrease flood duration of wetlands [*Meehl et al.*, 2007]. Associated soil drying and drop in water table may turn existing wetlands from carbon sinks to sources by aerating large quantities of labile carbon stored in previously saturated soils, although the opposing effects between enhanced plant productivity and increased soil decomposition rate are still uncertain [*Ise and Moorcroft*, 2006; *Kirschbaum*, 2000; *Moore*, 2002]. Sea level rise, which has been estimated recently at 3.4±0.4 mm annually and is expected to accelerate over the coming

century, may cause losses of wetlands exacerbated by modified shorelines which restrict lateral landward wetland migration [*Junk et al.*, 2013; *Meehl et al.*, 2007; *Webb et al.*, 2013].

The conversion of wetlands to agriculture and other land uses through drainage may impose additional climate forcing [*Murray and Vegh*, 2012]. Earlier studies suggested 0.03-0.37 Pg C yr^{-1} of carbon loss from drained organic soils from a drained area of 0.35 million km^2 [*Armentano*, 1980]. Pendleton et al. [2012] recently estimated that the conversion and degradation of vegetated coastal ecosystems is releasing 0.003-0.023 Pg C yr^{-1} with the estimated area of 0.34-1.15 million km^2. This carbon emission is equivalent to 3-19% of the emission from deforestation globally [*Pendleton et al.*, 2012]. Compared with the above estimated carbon accumulation rate of global wetlands, the carbon emission from the conversion and degradation of wetlands might offset a large proportion of the ecosystem service of wetlands as carbon sink. However, there is large variance between studies, implying large uncertainties in estimating the carbon budget of wetlands. While these previous studies suggest that wetland carbon emissions could have a significant impact on climate, more data and better understanding on the carbon dynamics in wetlands are necessary for future climate prediction and ecosystem services management.

1.3 Hydrologic effects and microtopography variation in wetlands

One of the most important physical characteristics among wetlands regardless of vegetation type and soil type is hydroperiod, the seasonal pattern of the water table depth [*Mitsch and Gosselink*, 2007]. The amplitude, frequency and duration of water table fluctuation determine the transition between aerobic and anaerobic status of soils and plant activities [*Wheeler*,

1999]. Hydrologic regime also interacts with microtopography, which is associated with plant distributions and soil chemical and physical properties [*Frei et al.*, 2012; *Van der Ploeg et al.*, 2012; *Waddington and Roulet*, 1996; *Wheeler*, 1999]. As a result, the carbon balance between CO_2 uptake, CO_2 emission and CH_4 emission will be altered along with the change of flooding conditions. Although only a few studies specifically investigated the microtopographic effects on carbon exchange in wetlands, most observed a general trend that topographically lower areas have lower CO_2 emissions and higher CH_4 emissions than topographically higher areas [*Alm et al.*, 1999; *Kim and Verma*, 1992; *Waddington and Roulet*, 1996]. Waddington and Roulet [1996] found the net CO_2 exchange differed at microsites, with hollows acting as large sources of CO_2 and hummocks net sinks. Ignoring the heterogeneity of landscape features will result in bias in carbon balance estimates at a large scale [*Dai et al.*, 2011].

2. Brief literature review on respiration

Respiration of a terrestrial ecosystem refers to the processes that release carbon into the atmosphere. The difference between the large amount of carbon from respiration and another large carbon flux, photosynthesis, determines the net carbon exchange. Small uncertainties in either flux could lead to significant bias of the net exchange [*Trumbore*, 2006; *Valentini et al.*, 2000]. For example, Beer et al. [2010] estimated the global gross primary productivity (GPP) of terrestrial ecosystems at 123±8 Pg C yr^{-1}. Le Quéré et al. [2009] estimated the net land carbon sink in 2008 was 4.7±1.2 Pg C yr^{-1}.

In contrast to photosynthesis as the single process in which carbon enters terrestrial

ecosystems, respiration integrates a variety of plant and microbial processes (Figure 1-2). Every component may exhibit different sensitivities to changes in environmental drivers, which would influence estimates of carbon residence time and long-term responses of terrestrial ecosystems to climate change [*Boone et al.*, 1998; *Trumbore*, 2006]. This complexity imposes greater uncertainties and difficulties in investigating the mechanisms of respiration and responses to climate change.

2.1 Modeling respiration

The number of studies on respiration has been increasing rapidly during recent decades [*Baldocchi*, 2008; *Bond-Lamberty and Thomson*, 2010]. With more measurements and larger data sets available, models for quantifying respiration have been developed from single-factor to multiple-factor with better parameterization of mechanisms involved [*Conant et al.*, 2011; *Davidson et al.*, 2006; *Davidson et al.*, 2012; *Moyano et al.*, 2013; *Noormets et al.*, 2008].

Most models used in current studies were developed based on the empirical exponential relationship between respiration rate and temperature, e.g. the most widely used Q_{10} model modified from van't Hoff equation and Arrhenius equation [*Arrhenius*, 1889; *Davidson and Janssens*, 2006; *Lloyd and Taylor*, 1994; *Sierra*, 2012; *van't Hoff*, 1898]. In spite of the existence of interaction between temperature and water content, by which the confounding effects of water content can be partly represented by temperature effects, it has been well acknowledged that temperature alone is not sufficient for good simulation of respiration [*Moyano et al.*, 2013; *Noormets et al.*, 2008; *Reichstein et al.*, 2002]. In addition, both

temperature and water content (related to precipitation) are the main physical manifestations of climate change. Predicted changes in climate might result in opposing feedbacks of respiration in a given ecosystem, leading to investigation on the effects of soil water content on respiration [*Denman et al.*, 2007; *Falloon et al.*, 2011; *Melillo et al.*, 2002].

Biotic factors have additional effects on respiration although incorporating them into models is still in its infancy. Migliavacca et al. [2011] suggested that incorporating leaf area index, recent productivity or soil carbon content into models could improve simulation of ecosystem respiration. For soil respiration, substrate availability is being given more attention in models [*Conant et al.*, 2011; *Davidson et al.*, 2006; *Davidson et al.*, 2012]. Due to the difficulties in directly measuring substrate availability, attempts to quantify it are still in the conceptual stage. One strategy is to modify the parameters which are constant in traditional models with the functions related to substrate availability. In other words, the traditional models are modified with dynamic parameters, e.g. the Dual Arrhenius and Michaelis-Menten kinetics (DAMM) model developed by Davidson et al. [*Davidson et al.*, 2012].

The driver sensitivities of respiration may exhibit different patterns in varying temporal and spatial scales, which also complicates the quantification and prediction of respiration [*Baldocchi et al.*, 2001; *Savage et al.*, 2009]. It has been found that the extrapolation from short-term to long-term leads to an overestimation of ecosystem respiration for ecosystems in which the long-term temperature sensitivity exceeds the short-term sensitivity, whereas an underestimation occurs in those ecosystems with lower long-term temperature sensitivity

than short-term [*Reichstein et al.*, 2005].

2.2 Methods of partitioning respiration

Ecosystem respiration is usually partitioned by measuring individual components directly, such as the aboveground respiratory components and the belowground components (Figure 1-2), and estimating the remaining components by difference between the total and the measured components [*Chambers et al.*, 2004; *Griffis et al.*, 2004]. The contribution from each component may differ between ecosystems and seasons.

For some ecosystems and especially forests with severe natural or anthropogenic disturbances, an increase in tree mortality potentially has important impacts on carbon balance. Therefore, coarse woody debris might become a main contributor to the carbon loss and has received more attentions as well [*Chambers et al.*, 2001; *Harmon et al.*, 2004; *Moore et al.*, 2013; *Noormets et al.*, 2012].

Soil respiration is the largest component of carbon emission from terrestrial ecosystems and also an integration of various components (Figure 1-2). The global annual soil CO_2 flux has been estimated to be 68±4 Pg C yr^{-1} [*Raich and Schlesinger*, 1992]. Because of its importance, soil respiration partitioning methods have been well studied [*Hanson et al.*, 2000; *Kuzyakov*, 2006]. Briefly, the methods of partitioning soil respiration can be divided into invasive and noninvasive.

Different from ecosystem respiration, measuring individual components in soil implies significant soil disturbance and alteration to natural conditions. Incubating root and soil separately *in vitro* breaks the root-soil interface, changes the soil atmosphere and the

interaction between root and microbial community [*Baggs*, 2006; *Hanson et al.*, 2000; *Kuzyakov*, 2006]. Root-exclusion or trenching experiments *in situ* also change the interaction between root and soil, and may affect soil water content and nutrient cycling [*Kuzyakov*, 2006; *Ross et al.*, 2001].

Isotope methods, both stable and radiocarbon isotopes, have long been recognized for their noninvasiveness and as tracers of ecological and physiological processes [*Bowling et al.*, 2008; *Brüggemann et al.*, 2011; *Ehleringer et al.*, 2000; *Ehleringer et al.*, 2002; *Staddon*, 2004; *Trumbore*, 2000]. The isotopic composition of soil-respired CO_2 can reflect the contribution from different carbon sources because each source, theoretically, has unique isotopic signature. However, the requirement of distinct isotopic signatures for all carbon sources still remains a challenge to the application of isotope methods for partitioning soil respiration. Continuous labeling as well as the use of ^{13}C-depleted CO_2 in free air CO_2 enrichment experiments (FACE) provide external tracers for distinguishing autotrophic and heterotrophic respiration [*Andrews et al.*, 1999; *Meharg*, 1994], but are complicated and expensive. Use of natural abundance of isotopes is still limited because soil encompasses the continuum from new carbon in the plant litter to progressively decayed organic matter [*Dungait et al.*, 2012], from which the traditional statistical analysis is unable to separate the respiratory components from disparate sources [*Formanek and Ambus*, 2004].

Another noninvasive approach can be used to estimate heterotrophic respiration, based on the assumption that soil respiration is linearly related with root biomass. The intercept of this linear regression is estimated as heterotrophic respiration, i.e. the soil respiration in the

absence of roots [*Baggs*, 2006; *Kucera and Kirkham*, 1971; *Kuzyakov*, 2006; *Rodeghiero and Cescatti*, 2006]. However, this approach has been used rarely despite the advantage of minimal disturbance, perhaps because precise quantification of root biomass and its relationship with soil respiration is still problematic [*Makita et al.*, 2012; *Marsden et al.*, 2008].

2.3 Respiration in wetlands

Responses of respiration in wetlands to environmental drivers are similar to those in upland ecosystems, especially under aerobic conditions in intermittently flooded wetlands. Generally, the relationship between respiration and temperature exhibits an exponential pattern in wetlands (e.g. most wetland studies in SRDB). Soil water content effects, however, usually result in different seasonal patterns of respiration between wetlands and upland ecosystems. For dry seasons or drought events, the aerobic respiration rate increases in wetlands when the water table sinks below the surface and oxygen and substrate availabilities increase correspondingly [*Laiho*, 2006; *Mast et al.*, 1998; *Schreader et al.*, 1998]. In upland ecosystems dry conditions represent a significant decrease in water content and respiration rate decreases [*Law et al.*, 2001; *Reichstein et al.*, 2002; *Wen et al.*, 2010]. Integrating effects of both temperature and water content implies that in wetlands the warmer and drier conditions may stimulate respiration rate whereas in many upland ecosystems drier conditions likely offset the increase that would result from the warming. Therefore, similarity in temperature effects implies the possibility of applying the respiration models for upland ecosystems into wetlands, but soil water content determines the difference in model structure.

While significant effects of water table fluctuation on respiration have been found in most existing wetland studies, they are rather specific between sites and associated with vegetation type, nutrient availability and other factors [*Laiho*, 2006]. Some studies have shown that respiration was not affected by water table fluctuation [*Parmentier et al.*, 2009; *Updegraff et al.*, 2001], or responded differently between sites or microsites [*Alm et al.*, 1999; *Sulman et al.*, 2010].

3. Study site

This dissertation research was conducted in the Alligator River National Wildlife Refuge (ARNWR) located on the Albemarle-Pamlico peninsula in eastern North Carolina, USA ($35^0$47′N, $75^0$54′W). ARNWR is the first and largest conservation holding in eastern North Carolina, established in 1984 to provide protection for pocosins [*Bryant et al.*, 2008]. Astronomic tides are absent in this peninsula because of the specific combination of geomorphic features and lagoonal environment. Precipitation is the main source of water to this wetland [*Moorhead and Brinson*, 1995]. The mean annual temperature and precipitation, from climate records of an adjacent meteorological station (Manteo AP, NC, $35^0$55′N, $75^0$42′W) for the period 1981-2010, are 16.9°C and 1270 mm, respectively.

Sea level rise (SLR) has already begun in this area, of which the magnitude is larger than northern Atlantic coast [*Kemp et al.*, 2009]. Management activities, such as installing riser-board structures and tide gates in old drainage ditches, have been adopted to enhance wetland functioning by preventing saltwater intrusion and flooding and help buffer these coastal ecosystems from SLR [*Lawler et al.*, 2008]. The vulnerability of these ecosystems to the

changing climate, SLR and extreme storm events warrants research to understand mechanisms of response that will aid in development of management strategies to optimize conservation [*Pearsall*, 2005].

Major soil types are hydric soil, such as Pungo muck (41% of the land area), Belhaven muck (31.6%), Ponzer muck (4.6%), Hobonny muck (3.6%), Currituck muck (2.5%), Scuppernong muck (1.8%) and etc. There are also several mineral soil type, such as Hyde, Cape Fear, Udorthents (sands), Ousley fine sand and Baymeade fine sand (Figure 1-3) [*Bryant et al.*, 2008; *USDA Soil Conservation Service*, 1992]. Large proportion of the vegetation types are mixed pine and hardwood forests (Figure 1-4) [*Bryant et al.*, 2008]. Our study site was set in a mixed hardwood stand area in the center of the peninsular (star symbol in Figure 1-3 and 1-4).

4. Dissertation objectives and framework

The major objective of this research was to characterize respiratory processes, especially soil respiration, in a forested wetland in the lower coastal plain of the southeastern USA. Only CO_2 emission was investigated for each component and the following research questions were addressed:

(1) How do the respiratory components in this forested wetland respond to temperature and especially water table fluctuation?

(2) Could existing models mostly developed for upland ecosystems adequately represent the response of respiratory components to environmental drivers in this forested wetland?

(3) What is the best way to upscale estimates of respiratory components from small sampling locations to the ecosystem scale in this forested wetland with typical microtopographic variation?

(4) How much CO_2 is released annually from these respiratory components in this forested wetland to the atmosphere?

(5) What is the difference in these respiratory components between this forested wetland and other types of ecosystems, especially upland forests?

Chapter 2 explored questions 1, 2, 4 and 5 related to **soil respiration**. Soil CO_2 efflux was measured continuously with an automated system from summer 2009 to the end of 2010. Two environmental drivers, soil temperature and water table depth, were characterized to model soil respiration. A nested model accounting for water table depth effects was developed for characterizing aerobic soil respiration and provided a significantly better fit with observations. Two traditional models were also tested for modeling performance and compared with the nested model. To understand spatial variation due to microtopography and associated differences in hydrology and vegetation, the above studies were applied to three microsites along a microtopographic gradient, representing the mound area where trees grow, the low-lying non-vegetated area, and the transitional area between the mound and low-lying areas.

In Chapter 3, the study was expanded to other respiratory components, including **ecosystem respiration (R_e)**, **soil respiration (R_s)** and **coarse woody debris respiration (R_{CWD}).** Measurements on R_e, R_s, and R_{CWD} were conducted from 2009 to 2011. Analysis

similar to those in Chapter 2 (i.e. for questions 1, 2, 4 and 5) was also conducted for the other two components. The strategy of modeling soil respiration developed in Chapter 2 was applied for ecosystem respiration to account for water table depth effects. Because the spatial scale of measurements was different for the three components, question 3 was also addressed in this chapter. With a **microtopography distribution analysis**, soil respiration was upscaled from a single location to the ecosystem scale. The seasonal variation of contributions from soil respiration and coarse woody debris respiration to ecosystem respiration was investigated. I specifically studied the ratio of soil respiration to ecosystem respiration, characterizing its seasonal variation and response to water table fluctuation.

Chapter 4 used stable carbon isotope methods to address question 1 indirectly for **the components of soil respiration**. The ^{13}C composition of soil CO_2 efflux is thought to reflect the relative contribution of components, and therefore the seasonal variation of $\delta^{13}C_{Rs}$ implies the seasonal variation of the relative contribution. Gas samples of soil-respired CO_2 were collected at mound microsites and low-lying microsites in 2010 and 2011. The seasonal variation, spatial variation of $\delta^{13}C_{Rs}$, and also the hydrologic effects on these variations were investigated. The implications of the variations and hydrologic effects provided insights on how to improve the noninvasive method of partitioning soil respiration under natural conditions.

Chapter 5 synthesizes the individual study results according to the above five questions, mainly with respect to responses of respiratory components to hydrologic regime and effects on the carbon budget estimate. Implications for further studies are also discussed.

References

Alm, J., L. Schulman, J. Walden, H. Nykanen, P. J. Martikainen, and J. Silvola (1999), Carbon balance of a boreal bog during a year with an exceptionally dry summer, *Ecology*, *80*(1), 161-174.

Andrews, J. A., K. G. Harrison, R. Matamala, and W. H. Schlesinger (1999), Separation of Root Respiration from Total Soil Respiration Using Carbon-13 Labeling during Free-Air Carbon Dioxide Enrichment (FACE), *Soil Sci. Soc. Am. J.*, *63*(5), 1429-1435.

Armentano, T. V. (1980), Drainage of Organic Soils as a Factor in the World Carbon Cycle, *BioScience*, *30*(12), 825-830.

Arrhenius, S. (1889), Uber die Reaktionsgeschwindigkeit bei der Inversion von Rohrzucker durch Sauren, *Zeitschrift fur Physik Chemique*, *4*, 226-248.

Aselmann, I., and P. J. Crutzen (1989), Global distribution of natural freshwater wetlands and rice paddies, their net primary productivity, seasonality and possible methane emissions, *J Atmos Chem*, *8*(4), 307-358.

Baggs, E. M. (2006), Partitioning the components of soil respiration: a research challenge, *Plant Soil*, *284*(1-2), 1-5.

Baldocchi, D. (2008), 'Breathing' of the terrestrial biosphere: lessons learned from a global network of carbon dioxide flux measurement systems, *Australian Journal of Botany*, *56*(1), 1-26.

Baldocchi, D., E. Falge, and K. Wilson (2001), A spectral analysis of biosphere-atmosphere trace gas flux densities and meteorological variables across hour to multi-year time scales, *Agricultural and Forest Meteorology*, *107*(1), 1-27.

Battin, T. J., S. Luyssaert, L. A. Kaplan, A. K. Aufdenkampe, A. Richter, and L. J. Tranvik (2009), The boundless carbon cycle, *Nature Geosci*, *2*(9), 598-600.

Beer, C., et al. (2010), Terrestrial Gross Carbon Dioxide Uptake: Global Distribution and Covariation with Climate, *Science, 329*(5993), 834-838.

Bond-Lamberty, B., and A. Thomson (2010), A global database of soil respiration data, *Biogeosciences, 7*, 1915-1926.

Boone, R. D., K. J. Nadelhoffer, J. D. Canary, and J. P. Kaye (1998), Roots exert a strong influence on the temperature sensitivityof soil respiration, *Nature, 396*(6711), 570-572.

Bowling, D. R., D. E. Pataki, and J. T. Randerson (2008), Carbon isotopes in terrestrial ecosystem pools and CO_2 fluxes, *New Phytologist, 178*(1), 24-40.

Bridgham, S., J. P. Megonigal, J. Keller, N. Bliss, and C. Trettin (2006), The carbon balance of North American wetlands, *Wetlands, 26*(4), 889-916.

Brinson, M. M., A. I. Malvárez, and eacute (2002), Temperate freshwater wetlands: types, status, and threats, *Environ. Conserv., 29*(02), 115-133.

Brüggemann, N., et al. (2011), Carbon allocation and carbon isotope fluxes in the plant-soil-atmosphere continuum: a review, *Biogeosciences, 8*(11), 3457-3489.

Bryant, M., P. Jerome, and J. Andrew (2008), Alligator River National Wildlife Refuge Comprehenisve Conservation Plan*Rep.*, Fish and Wildlife Service, Southeast Region, Atlanta, Georgia.

Chambers, J. Q., J. P. Schimel, and A. D. Nobre (2001), Respiration from coarse wood litter in central Amazon forests, *Biogeochemistry, 52*(2), 115-131.

Chambers, J. Q., E. S. Tribuzy, L. C. Toledo, B. F. Crispim, N. Higuchi, J. d. Santos, A. C. Araújo, B. Kruijt, A. D. Nobre, and S. E. Trumbore (2004), Respiration from a Tropical Forest Ecosystem: Partitioning of Sources and Low Carbon Use Efficiency, *Ecological Applications, 14*(4), S72-S88.

Chimner, R. A. (2004), Soil respiration rates of tropical peatlands in Micronesia and Hawaii,

Wetlands, 24(1), 51-56.

Chmura, G. L., S. C. Anisfeld, D. R. Cahoon, and J. C. Lynch (2003), Global carbon sequestration in tidal, saline wetland soils, *Global Biogeochemical Cycles*, *17*(4), 1111.

Ciais, P., P. P. Tans, M. Trolier, J. W. C. White, and R. J. Francey (1995), A Large Northern Hemisphere Terrestrial CO_2 Sink Indicated by the $^{13}C/^{12}C$ Ratio of Atmospheric CO_2, *Science*, *269*(5227), 1098-1102.

Conant, R. T., et al. (2011), Temperature and soil organic matter decomposition rates – synthesis of current knowledge and a way forward, *Global Change Biology*, *17*(11), 3392-3404.

Dai, Z., C. C. Trettin, C. Li, H. Li, G. Sun, D. M. Amatya (2011), Effect of assessment scale on spatial and temporal variations in CH_4, CO_2, and N_2O fluxes in a forested wetland. *Water, Air and Soil Pollution*. DOI: 10.1007/s11270-011-0855-0.

Davidson, E. A. (2010), Permafrost and Wetland Carbon Stocks, *Science*, *330*(6008), 1176-1177.

Davidson, E. A., and I. A. Janssens (2006), Temperature sensitivity of soil carbon decomposition and feedbacks to climate change, *Nature*, *440*(7081), 165-173.

Davidson, E. A., I. A. Janssens, and Y. Luo (2006), On the variability of respiration in terrestrial ecosystems: moving beyond Q_{10}, *Global Change Biology*, *12*(2), 154-164.

Davidson, E. A., S. Samanta, S. S. Caramori, and K. Savage (2012), The Dual Arrhenius and Michaelis–Menten kinetics model for decomposition of soil organic matter at hourly to seasonal time scales, *Global Change Biology*, *18*(1), 371-384.

Denman, K. L., et al. (2007), Couplings between changes in the climate system and biogeochemistry, in *Climate Change 2007: The Physical Science Basis. Contribution of Working Group I to the Fourth Assessment Report of the Intergovernmental Panel on Climate Change*, edited by S. Solomon, D. Qin, M. Manning, Z. Chen, M. Marquis, K. B.

Averyt, M. Tignor and H. L. Miller, Cambridge University Press, Cambridge, United Kingdom and New York, NY, USA.

Dungait, J. A. J., D. W. Hopkins, A. S. Gregory, and A. P. Whitmore (2012), Soil organic matter turnover is governed by accessibility not recalcitrance, *Global Change Biology*, *18*(6), 1781-1796.

Ehleringer, J. R., N. Buchmann, and L. B. Flanagan (2000), Carbon isotope ratios in belowground carbon cycle processes, *Ecological Applications*, *10*(2), 412-422.

Ehleringer, J. R., D. R. Bowling, L. B. Flanagan, J. Fessenden, B. Helliker, L. A. Martinelli, and J. P. Ometto (2002), Stable Isotopes and Carbon Cycle Processes in Forests and Grasslands, *Plant Biology*, *4*(2), 181-189.

Erwin, K. (2009), Wetlands and global climate change: the role of wetland restoration in a changing world, *Wetlands Ecol Manage*, *17*(1), 71-84.

Falloon, P., C. D. Jones, M. Ades, and K. Paul (2011), Direct soil moisture controls of future global soil carbon changes: An important source of uncertainty, *Global Biogeochemical Cycles*, *25*, GB3010.

Formanek, P., and P. Ambus (2004), Assessing the use of delta C-13 natural abundance in separation of root and microbial respiration in a Danish beech (Fagus sylvatica L.) forest, *Rapid Commun. Mass Spectrom.*, *18*(8), 897-902.

Frei, S., K. H. Knorr, S. Peiffer, and J. H. Fleckenstein (2012), Surface micro-topography causes hot spots of biogeochemical activity in wetland systems: A virtual modeling experiment, *Journal of Geophysical Research: Biogeosciences*, *117*(G4), G00N12.

GLOBALVIEW-CO2 (2012), Cooperative Atmospheric Data Integration Project - Carbon Dioxide, edited by NOAA-ESRL, http://www.esrl.noaa.gov/gmd/ccgg/globalview/, Boulder, Colorado.

Gorham, E. (1991), Northern Peatlands: Role in the Carbon Cycle and Probable Responses to

Climatic Warming, *Ecological Applications, 1*(2), 182-195.

Griffis, T. J., T. A. Black, D. Gaumont-Guay, G. B. Drewitt, Z. Nesic, A. G. Barr, K. Morgenstern, and N. Kljun (2004), Seasonal variation and partitioning of ecosystem respiration in a southern boreal aspen forest, *Agricultural and Forest Meteorology, 125*(3–4), 207-223.

Hanson, P. J., N. T. Edwards, C. T. Garten, and J. A. Andrews (2000), Separating root and soil microbial contributions to soil respiration: A review of methods and observations, *Biogeochemistry, 48*(1), 115-146.

Harmon, M. E., et al. (2004), Ecology of Coarse Woody Debris in Temperate Ecosystems, in *Advances in Ecological Research*, edited by H. Caswell, pp. 59-234, Academic Press.

Ise, T., and P. R. Moorcroft (2006), The global-scale temperature and moisture dependencies of soil organic carbon decomposition: an analysis using a mechanistic decomposition model, *Biogeochemistry, 80*(3), 217-231.

Ise, T., A. L. Dunn, S. C. Wofsy, and P. R. Moorcroft (2008), High sensitivity of peat decomposition to climate change through water-table feedback, *Nature Geoscience, 1*, 763-766.

Junk, W., S. An, C. M. Finlayson, B. Gopal, J. Květ, S. Mitchell, W. Mitsch, and R. Robarts (2013), Current state of knowledge regarding the world's wetlands and their future under global climate change: a synthesis, *Aquat Sci, 75*(1), 151-167.

Keller, J. K. (2011), Wetlands and the global carbon cycle: what might the simulated past tell us about the future?, *New Phytologist, 192*(4), 789-792.

Kemp, A. C., B. P. Horton, S. J. Culver, D. R. Corbett, O. van de Plassche, W. R. Gehrels, B. C. Douglas, and A. C. Parnell (2009), Timing and magnitude of recent accelerated sea-level rise (North Carolina, United States), *Geology, 37*(11), 1035-1038.

Kim, J., and S. B. Verma (1992), Soil surface CO_2 flux in a Minnesota peatland,

Biogeochemistry, *18*, 37-51.

Kirschbaum, M. U. F. (2000), Will changes in soil organic carbon act as a positive or negative feedback on global warming?, *Biogeochemistry*, *48*(1), 21-51.

Kucera, C. L., and D. R. Kirkham (1971), Soil respiration studies in tallgrass prairie in Missouri, *Ecology*, *52*(5), 912-915.

Kuzyakov, Y. (2006), Sources of CO_2 efflux from soil and review of partitioning methods, *Soil Biology and Biochemistry*, *38*(3), 425-448.

Laiho, R. (2006), Decomposition in peatlands: Reconciling seemingly contrasting results on the impacts of lowered water levels, *Soil Biology and Biochemistry*, *38*(8), 2011-2024.

Law, B. E., F. M. Kelliher, D. D. Baldocchi, P. M. Anthoni, J. Irvine, D. Moore, and S. Van Tuyl (2001), Spatial and temporal variation in respiration in a young ponderosa pine forest during a summer drought, *Agricultural and Forest Meteorology*, *110*(1), 27-43.

Lawler, J. J., et al. (2008), Resource management in a changing and uncertain climate, *Frontiers in Ecology and the Environment*, *8*(1), 35-43.

Le Quere, C., M. R. Raupach, J. G. Canadell, G. Marland, and et al. (2009), Trends in the sources and sinks of carbon dioxide, *Nature Geosci*, *2*(12), 831-836.

Lelieveld, J. O. S., P. J. Crutzen, and F. J. Dentener (1998), Changing concentration, lifetime and climate forcing of atmospheric methane, *Tellus B*, *50*(2), 128-150.

Lloyd, J., and J. A. Taylor (1994), On the temperature dependence of soil respiration, *Functional Ecology*, *8*(3), 315-323.

Lugo, A. E., S. Brown, and M. Brinson (1990), *Forested wetlands*, Elsevier, Amsterdam, Netherlands.

Luyssaert, S., et al. (2007), CO2 balance of boreal, temperate, and tropical forests derived from a global database, *Global Change Biology*, *13*(12), 2509-2537.

Mahecha, M. D., et al. (2010), Global convergence in the temperature sensitivity of respiration at ecosystem level, *Science*, *329*(5993), 838-840.

Makita, N., Y. Kosugi, M. Dannoura, S. Takanashi, K. Niiyama, A. R. Kassim, and A. R. Nik (2012), Patterns of root respiration rates and morphological traits in 13 tree species in a tropical forest, *Tree Physiology*, *32*(3), 303-312.

Marsden, C., Y. Nouvellon, and D. Epron (2008), Relating coarse root respiration to root diameter in clonal Eucalyptus stands in the Republic of the Congo, *Tree Physiology*, *28*(8), 1245-1254.

Mast, M. A., K. P. Wickland, R. T. Striegl, and D. W. Clow (1998), Winter fluxes of CO_2 and CH_4 from subalpine soils in Rocky Mountain National Park, Colorado, *Global Biogeochemical Cycles*, *12*(4), 607-620.

Matthews, E., and I. Fung (1987), Methane emission from natural wetlands: Global distribution, area, and environmental characteristics of sources, *Global Biogeochemical Cycles*, *1*(1), 61-86.

Meehl, G. A., et al. (2007), Global climate projections, in *Climate Change 2007: The Physical Science Basis. Contribution of Working Group I to the Fourth Assessment Report of the Intergovernmental Panel on Climate Change*, edited by S. Solomon, D. Qin, M. Manning, Z. Chen, M. Marquis, K. B. Averyt, M. Tignor and H. L. Miller, Cambridge University Press, Cambridge, United Kingdom and New York, NY, USA.

Meharg, A. A. (1994), A critical review of labelling techniques used to quantify rhizosphere carbon-flow, *Plant Soil*, *166*(1), 55-62.

Melillo, J. M., P. A. Steudler, J. D. Aber, K. Newkirk, H. Lux, F. P. Bowles, C. Catricala, A. Magill, T. Ahrens, and S. Morrisseau (2002), Soil warming and carbon-cycle feedbacks to the climate system, *Science*, *298*(5601), 2173-2176.

Migliavacca, M., et al. (2011), Semiempirical modeling of abiotic and biotic factors controlling ecosystem respiration across eddy covariance sites, *Global Change Biology*, *17*(1), 390-409.

Mitsch, W. J., and J. G. Gosselink (2007), *Wetlands*, John Wiley & Sons, Inc., New York, NY, USA.

Moore, D. J. P., N. A. Trahan, P. Wilkes, T. Quaife, B. B. Stephens, K. Elder, A. R. Desai, J. Negron, and R. K. Monson (2013), Persistent reduced ecosystem respiration after insect disturbance in high elevation forests, *Ecology Letters*, *16*(6), 731-737.

Moore, P. D. (2002), The future of cool temperate bogs, *Environ. Conserv.*, *29*(1), 3-20.

Moorhead, K. K., and M. M. Brinson (1995), Response of wetlands to rising sea level in the lower coastal plain of North Carolina, *Ecological Applications*, *5*(1), 261-271.

Moyano, F. E., S. Manzoni, and C. Chenu (2013), Responses of soil heterotrophic respiration to moisture availability: An exploration of processes and models, *Soil Biology and Biochemistry*, *59*(0), 72-85.

Murray, B. C., and T. Vegh (2012), Incorporating blue carbon as a mitigation action under the United Nations Framework Convention on climate change: Technical issues to address. *Rep. Report NI R 12-05*, Nicholas Institute for Environmental Policy Solutions, Duke University, Durham, NC.

Noormets, A., S. G. McNulty, J.-C. Domec, M. Gavazzi, G. Sun, and J. S. King (2012), The role of harvest residue in rotation cycle carbon balance in loblolly pine plantations. Respiration partitioning approach, *Global Change Biology*, *18*(10), 3186-3201.

Noormets, A., et al. (2008), Moisture sensitivity of ecosystem respiration: Comparison of 14 forest ecosystems in the Upper Great Lakes Region, USA, *Agricultural and Forest Meteorology*, *148*, 216-230.

NRC, N. R. C. (1995), *Wetlands: Characteristics and Boundaries*, National Academy Press,

Washington, DC.

Parmentier, F. J. W., M. K. van der Molen, R. A. M. de Jeu, D. M. D. Hendriks, and A. J. Dolman (2009), CO_2 fluxes and evaporation on a peatland in the Netherlands appear not affected by water table fluctuations, *Agricultural and Forest Meteorology*, *149*(6–7), 1201-1208.

Pearsall, S. H. I. (2005), Managing for future change on the Albemarle Sound, in *Climate change and biodiversity*, edited by L. Hannah and T. E. Lovejoy, Yale University Press, New Haven, CT.

Pendleton, L., D. C. Donato, B. C. Murray, S. Crooks, and W. A. Jenkins (2012), Estimating global 'blue carbon' emissions from conversion and degradation of vegetated coastal ecosystems, *PLoS ONE*, *7*(9), e43542.

Raich, J. W., and W. H. Schlesinger (1992), The global carbon dioxide flux in soil respiration and its relationship to vegetation and climate, *Tellus B*, *44*(2), 81-99.

Reichstein, M., J. D. Tenhunen, O. Roupsard, J.-M. Ourcival, S. Rambal, S. Dore, and R. Valentini (2002), Ecosystem respiration in two Mediterranean evergreen Holm Oak forests: drought effects and decomposition dynamics, *Functional Ecology*, *16*, 27-39.

Reichstein, M., et al. (2005), On the separation of net ecosystem exchange into assimilation and ecosystem respiration: review and improved algorithm, *Global Change Biology*, *11*(9), 1424-1439.

Rodeghiero, M., and A. Cescatti (2006), Indirect partitioning of soil respiration in a series of evergreen forest ecosystems, *Plant Soil*, *284*(1-2), 7-22.

Ross, D. J., N. A. Scott, K. R. Tate, N. J. Rodda, and J. A. Townsend (2001), Root effects on soil carbon and nitrogen cycling in a Pinus radiata D. Don plantation on a coastal sand, *Aust. J. Soil Res.*, *39*(5), 1027-1039.

Savage, K., E. A. Davidson, A. D. Richardson, and D. Y. Hollinger (2009), Three scales of

temporal resolution from automated soil respiration measurements, *Agricultural and Forest Meteorology*, *149*(11), 2012-2021.

Schimel, D. S. (1995), Terrestrial ecosystems and the carbon cycle, *Global Change Biology*, *1*(1), 77-91.

Schreader, C. P., W. R. Rouse, T. J. Griffis, L. D. Boudreau, and P. D. Blanken (1998), Carbon dioxide fluxes in a northern fen during a hot, dry summer, *Global Biogeochemical Cycles*, *12*(4), 729-740.

Sierra, C. (2012), Temperature sensitivity of organic matter decomposition in the Arrhenius equation: some theoretical considerations, *Biogeochemistry*, *108*(1-3), 1-15.

Staddon, P. L. (2004), Carbon isotopes in functional soil ecology, *Trends in Ecology & Evolution*, *19*(3), 148-154.

Sulman, B. N., A. R. Desai, N. Z. Saliendra, P. M. Lafleur, L. B. Flanagan, O. Sonnentag, D. S. Mackay, A. G. Barr, and G. van der Kamp (2010), CO_2 fluxes at northern fens and bogs have opposite responses to inter-annual fluctuations in water table, *Geophysical Research Letters*, *37*(19), L19702.

Trettin, C. C., and M. F. Jurgensen (2003), Carbon cycling in wetland forest soils, in *The Potential of U.S. Forest Soils to Sequester Carbon and Mitigate the Greenhouse Effect*, edited by J. M. Kimble, L. S. Heath, R. A. Birdsey and R. Lal, CRC Press, Boca Raton.

Trumbore, S. (2000), Age of soil organic matter and soil respiration: Radiocarbon constraints on belowground carbon dynamics, *Ecological Applications*, *10*(2), 399-411.

Trumbore, S. (2006), Carbon respired by terrestrial ecosystems – recent progress and challenges, *Global Change Biology*, *12*(2), 141-153.

Updegraff, K., S. D. Bridgham, J. Pastor, P. Weishampel, and C. Harth (2001), Response of CO_2 and CH_4 emissions from peatlands to warming and water table manipulation. *Ecological Applications*, *11*(2), 311-326.

USDA (U.S. Department of Agriculture), Soil Conservation Service (1992), *Soil Survey of Dare County, North Carolina*. USDA Soil Conservation Service, Washington, DC.

Valentini, R., et al. (2000), Respiration as the main determinant of carbon balance in European forests, *Nature*, *404*(6780), 861-865.

van't Hoff, J. H. (1898), *Lectures on Theoretical and Physical Chemistry. Part 1. Chemical Dynamics*, Edward Arnold, London.

Van der Ploeg, M. J., W. M. Appels, D. G. Cirkel, M. R. Oosterwoud, J.-P. M. Witte, and S. E. A. T. M. van der Zee (2012), Microtopography as a driving mechanism for ecohydrological processes in shallow groundwater systems, *Vadose Zone Journal*, *11*(3), DOI: 10.2136/vzj2011.0098.

Waddington, J. M., and N. T. Roulet (1996), Atmosphere-wetland carbon exchanges: Scale dependency of CO_2 and CH_4 exchange on the developmental topography of a peatland, *Global Biogeochemical Cycles*, *10*(2), 233-245.

Webb, E. L., D. A. Friess, K. W. Krauss, D. R. Cahoon, G. R. Guntenspergen, and J. Phelps (2013), A global standard for monitoring coastal wetland vulnerability to accelerated sea-level rise, *Nature Clim. Change*, *3*(5), 458-465.

Wen, X. F., H. M. Wang, J. L. Wang, G. R. Yu, and X. M. Sun (2010), Ecosystem carbon exchanges of a subtropical evergreen coniferous plantation subjected to seasonal drought, 2003-2007, *Biogeosciences*, *7*(1), 357-369.

Wheeler, B. D. (1999), Water and plants in freshwater wetlands, in *Ecohydrology: plants and water in terrestrial and aquatic environments*, edited by A. J. Baird and R. L. Wilby, pp. 119-169, Routledge, London.

Figures

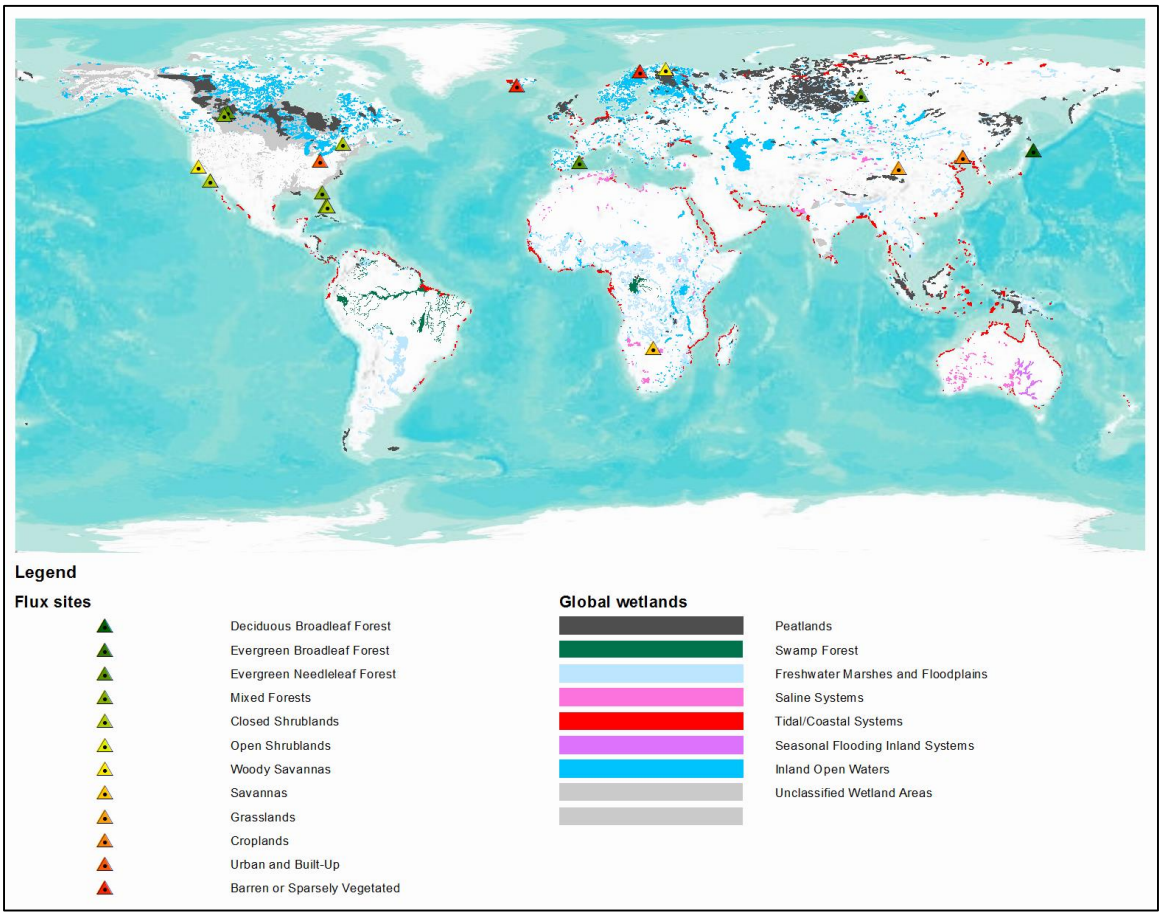

Figure 1-1 Distribution of global wetlands (from the global wetlands 1993 dataset) and identified wetland flux sites in global FLUXNET work. Twenty-five sites were located in wetlands including the IGBP-Land-Use defined 'permanent wetlands'. Searched words included: 'wetland', 'peatland', 'mire', 'bog', 'fen', and 'marsh' in site name. The vegetation types listed in Legend are defined by UMD-Land-Use (information from http://fluxnet.ornl.gov/).

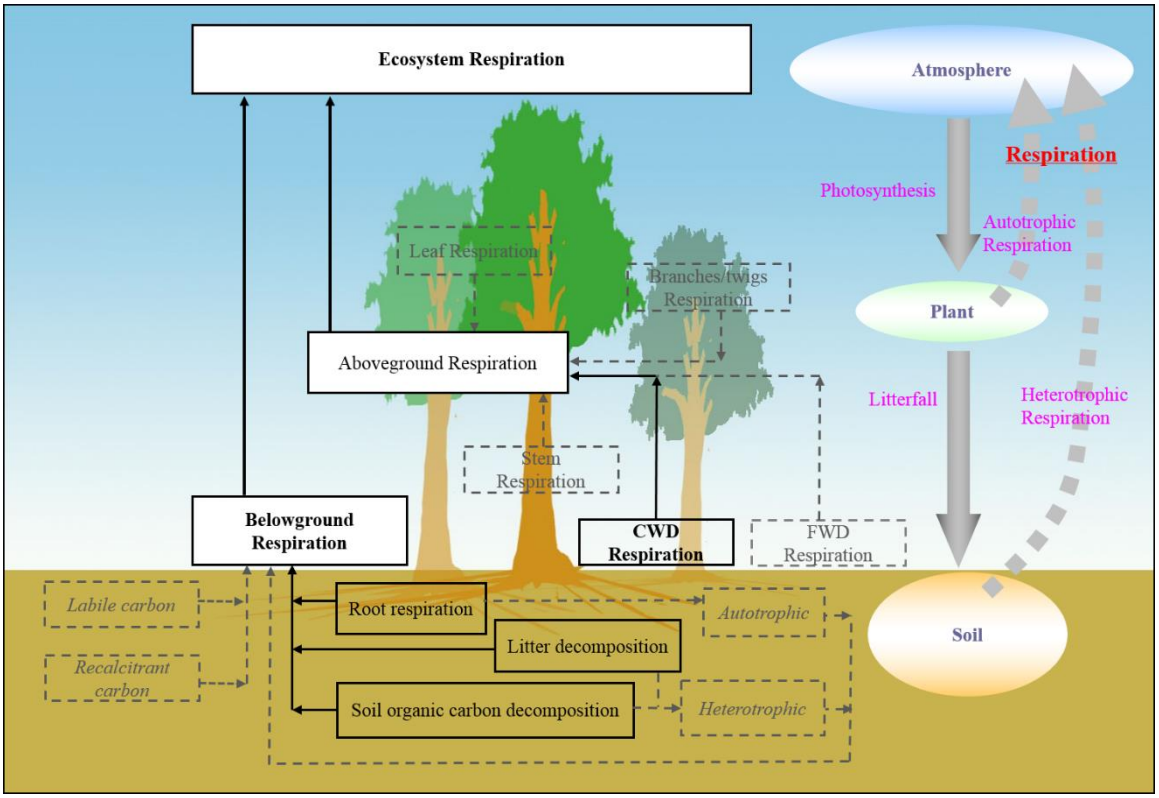

Figure 1-2 Simplified conceptual model of respiratory processes in an ecosystem. The components in solid frames are investigated in this study. Ecosystem respiration, belowground respiration and coarse woody debris (CWD) respiration (text in bold and black) were directly measured. Aboveground respiration, root respiration, litter decomposition and soil organic carbon decomposition (text in black) were discussed based on the measured components or indirect measurements. The terms in dashed frames were not measured in this study but presented to illustrate the complexity of respiration.

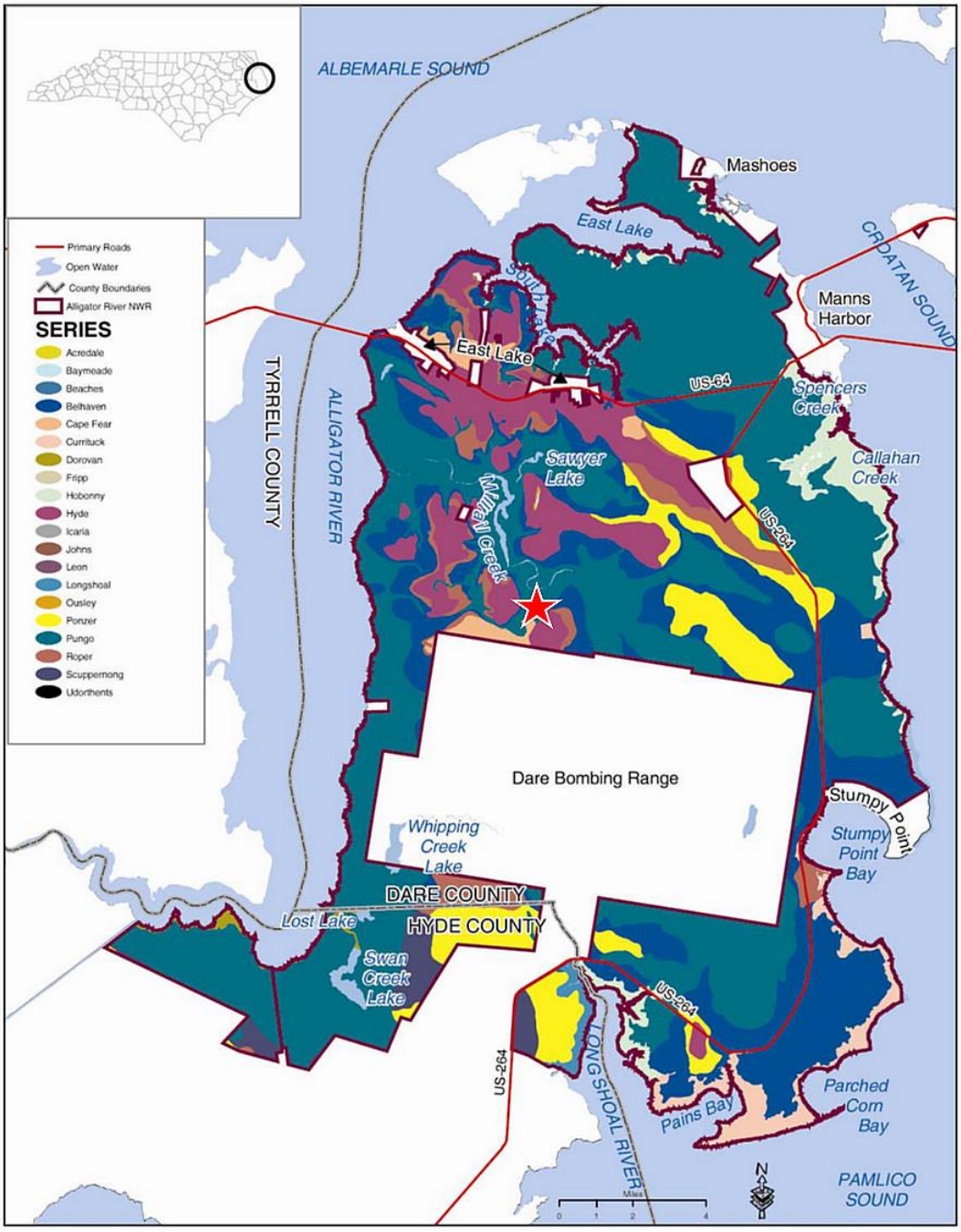

Figure 1-3 Soil types in the Alligator River National Wildlife Refuge (copy from Figure 3 in *Bryant et al.*, 2008). The red star symbol marks the site location of this study.

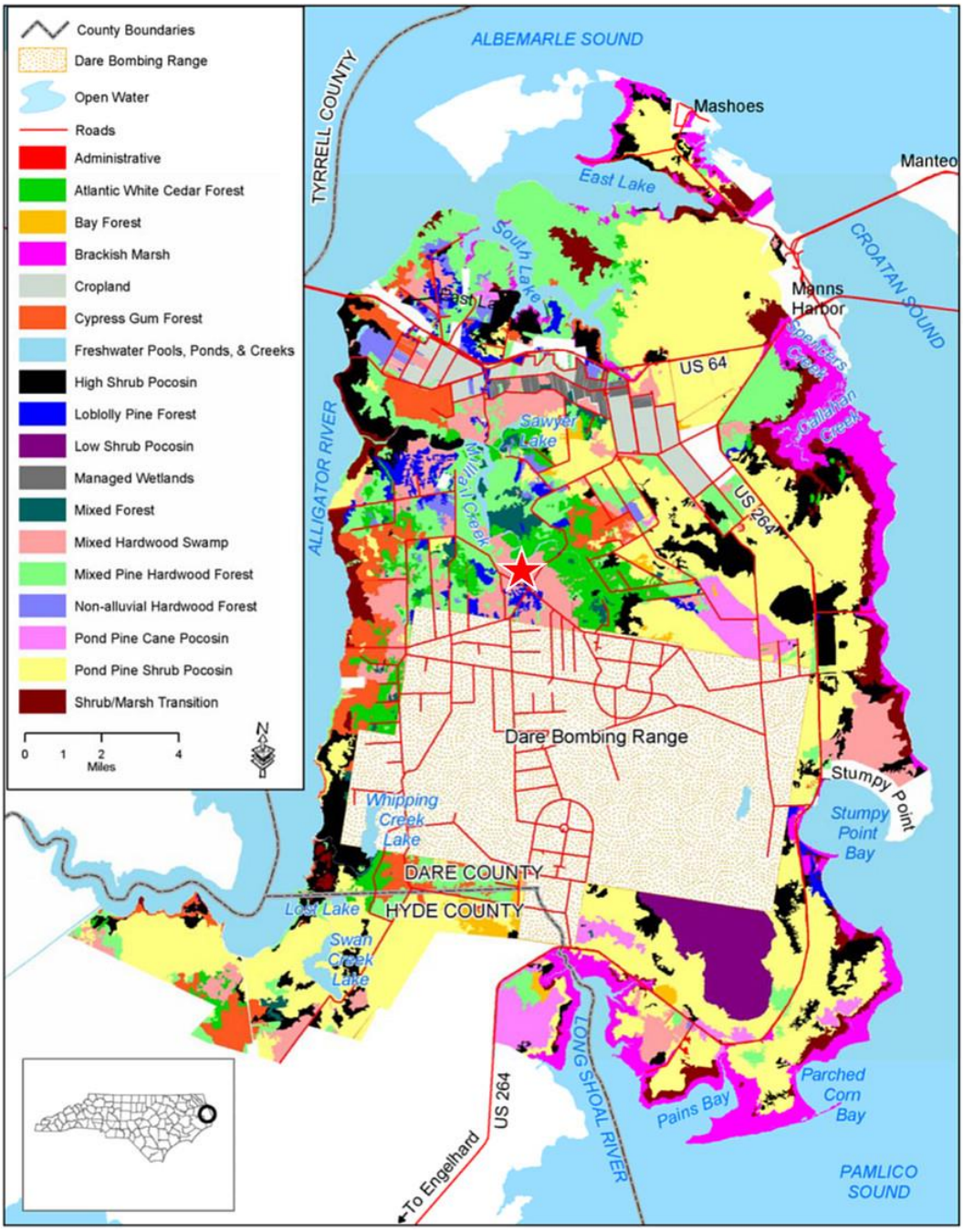

Figure 1-4 Vegetation types in the Alligator River National Wildlife Refuge (copy from Figure 4 in *Bryant et al.*, 2008). The red star symbol marks the site location of this study.

CHAPTER 2. THE EFFECT OF WATER TABLE FLUCTUATION ON SOIL RESPIRATION IN A LOWER COASTAL PLAIN FORESTED WETLAND IN THE SOUTHEASTERN USA

Abstract

The anthropogenic and environmental pressures on wetland hydrology may trigger changes in carbon (C) cycling, potentially exposing vast amounts of soil C to rapid decomposition. However, modeling soil C dynamics in wetlands has been challenging because of the fast-changing hydrologic regimes. In the current study, we measured soil CO_2 efflux (R_s) continuously in a lower coastal plain forested wetland in North Carolina, USA, to characterize its main environmental drivers. To account for spatial variation due to microtopography and associated differences in hydrology and vegetation, three microsites were positioned along a microtopographic gradient. There was a seasonal hysteresis in R_s because of the transitions between flooded (FL) and non-flooded (NFL) conditions, and differed by microtopographic location. Efflux dynamics during FL were characterized with a quadratic temperature-based model, whereas during NFL a nested Q_{10} model with dynamic parameters accounting for water table depth (WTD) effects provided a significantly better fit with observations compared to traditional models. The WTD effect was significant in both base respiration (R_b) and temperature sensitivity (Q_{10}). The diel variation of R_s was high and independent of soil temperature and WTD, which both had small diel variations. The fit of the models to daily R_s increased further, suggesting that the diel patterns in R_s were likely associated with vegetation activity. With the NFL- and FL-CO_2 fluxes estimated separately, the site-average soil CO_2-C emission was approximately 960-1103 g C m^{-2} yr^{-1} in 2010, of which 93% was released during NFL periods.

1. Introduction

It is estimated that wetland soils store 18-30% of the 1550 Pg of total global soil carbon while covering only 2-3% of the land area [*Trettin and Jurgensen*, 2003]. Information on soil carbon dynamics in wetlands, however, is very limited despite the large amount of C stored in these ecosystems. For example, in the global soil respiration database (SRDB version 20100517) [*Bond-Lamberty and Thomson*, 2010], there are only 135 data records for wetlands among the total of 3821 records. From this database, the global average annual soil CO_2 efflux (R_s, also representing the term of 'soil respiration' in this study) from wetlands was 344±278 (mean±SD) g C m^{-2} yr^{-1} as compared to an average 816±516 g C m^{-2} yr^{-1} in upland ecosystems. The proportion of total efflux from wetlands is relatively small, but the large amount of C may play important roles in terrestrial feedbacks to climate change. A recent modeling study has shown that wetland soil decomposition is highly sensitive to climate change [*Ise et al.*, 2008].

The hydrologic regime determines the difference in driving factors and mechanisms of temporal and spatial variation of R_s between wetlands and uplands. The hydroperiod confounds temporal variation on R_s in addition to the general seasonal variation regulated by temperature [*Mitsch and Gosselink*, 2007]. The water table depth (WTD) influences R_s through soil water content (SWC) or substrate availability to biological processes, and also through transitions between aerobic and anaerobic status [*Wheeler*, 1999]. This also implies the importance of microtopography in characterizing spatial heterogeneity of R_s in wetlands [*Alm et al.*, 1999]. However, only few studies in the past included the microtopography factor

into the field experiment design, which could significantly affect the estimate of R_s in ecosystem scale and wetland roles in global carbon cycle [*Alm et al.*, 1999; *Alm et al.*, 1997; *Jauhiainen et al.*, 2005; *Luken and Billings*, 1985].

The mechanistic response of R_s to its main environmental drivers remains poorly characterized for wetlands [*Davidson et al.*, 2006; *Lloyd and Taylor*, 1994; *Luo and Zhou*, 2006]. The WTD effect has been qualitatively investigated by laboratory controlled studies [*Blodau et al.*, 2004; *Dinsmore et al.*, 2009; *Moore and Dalva*, 1993; *Vicca et al.*, 2009]. Most published modeling studies, especially from intermittently flooded wetlands, have directly adapted the empirical models for R_s from upland systems, substituting WTD for SWC [Studies included in SRDB; *Bond-Lamberty and Thomson* 2010]. However, adaptation of models across sites has been complicated by the confounding temperature effects, large spatial variability and methodological differences among studies [*Chimner*, 2004; *Kim and Verma*, 1992; *Mäkiranta et al.*, 2009; *Silvola et al.*, 1996]. It has been shown that without proper accounting of hydrologic effects or other confounding influences, using the short-term temperature sensitivity to project soil responses to global change could result in significant bias [*Falloon et al.*, 2011; *Subke and Bahn*, 2010].

Efforts to quantify the effect of SWC or WTD on R_s (as well as on ecosystem respiration) have included SWC- or WTD-sensitive temperature sensitivity (e.g. Q_{10} in Q_{10} model or activation energy in Arrhenius equation) [*Mäkiranta et al.*, 2009; *Reichstein et al.*, 2002], as well as SWC-sensitive base respiration (R_b) [*Gaumont-Guay et al.*, 2006; *Noormets et al.*, 2008]. While the dynamic characteristics of Q_{10} and R_b have been well recognized and

different factors were considered for its mechanisms [*Pavelka et al.*, 2007; *Sampson et al.*, 2007; *Tjoelker et al.*, 2001; *Wang et al.*, 2010], to date few studies have combined both into a single model and none have directly quantified their ability to capture the variability of R_s. In this study, we evaluate the WTD effect on both Q_{10} and R_b in a forested wetland, present a model with dynamic parameterization, and evaluate its performance in different microtopographic location.

The objectives of this study were to: (1) quantify the seasonal variation and spatial heterogeneity of R_s in a seasonally-flooded coastal forested wetland on the lower coastal plain of North Carolina, USA; (2) develop a model for R_s under aerobic conditions to account for the covarying effect of WTD and T_s, and quantify the effects of WTD- and temperature-sensitivity parameters on capturing variation at different timescale; and (3) quantify the total soil CO_2 emission by distinguishing aerobic and anaerobic emissions given the microtopographic heterogeneity.

2. Materials and Methods

2.1 Site description

The study site was located at the Alligator River National Wildlife Refuge (ARNWR), on the Albemarle-Pamlico peninsula of North Carolina, USA (35°47´N, 75°54´W). This peninsula differs from coastlines to the north and the south because of the specific combination of geomorphic features and lagoonal environment, which results in astronomic tides being absent and rainfall being the main source of water [*Moorhead and Brinson*, 1995]. The peninsula has a deeper organic layer than the adjacent mainland areas due to having formed

at the outlet of the Alligator River which carries organic sediments, and for lower intensity of drainage due to very low topographic relief.

Climate records from an adjacent meteorological station (Manteo AP, NC) show the mean (1971-2000) annual precipitation is 1298 mm. Average annual temperature is 16.8 °C with 6.8 °C in January and 26.5 °C in July. Major soil types at the site are poorly drained Pungo and Belhaven mucks. The amounts of organic matter in surface soils are approximately 20-100% and 40-100%, respectively (Web Soil Survey accessed on 12/14/2009). The soils are acidic with pH of 4.2-4.8 at surface horizons. The overstorey is predominantly composed of black gum (*Nyssa sylvatica*), swamp tupelo (*Nyssa biflora*) and bald cypress (*Taxodium distichum*), with occasional red maple (*Acer rubrum*), white cedar (*Chamaecyparis thyoides*) and loblolly pine (*Pinus taeda*). The understory is predominantly fetterbush (*Lyonia lucida*), bitter gallberry (*Ilex galbra*), and red bay (*Persea borbonia*). Canopy height ranges from 15 to 20 m, with peak leaf area index of 3.5±0.3. Aboveground live biomass was estimated allometrically at 37.5±12.5 Mg C ha^{-1} in 2009 and 2010. Average live fine root biomass to a depth of 30 cm was 3.1±1.0 Mg C ha^{-1} during the same period.

2.2 Micrometeorology and water table measurement

Precipitation was measured with a model TE-525 tipping bucket rain gauge (Texas Electronic, TX, USA), air temperature and humidity with a model HMP45AC (Vaisala, Helsinki, Finland), soil temperature (T_s) at 5 and 20 cm with a model CS107 gauge (Campbell Scientific (CSI), UT, USA) and WTD with a pressure water level data logger (Infinities, Port Orange, FL, USA). Volumetric SWC (CS 616, CSI) was also measured as a

reference variable to WTD.

During the 1.5-year observation period, 2009 was a wet year, with 799 mm precipitation from July to December, while 2010 was a dry year, with only 673 mm during the second half of the year. The monthly mean WTD for July and August 2009 was 9.3 and 7.5 cm, respectively, at the water table probe location, while in July and August 2010 it was -13.8 and -6.7 cm (positive means water surface is above the ground and negative means below). The seasonal variation of soil temperature was not significantly different between 2009 and 2010 (Figure 2-1 a-c).

2.3 Soil CO_2 efflux measurement

Soil CO_2 efflux was measured with an automated soil respiration measuring system consisting a portable infrared gas analyzer (LI-8100, Licor Inc.), multiplexer (LI-8150, Licor Inc.), and three permanent sampling chambers (8100-104, Licor Inc.), starting in June, 2009. Three permanently installed PVC collars were located along a gradient of microsites from an elevated mound at the base of a tree to a low-lying non-vegetated area. The former was elevated above water table for most of the year, whereas the latter were inundated for part of the year. The relative elevations of the three microsites of automatic measurements were 12.9, 1.2 and -3.8 cm relative to the elevation of water table probe location (Figure 2-1 b). Microsite HIGH was at the base of a tree, microsite LOW was in the middle of a 2-m diameter non-vegetated low-lying area and microsite MID was intermediate along the elevation gradient, and about half a meter away from the nearest tree.

Soil CO_2 efflux data were collected every 30 minutes from July 2009 to December 2010

with the automated system. On November 11, 2009, hurricane Ida resulted in 40-cm increase in the water table in 2 days, flooding the chambers and causing a 4-month data gap, as the system had to be repaired (dark grey areas in Figure 2-1 d-f). Measurements continued on March 17th, 2010, and were discontinued again on September 17th due to hurricane Igor until November 14th. Data gaps were also caused by system protection under high relative humidity inside the chambers, occasional power problems at night and excessive flux coefficient of variation. Data coverage was 28% of time in 2009 and increased to above 50% as the result of improved power system, and less frequent high-humidity shut-down due to dry spring and summer of 2010. The LOW chamber was used for other purposes after August 5, 2010.

Data were separated to non-flooded (NFL, white areas in Figure 2-1 d-f) and flooded (FL, light grey areas) subsets in terms of the WTD at each microsite, which corresponded to aerobic and anaerobic states, respectively. During the 1.5-year study, HIGH microsite had 90% of NFL records spanning all seasons in both 2009 and 2010. MID and LOW were not flooded only in spring and summer of 2010, with the percentages of 46% and 54% of the time, respectively. For the FL records, due to the continuous change of surface water depth resulting in the change of collar headspace, the volume of headspace at each microsite was calculated based on the level of WTD above ground and the CO_2 effluxes were adjusted accordingly.

2.4 Model development

Models were developed separately for FL and NFL conditions due to the distinct phase shift.

During NFL periods, with aerobic processes dominating the efflux, both T_s and WTD effects were evaluated. During anaerobic FL conditions, T_s was the only independent factor considered.

2.4.1 Non-flooded model

Many soil respiration studies used Q_{10} model (Equation 1) for both upland and wetland ecosystems. Different improved versions have also been published by involving additional factors. For this forested wetland, we hypothesized that if the temperature response of aerobic R_s was affected by WTD, the R_b and Q_{10} would exhibit relationships with WTD. We therefore proposed a nested model (Equation 2).

$$R_s = R_b Q_{10}^{\frac{T_s - T_b}{10}} \tag{1}$$

$$R_s = f_{R_b}(WTD)\left[f_{Q_{10}}(WTD)\right]^{\frac{T_s - T_b}{10}} \tag{2}$$

where $f_{R_b}(WTD)$ and $f_{Q_{10}}(WTD)$ represent R_b and Q_{10} as the function of WTD; T_b is base temperature.

The functions of R_b and Q_{10} were derived by separating out the continuous NFL data in terms of specific temperature or WTDs, i.e. minimizing the correlation between temperature and WTD, and then fitting their respective patterns. T_s at 5 cm depth was used. Base temperature was defined as the temperature with the broadest range of WTD and set at 24°C. This is higher than the mean temperature during the study period, which was 19°C. The R_s with the range of temperatures constrained to within ±0.5°C, i.e. 23.5-24.5°C, were then

separated out as R_b data. With the data in a narrow range of temperature and the widest coverage of WTD, the relationship between R_b and WTD (i.e. $f_{R_b}(WTD)$) was analyzed.

Over the T_s range of one degree, R_s did not exhibit any pattern with temperature, whereas the variation with WTD exhibited a strong response (Figure 2-2). There was a pattern of increasing R_s as WTD dropped from 0 to -10 or -20 cm (varied by microsites) with nearly constant R_s at deeper WTD. As this pattern resembled the saturating pattern of Michaelis-Menten reaction, we simulated the dependence of R_b on WTD as (Equation 3):

$$R_b = f_{R_b}(WTD) = \frac{V_{\max} WTD}{K_m + WTD} \tag{3}$$

where V_{max} is the maximum R_b rate at T_b, and K_m the water depth at half maximum R_b.

For quantifying temperature sensitivity of R_s, data were binned by WTD in 5 cm intervals when WTD was shallower than 30 cm below ground (i.e. from -30 cm up to ground level). The interval was set greater when WTD was deeper due to the limited sample size. We assumed T_s was the primary driver of R_s within a given WTD class and estimated Q_{10} according to conventional Q_{10} model (Equation 1). Due to the interdependence between R_b and Q_{10} [*Janssens and Pilegaard* 2003], two methods were used to derive Q_{10} of each group of data: (i) R_b was calculated with $f_{R_b}(WTD)$ first and only Q_{10} was estimated by regression; and (ii) both R_b and Q_{10} were estimated by regression. Ultimately, the WTD was averaged for each group and used to analyze the relationship between Q_{10} and WTD (i.e. $f_{Q_{10}}(WTD)$).

In contrast to R_b extracted from measurements directly, Q_{10} was estimated by regression,

which resulted in greater uncertainties of the relationship between Q_{10} and WTD. At deeper WTD, the narrower T_s range and the large diurnal R_s variation resulted in poorer fit and less well-defined Q_{10}. The pattern of Q_{10} varying with WTD, however, was mostly consistent between the two methods despite the estimation uncertainty (Table 2-1). We then simplified the dependence of Q_{10} on WTD as an exponential function:

$$Q_{10} = f_{Q_{10}}(WTD) = \beta_1 \exp\left[\beta_2 (WTD + 10)\right] \quad (4)$$

where β_1 is Q_{10} at WTD = -10 cm and β_2 is a fitted WTD-effect parameter. The β_1 indicates that R_s at WTD = -10 cm increases $(\beta_1 - 1)$ times for every 10 degree rise in temperature. The β_2 means that per unit decrease in WTD (i.e. -1 cm) would cause Q_{10} to decrease by $\left[1 - \exp(\beta_2)\right]$.

By combining Equation 3 and 4, we derived the aerobic R_s model accounting for the effect of WTD as Equation 5. The model was then fitted to the continuous NFL data sets at each microsite.

$$R_s = \frac{V_{\max} WTD}{K_m + WTD} \left\{\beta_1 \exp\left[\beta_2 (WTD + 10)\right]\right\}^{\frac{T_s - 24}{10}} \quad (5)$$

2.4.2 Performance comparison between models

Performance of the nested Q_{10} model was compared with those of the conventional Q_{10} (Equation 1, T_b=24°C) and multiplicative model (Equation 6). The multiplicative model can be viewed as a special form of nested Q_{10} model, i.e. only R_b is dynamic and Q_{10} is constant, and is sometimes used as an improved Q_{10} model [*Davidson et al.*, 1998; *Tang et al.*, 2005b].

Both the coefficient of determination (R^2, Equation 7) and Akaike's Information Criterion (AIC, Equation 8) were calculated to evaluate the model performance [*Anderson et al.*, 2000; *Motulsky and Christopoulos*, 2004]. R^2 describes how well the model fits the data. AIC introduces a penalty for additional parameters to assess if the model is truly better or an overfit of the data. All computations were done with MATLAB 7.11 R2010b (The MathWorks Inc., U.S.A.).

$$R_s = R_b \exp\left[\beta\left(WTD + 10\right)\right] Q_{10}^{\frac{T_s - 24}{10}} \tag{6}$$

$$R^2 = 1.0 - \frac{RSS}{TSS} \tag{7}$$

$$AIC = n \ln \frac{RSS}{n} + 2K \tag{8}$$

where RSS represents the residual sum of squares and TSS the total sum of squares. n is the number of observations and K is the number of parameters.

2.4.3 Modeling with two datasets

One of the uncertainties of modeling R_s with 30-min data is from the variability at different time scales under which the factors influencing R_s may vary [*Baldocchi et al.*, 2001; *Riveros-Iregui et al.*, 2007]. We hypothesized that the model fit would increase with daily data due to reduced lags and temperature-independent variability in the diel cycle. For reference, we then fitted equations 1, 5 and 6 to daily integrated R_s data, where all 48 half-hourly records were present and had passed the quality assurance criteria. Both R^2 and AIC were calculated to compare model performance as well.

2.4.4 Flooded model

We tested two temperature-dependent models for modeling FL CO_2 efflux: a diffusion model from aquatic ecosystems [*Casper et al.*, 2000; *Maberly*, 1996], and a simple quadratic equation derived from regression between observed FL CO_2 efflux and T_s. Performance was similar between the two models; we then chose the simpler quadratic equation. The regression was done separately for three microsites (Table 2-2).

2.5 Gap filling and estimation of annual total soil CO_2-C emission

Missing 30-min flux data were gap-filled separately for NFL and FL periods. Non-flooded CO_2 efflux was gap-filled with the nested model (Equation 5). During FL periods, two criteria were used to fill the missing values. (i) If there were valid measurements during a given FL day, the missing flux values were simply set equal to the arithmetic mean of existing observed fluxes because of minimal diurnal fluctuation in FL fluxes. (ii) If there were no measurements during a day or continuous days, the missing values were filled with the quadratic equation (Equations in Table 2-2). The total annual CO_2-C loss was estimated as the sum of CO_2 efflux during NFL and FL periods. The NFL CO_2 efflux was also predicted based on T_s and/or WTD with the three models.

3. Results

3.1 Seasonal CO_2 efflux and spatial heterogeneity

Soil CO_2 efflux varied significantly by microsite and season (Figure 2-1 d-f). In general, the site was driest during summer (Jun., Jul. and Aug., Figure 2-1 b) with WTD below surface (mean WTD = -10 cm in summer 2010) and had the greatest CO_2-C release of the year.

During summer the individual peak efflux reached 21.0 μmol CO_2 m^{-2} s^{-1} and the mean value at HIGH microsite was 8.5±3.7 (mean±SD) μmol CO_2 m^{-2} s^{-1}. The mean CO_2 flux at MID and LOW microsites was 5.7±3.1 and 3.8±1.6 μmol CO_2 m^{-2} s^{-1}, respectively. The maximum daily total CO_2-C loss was 12.9, 9.8 and 6.0 g CO_2-C m^{-2} d^{-1} in HIGH, MID, and LOW microsites, respectively. Rain events during summer caused temporary flooding, resulting in uniformly low CO_2 efflux, with no significant difference between the three microsites. Flooded CO_2 flux during summer averaged 0.6 μmol CO_2 m^{-2} s^{-1} and ranged from 0.1-3.5 μmol CO_2 m^{-2} s^{-1}.

Most of the soil surface was submerged during autumn (Sep., Oct. and Nov., mean WTD = 14 cm in 2010) and winter (Dec., Jan., and Feb., mean WTD = 12 cm). CO_2 flux was generally less than 1.0 μmol CO_2 m^{-2} s^{-1} during this time. The flux during winter was the lowest due to the combination of flooding and low temperature, and averaged about 0.3 μmol CO_2 m^{-2} s^{-1} at all microsites. The water table drew down gradually in winter and the following spring (Mar., Apr. and May; mean WTD = 2 cm in spring 2011). The HIGH microsite was first exposed to the air in spring, and as a result CO_2 flux increased despite the similar temperatures in spring and autumn. The low-lying microsites were still submerged during spring and had comparable magnitude of CO_2 flux between spring and autumn. The respective mean CO_2 efflux at HIGH microsite during spring and autumn was 3.2 and 0.9 μmol CO_2 m^{-2} s^{-1}, respectively, whereas at MID it was 0.8 and 0.6 μmol CO_2 m^{-2} s^{-1}.

3.2 Nested Q_{10} model and model parameters

The difference in Q_{10} among the three microsites, determined by β_1 and β_2 in the nested

model, varied with WTD (Table 2-3 a, Figure 2-3 f). Higher β_1 implies higher Q_{10} at WTD = -10 cm, and higher β_2 implies faster change of Q_{10} with WTD. Both β_1 and β_2 were lower at HIGH than at LOW microsite, and as a result Q_{10} was lower at HIGH than LOW microsite when WTD was relatively shallow (from -5 to -15 cm), but higher when WTD was deeper. When the WTD decreased from -5 to -15 cm, Q_{10} decreased from 4.7 to 2.8 at HIGH microsite, whereas it decreased from 5.5 to 2.8 at LOW microsite. When the WTD decreased further from -15 to -25 cm, the Q_{10} decreased from 2.8-1.6 and 2.8-1.4 at HIGH and LOW microsite, respectively.

The parameters in the nested model were much higher at MID than at the other two microsites (Table 2-3 a). While this modeled greater sensitivity to environmental drivers might be real at MID than other microsites, it is more likely that the weakly defined asymptotic relationship between R_b and WTD due to limited WTD range (Figure 2-2) led to parameter convergence at unrealistic values. To aid model convergence at the MID microsite, we interpolated the V_{max} and β_2 parameter values based on the HIGH and LOW microsites (V_{max} = 11 μmol C m^{-2} s^{-1} and β_2 = 0.06 m^{-1}, MID-2 in Table 2-3). With these two parameter corrections, the K_m was estimated as 8 cm below ground and β_1 as 6.1.

In contrast to the dynamic trends of spatial difference reflected in parameters of the nested model, the trends resulting from the conventional Q_{10} and multiplicative models were fixed and differed between the two models (Table 2-3 a, Figure 2-3). The HIGH microsite had the lowest Q_{10} and the highest R_b according to all models throughout most of the year. The Q_{10} of the conventional Q_{10} model was not significantly different between MID and

LOW microsites, while from the multiplicative model the MID microsite had lower Q_{10} and more negative β, i.e. lower temperature sensitivity but greater WTD effect ($p<0.01$).

3.3 Comparison of model performances and two datasets

The conventional Q_{10} model captured 50-60% of the R_s variation with variability in T_s. The multiplicative model improved the performance by accounting for the effects of WTD, and increased R^2 to 70-80%. The nested model increased model fit by an additional 4-10%. For MID microsite, the R^2 decreased 5% with the manually-set values in the nested model, but was still high at 78% with increases of 26% and 4% relative to the conventional Q_{10} and multiplicative models, respectively. The lower AICs of the nested model with both the 30-min and daily data also indicated that the nested model performed better than the conventional models, even as penalized for the higher number of parameters (Table 2-3). Moreover, the residual analysis showed that the nested model provided the most consistency with observations, although it was not entirely unbiased (Figure 2-4 d-f, j-l).

Differences in model parameters among the microsites were consistent at both 30-minute and daily timescale, but improvement in model performance differed by microsite (Table 2-3 b). Through the comparison of R^2, AIC and the distribution of residuals, modeling with daily data performed better at MID and LOW compared to HIGH microsites. The R^2 of 30-min data at LOW microsite was 91% while the daily data reached 96%, indicating that the two environmental drivers can account for nearly all of the seasonal variation at this location (Table 2-3 b, Figure 2-4). In contrast, at HIGH microsite the R^2 increased from 82% to 87%, with 13% still unaccounted for (Table 2-3 b). In other words, the diel variability independent

of T_s and WTD was greatest at the HIGH microsite.

3.4 Estimation of annual total soil CO_2-C emissions

With the gaps filled separately for NFL and FL records, i.e. the nested model for NFL and the quadratic temperature-response equation for FL, the annual soil CO_2-C emissions at HIGH microsite was estimated at 1325 (95% CI: 1291-1365) g C m^{-2} in 2010, while MID and LOW microsites released an estimated 621 (555-710) and 430 (319-694) g C m^{-2}, respectively. The NFL periods contributed most of the CO_2-C loss annually, ranging from 72 to 97% at the different microsites (Table 2-4).

The difference of cumulative R_s between 2009 and 2010 was attributable to the differences in the number of FL and NFL days between the two years. From July to December, the percentage of NFL days at HIGH microsite was 51% (ca. 185 days) in 2009 and 85% (ca. 305 days) in 2010, which resulted in 308 and 704 g C m^{-2} of CO_2-C emission. At MID and LOW microsites, the R_s over the same period was approximately 2-3 times higher in the drier 2010 than in 2009.

The prediction of CO_2-C emission during NFL periods differed markedly between the three models (Table 2-5). Generally, the conventional Q_{10} and multiplicative models overestimated R_s compared to the nested model. However, the difference between the models may have been exaggerated by the unequal data coverage between the years. For example, 87% of the data at HIGH microsite came from 2010, and only 13% came from 2009. Thus, it should perhaps not be a surprise that the annual fluxes estimated with the conventional model and the multiplicative model differed by as much 105% and 48% from that with the nested

model in 2009. The annual estimates for 2010 by the three models were within 5% of each other.

4. Discussion

4.1 Temperature and WTD effects on soil respiration

In this southern forested wetland, the T_s-R_s relationship exhibited seasonal hysteresis, but differed among the three microsites due to their elevation and associated hydrology. R_s at HIGH microsite was higher earlier in the growing season than later. This pattern was similar to the hysteresis observed in R_s in a boreal aspen forest and a mixed conifer and oak forest in California, which was attributed to high rates of fine-root production early in the growing season and/or the drought conditions during late summer [*Gaumont-Guay et al.*, 2006; *Vargas and Allen*, 2008]. The opposite pattern, documented in some other boreal and temperate forests, has been attributed to higher microbial activity due to deeper soil warming [*Drewitt et al.*, 2002; *Goulden et al.*, 1998; *Morén and Lindroth*, 2000; *Phillips et al.*, 2010]. In the current study, both root growth and soil warming may have contributed to the seasonal dynamics of R_s, but both are ultimately linked to WTD and flooding status. The higher WTD (i.e. FL conditions) during autumn resulted in the lower R_s, and lower WTD (i.e. NFL conditions) during spring and summer corresponded to higher R_s. Compared with the HIGH microsite, the difference in R_s between spring and autumn at MID and LOW microsites was less pronounced as these microsites were flooded during both spring and summer (Figure 2-5).

The year-to-year difference in R_s during NFL periods shown in the two growing seasons

of observation at HIGH microsite also suggested that WTD had significant effects on R_s. For example, the mean value of recorded T_s was 21.8±0.9 (mean±SD) ˚C in July of 2009 and 23.3±1.0 ˚C in July of 2010, while the WTD at HIGH microsite was -3.3±2.7 cm and -29.1±6.4 cm, respectively. Correspondingly, R_s was 2.3±2.3 μmol CO_2 m^{-2} s^{-1} in 2009 and 10.0±2.8 μmol CO_2 m^{-2} s^{-1} in 2010. Different fine root production rate during earlier period in each year might be one reason causing the year-to-year variation [*Savage and Davidson*, 2001]. The key mechanisms associated with WTD-driven regulation include aeration, enzyme activity and the composition of decomposer communities, but none of these were explicitly measured in the current study. [*Freeman et al.*, 2001; *Freeman et al.*, 2004; *Jaatinen et al.*, 2007].

4.2 Quantifying driver effects during non-flooded periods

Due to the T_s-WTD interaction, some of WTD effect may be embedded in the simulation of T_s effect. For example, the bifurcation in the modeled WTD-R_s relationship was captured by the temperature-only conventional Q_{10} model (Figure 2-6 d). However, the seasonal hysteresis and year-to-year difference (i.e. the bifurcation shown in T_s-R_s relationship, grey dots in Figure 2-6 a), which is the WTD effect independent of T_s effect, is usually omitted by temperature-only models (black dots in Figure 2-6 a).

In previous studies, several strategies have been adopted to model the seasonal hysteresis and couple the effects from multiple drivers into models. Most studies have used the residual method: (1) fitting temperature-only models first (e.g. conventional Q_{10} model or Lloyd-Taylor model); (2) analyzing relationship between residuals and another driver (e.g. SWC);

(3) either adding or multiplying the additional-driver function to the temperature-only model, in which the residual pattern is generally site-specific [*Davidson et al.*, 1998; *Mäkiranta et al.*, 2009; *Savage and Davidson*, 2001; *Vincent et al.*, 2006]. There have also been studies applying the same model to different ecosystems without site-specific analysis [*Tang et al.*, 2005b; *Vargas and Allen*, 2008], which could also provide a better fit to observations like the multiplicative model we presented in this study. Few studies constructed dynamic R_b and/or Q_{10} separately through specific data classification and then combined them into one model [*Noormets et al.*, 2008; *Reichstein et al.*, 2002]. All these methods created empirical models, but the third one might be better connected with mechanisms as the dynamic pattern is derived directly from observations, whereas the residual method is based on indirect statistical results. Application of the third method has been limited by measurement technology and sample size at earlier periods, but the deployment of automated measuring system is currently reducing that limitation [*Carbone and Vargas*, 2008; *Savage and Davidson*, 2003].

The dynamic pattern of R_b and Q_{10} (Table 2-1, Figure 2-2 and Figure 2-3) provides a comparison between methods. At a casual look, the multiplicative model seems to offer improved performance compared to the conventional Q_{10} model in terms of increased R^2 and decreased AIC, but the pattern of WTD-R_b relationship reflected in the model (Figure 2-3 b) was fundamentally in disagreement with observations (Figure 2-2). The multiplicative model also did not capture the T_s-R_s relationship as well as the nested model (Figure 2-6 b-c), and its range of applicability seems restricted to WTD>-30 cm (Figure 2-6 e). At deeper WTD,

the multiplicative model would predict further increase in R_s, which is not supported by observations.

However, the dynamic R_b and Q_{10} based on classification of observations was affected by the selection of T_b and the assumption of consistent mechanism of regulation within each class. For example, the WTD-R_b relationship may not follow Michaelis-Menten relationship at all T_b levels, and the processes of CO_2 production and mechanisms of regulation may differ by depth. It is possible that the dynamic pattern may change if the criteria of data classification do. The robustness of the model can be tested further as the T_s-WTD parameter space gets filled more densely and in areas that are currently blank.

4.3 Implication of R_b and Q_{10} pattern in soil respiration modeling

As the net soil CO_2 efflux is the sum of multiple components with different regulatory mechanisms [*Davidson et al.*, 2006], the pattern of the apparent mean R_b and Q_{10} is determined by the response of respiration components to drivers and their relative contribution. For example, if two respiration components responded to driver variation oppositely and contributed equally to R_s, the apparent R_b and Q_{10} would both be constant. Thus, the mechanistic meaning of dynamic parameters fitted to the compound process of total R_s is to a degree speculative. It is also confounded by the nature of regression analysis, such as the statistically increased model performance with more parameters, or the interdependence between R_b and Q_{10} [*Janssens and Pilegaard*, 2003; *Kirschbaum*, 2006; *Subke and Bahn*, 2010].

Quantifying the role of individual parameters on improved performance may provide a

method for differentiating the biophysical basis from the statistical interaction between parameters. To our knowledge, none of previous studies improving R_s modeling through dynamic parameterization have explicitly compared the roles of individual parameters and explored the implications on mechanisms. In the current study, the improved performance of the multiplicative model with dynamic R_b and constant Q_{10} implicitly demonstrated the significance of R_b, while the small improvement with dynamic Q_{10} involved in the nested model might imply the smaller contribution by Q_{10}. To explicitly quantify the role of dynamic parameters, we did additional regression analysis in which the effects of WTD on R_b and Q_{10} were included into the nested model separately and in different order. The individual contribution of R_b to model improvement was more significant than that of Q_{10} for R_s of this forested wetland ecosystem (Table 2-6).

The partitioning of R^2 indicated that dynamic R_b contributed more than dynamic Q_{10} to capturing the dynamics of R_s at all three microsites. Although we derived consistent Q_{10} pattern regardless of the R_b pattern (Table 2-1), the small contribution of Q_{10} to increased R^2 implies uncertainty in the dynamic Q_{10} (Table 2-6). On one hand, this was expected as the statistical regression might obscure the dynamic pattern of Q_{10}. On the other hand, Q_{10} might play a role in simulating the higher end of R_s range (Figure 2-7), which corresponds to the deeper of WTD (deeper than -30 cm) and is usually statistically neglected because of its small weight in datasets. Also, the contribution of Q_{10} to seasonal variation of R_s in the forested wetland varied by microsite, likely reflecting different component processes.

4.4 Effect of time scale on model performance

As expected, model fit increased when applied to daily data, even though the smaller sample size led to higher uncertainty of parameter estimates (Table 2-3 b). The results confirmed the hypothesis that eliminating the diel variation would improve the simulation of seasonal variation. The greater improvement of performance at LOW than HIGH microsite (Table 2-3) may be caused by greater contribution of root respiration on diel cycle in the latter.

Compared with some upland ecosystems where diel variation of R_s is related to high diel temperature variation [*Ruehr et al.*, 2010], the forested wetland had small diel variation in T_s due to the buffering influence of high water table. For example, the daily range of T_s during the summer of 2010 was 0.54±0.17 ˚C (mean±SD), while the range of R_s at HIGH, MID and LOW microsite was 8.0±2.1, 5.7±2.8 and 3.6±2.8 μmol C m^{-2} s^{-1}, respectively. The diel variation of WTD was also small with the daily range at 1.7±0.6 cm excluding days with precipitation. This suggests that the diel variation in R_s was relatively independent of the T_s and WTD fluctuations, which were the primary drivers of the seasonal cycle. Plant processes which were not quantified in the current study may have dominated the diel dynamics. The role of new carbohydrate availability on R_s dynamics has been demonstrated in upland ecosystems [*Liu et al.*, 2006; *Tang et al.*, 2005a], but the evidence is less clear in wetland ecosystems where the trees are acclimated to wet conditions [*Lugo et al.*, 1990; *Mitsch and Gosselink*, 2007].

4.5 Annual soil CO_2-C emissions and spatial heterogeneity

The annual soil CO_2 emissions at MID and HIGH microsites (Table 2-4) were similar to

those reported for nearby pocosin and gum swamp ecosystems in North Carolina (672-1086 g C m^{-2} yr^{-1}) [*Bridgham and Richardson*, 1992], and a freshwater marsh in Louisiana (618 g C m^{-2} yr^{-1}) [*Smith et al.*, 1983]. The smaller flux at LOW microsite was similar to the salt marsh in the same study from Louisiana (418 g C m^{-2} yr^{-1}). Compared with upland systems, the magnitude of annual CO_2-C emissions at HIGH, MID and LOW microsite in 2010 were comparable with average soil CO_2 efflux of tropical evergreen broadleaf forest (1540 g C m^{-2} yr^{-1}), boreal deciduous broadleaf (650 g C m^{-2} yr^{-1}) and boreal evergreen needle-leaf forest (360 g C m^{-2} yr^{-1}), respectively [*Gower*, 2003].

Such high spatial variation of R_s has been documented by earlier studies in other wetland ecosystems [*Alm et al.*, 1999; *Jauhiainen et al.*, 2005; *Luken and Billings*, 1985]. The range of 430-1320 g C m^{-2} yr^{-1} observed in the current study highlights the need for spatially explicit estimates of soil CO_2 efflux when scaling point data to the stand scale to estimate ecosystem C balance (Table 2-4). Given the areal contribution of different microtopographic positions in the landscape, 60% in HIGH, 23% in MID and 17% in LOW, result in the mean site-average efflux of 1015 g C m^{-2} yr^{-1} with 95% confidence interval of 960 to 1103 g C m^{-2} yr^{-1} in 2010, of which 93% was released during NFL periods. This estimate awaits further refinements in R_s data coverage, model development, and further quantification of the distribution of microsites.

The soil C emission from this southern forested wetland was much higher than that reported for northern wetlands and similar to some tropical wetlands. For example, the annual estimate is more than 2 times of the soil CO_2 flux at the wetlands at Harvard and

Howland Forests (370-480 g CO_2-C m^{-2} yr^{-1}) in northeast USA [*Savage and Davidson*, 2001], 2-4 times higher than those at a southern boreal peatland of Finland (220-320 g CO_2-C m^{-2} yr^{-1}) [*Alm et al.*, 1999], and 5-10 times higher than at a subarctic peatland (80-180 g CO_2-C m^{-2} yr^{-1}) [*Moore*, 1986], but similar to a tropical peat swamp forest in Indonesia (900-1100 g CO_2-C m^{-2} yr^{-1}) [*Jauhiainen et al.*, 2005]. As 2010 was a dry year in this study area, the soil C emission estimation may be higher than its long-term average, but this also indicates its potential for high emissions under drier conditions.

4.6 Uncertainties and implication of this study

Explicit accounting for WTD effects on Q_{10} showed that there is a positive relationship between them (Figure 2-3 f). In addition to being helpful for understanding temporal dynamics of R_s, this relationship allows us to explore the circumstances when site hydrology changes beyond currently observable conditions. The WTD-Q_{10} relationship suggests that there exists a WTD below which $Q_{10}<1$, i.e. R_s will begin to decrease with temperature. While there is a recognized temperature optimum on physiological processes [*Larcher*, 2003], and a negative T_s-R_s relationship has sometimes been reported [*Lellei-Kovács et al.*, 2011; *Tang et al.*, 2005a], the possibility of $Q_{10}\leq1$ is rarely considered in models. In the current study, only HIGH microsite had the records of WTD deeper than the modeled critical depth, i.e. about -35 cm. Although R_s was nearly constant with the increase of T_s at this relatively dry condition, the narrow temperature range (within 2.5°C) imposed large uncertainties.

With dynamic parameters, the model results suggested that the spatial differences in

temperature sensitivity of R_s are not consistent and the trend may be opposite at different WTD (Figure 2-3 f), which might be related to the varying contribution of respiration components [*Högberg*, 2010; *Zhou et al.*, 2010]. Given the spatial differences in microtopography and vegetation coverage at HIGH and LOW microsites, we expected the contribution of autotrophic component to be higher at the HIGH microsite near the tree base. Thus, the smaller decline in Q_{10} with decreasing WTD at HIGH than LOW microsite might suggest smaller suppression/sensitivity of autotrophic than heterotrophic component.

These results suggest that the regression approach [*Kucera and Kirkham*, 1971], whereby heterotrophic respiration is estimated as the intercept with R_s regressed against root biomass, may work well at this ecosystem. Despite other method-specific challenges such as the lack of replication of microsites in the current study, this approach offers lower disturbance and higher universality than the various root exclusion techniques currently in use [*Kuzyakov*, 2006].

5. Conclusions

Soil CO_2 efflux was measured continuously in a lower coastal plain forested wetland in North Carolina, USA, from 2009 to 2010. The R_s in the forested wetland varied by more than 2-fold as a function of microtopographic position. During summer non-flooded conditions, R_s rates averaged at 8.5±3.7 (mean±SD) μmol CO_2 m^{-2} s^{-1} in HIGH, 5.7±3.1 μmol CO_2 m^{-2} s^{-1} in MID, and 3.8±1.6 μmol CO_2 m^{-2} s^{-1} in LOW microsites. During submerged conditions, R_s rates decreased to less than 1 μmol CO_2 m^{-2} s^{-1} at all microsites. The seasonality of water table dynamics and flooding state overrode temperature effects on R_s at HIGH microsite,

resulting in seasonal hysteresis in the R_s-T_s relationship. This was not the case at MID and LOW microsites, which had similar hydrologic conditions during both seasons.

The spatial variability and interacting effects of T_s and WTD were successfully captured with a nested Q_{10} model where both base respiration and temperature sensitivity varied with WTD. The WTD effect on R_b followed Michaelis-Menten-reaction pattern, whereas Q_{10} varied exponentially. The dynamic parameters also reflected the dynamic trends of spatial difference in temperature sensitivity of R_s along with the WTD.

The diel range of R_s (3.6-8.0 μmol CO_2 m^{-2} s^{-1}) was much higher and not attributable to T_s and WTD, which had diel ranges of 0.54±0.17°C and 1.7±0.6 cm, respectively. The fit of the models to daily total CO_2 effluxes increased the model fit further, suggesting that the diel patterns were likely associated with vegetation activity.

With CO_2 effluxes estimated separately for flooded and non-flooded periods, and weighed by the areal contribution of different microsites, the total site mean annual soil CO_2 emission was 1015 (95% CI: 960-1103) g C m^{-2} s^{-1}, of which 93% was released during non-flooded periods.

Acknowledgements

This work was supported primarily by DOE NICCR (award number 08-SC-NICCR-1072) and USDA Forest Service Eastern Forest Environmental Threat Assessment Center (award 08-JV-11330147-38). GM was partly supported by a graduate research assistantship from the USGS Southeast Climate Science Center (award G10AC00624). Partial support for the study was also provided by DOE-TES program (award 11-DE-SC-0006700).

References

Alm, J., L. Schulman, J. Walden, H. Nykanen, P. J. Martikainen, and J. Silvola (1999), Carbon balance of a boreal bog during a year with an exceptionally dry summer, *Ecology*, *80*(1), 161-174.

Alm, J., A. Talanov, S. Saarnio, J. Silvola, E. Ikkonen, H. Aaltonen, H. Nykänen, and P. J. Martikainen (1997), Reconstruction of the carbon balance for microsites in a boreal oligotrophic pine fen, Finland, *Oecologia*, *110*(3), 423-431.

Anderson, D. R., K. P. Burnham, and W. L. Thompson (2000), Null hypothesis testing: problems, prevalence and an alternative, *The Journal of Wildlife Management*, *64*, 912-923.

Baldocchi, D., E. Falge, and K. Wilson (2001), A spectral analysis of biosphere-atmosphere trace gas flux densities and meteorological variables across hour to multi-year time scales, *Agricultural and Forest Meteorology*, *107*(1), 1-27.

Blodau, C., N. Basiliko, and T. R. Moore (2004), Carbon turnover in peatland mesocosms exposed to different water table levels, *Biogeochemistry*, *67*(3), 331-351.

Bond-Lamberty, B., and A. Thomson (2010), A global database of soil respiration data, *Biogeosciences*, *7*, 1915-1926.

Bridgham, S. D., and C. J. Richardson (1992), Mechanisms controlling soil respiration (CO_2 and CH_4) in southern peatlands, *Soil Biology & Biochemistry*, *24*(11), 1089-1099.

Carbone, M. S., and R. Vargas (2008), Automated soil respiration measurements: new information, opportunities and challenges, *New Phytologist*, *177*, 295-297.

Casper, P., S. C. Maberly, G. H. Hall, and B. J. Finlay (2000), Fluxes of methane and carbon dioxide from a small productive lake to the atmosphere, *Biogeochemistry*, *49*, 1-19.

Chimner, R. A. (2004), Soil respiration rates of tropical peatlands in Micronesia and Hawaii, *Wetlands*, *24*(1), 51-56.

Davidson, E. A., E. Belk, and R. D. Boone (1998), Soil water content and temperature as independent or confounded factors controlling soil respiration in a temperate mixed hardwood forest, *Global Change Biology*, *4*(2), 217-227.

Davidson, E. A., I. A. Janssens, and Y. Luo (2006), On the variability of respiration in terrestrial ecosystems: moving beyond Q10, *Global Change Biology*, *12*(2), 154-164.

Dinsmore, K. J., U. M. Skiba, M. F. Billett, and R. M. Rees (2009), Effect of water table on greenhouse gas emissions from peatland mesocosms, *Plant and Soil*, *318*(1-2), 229-242.

Drewitt, G. B., T. A. Black, Z. Nesic, E. R. Humphreys, E. M. Jork, R. Swanson, G. J. Ethier, T. Griffis, and K. Morgenstern (2002), Measuring forest floor CO_2 fluxes in a Douglas-fir forest, *Agricultural and Forest Meteorology*, *110*, 299-317.

Falloon, P., C. D. Jones, M. Ades, and K. Paul (2011), Direct soil moisture controls of future global soil carbon changes: An important source of uncertainty, *Global Biogeochemical Cycles*, *25*, GB3010.

Freeman, C., N. Ostle, and K. H. (2001), An enzymic 'latch' on a global carbon store, *Nature*, *409*, 149.

Freeman, C., N. J. Ostle, N. Fenner, and H. Kang (2004), A regulatory role for phenol oxidase during decomposition in peatlands, *Soil Biology & Biochemistry*, *36*, 1663-1667.

Gaumont-Guay, D., T. A. Black, T. J. Griffis, A. G. Barr, R. S. Jassal, and Z. Nesic (2006), Interpreting the dependence of soil respiration on soil temperature and water content in a boreal aspen stand, *Agricultural and Forest Meteorology*, *140*(1–4), 220-235.

Goulden, M. L., et al. (1998), Sensitivity of boreal forest carbon balance to soil thaw, *Science*, *279*(5348), 214-217.

Gower, S. T. (2003), Patterns and mechanisms of the forest carbon cycle, *Annu. Rev. Environ. Resour.*, *28*, 169-204.

Högberg, P. (2010), Is tree root respiration more sensitive than heterotrophic respiration to changes in soil temperature?, *New Phytologist*, *188*, 9-10.

Ise, T., A. L. Dunn, S. C. Wofsy, and P. R. Moorcroft (2008), High sensitivity of peat decomposition to climate change through water-table feedback, *Nature Geoscience*, *1*, 763-766.

Jaatinen, K., H. Fritze, J. Laine, and R. Laiho (2007), Effects of short- and long-term water-level drawdown on the populations and activity of aerobic decomposers in a boreal peatland, *Global Change Biology*, *13*, 491-510.

Janssens, I. A., and K. Pilegaard (2003), Large seasonal changes in Q_{10} of soil respiration in a beech forest, *Global Change Biology*, *9*(6), 911-918.

Jauhiainen, J., H. Takahashi, J. E. P. Heikkinen, P. J. Martikainen, and H. Vasander (2005), Carbon fluxes from a tropical peat swamp forest floor, *Global Change Biology*, *11*, 1788-1797.

Kim, J., and S. B. Verma (1992), Soil surface CO_2 flux in a Minnesota peatland, *Biogeochemistry*, *18*, 37-51.

Kirschbaum, M. U. F. (2006), The temperature dependence of organic-matter decomposition-still a topic of debate, *Soil Biology & Biochemistry*, *38*, 2510-2518.

Kucera, C. L., and D. R. Kirkham (1971), Soil respiration studies in tallgrass prairie in Missouri, *Ecology*, *52*(5), 912-915.

Kuzyakov, Y. (2006), Sources of CO_2 efflux from soil and review of partitioning methods, *Soil Biology & Biochemistry*, *38*, 425-448.

Larcher, W. (2003), *Physiological plant ecology: ecophysiology and stress physiology of functional groups*, Springer-Verlag, Berlin, Germany.

Lellei-Kovács, E., E. Kovács-Láng, Z. Botta-Dukát, T. Kalapos, B. Emmett, and C. Beier

(2011), Thresholds and interactive effects of soil moisture on the temperature response of soil respiration, *European Journal of Soil Biology*, *47*, 247-255.

Liu, Q., N. T. Edwards, W. M. Post, L. Gu, J. Ledford, and S. Lenhart (2006), Temperature-independent diel variation in soil respiration observed from a temperate deciduous forest, *Global Change Biology*, *12*(11), 2136-2145.

Lloyd, J., and J. A. Taylor (1994), On the temperature dependence of soil respiration, *Functional Ecology*, *8*(3), 315-323.

Lugo, A. E., S. Brown, and M. Brinson (1990), *Forested wetlands*, Elsevier, Amsterdam, Netherlands.

Luken, J. O., and W. D. Billings (1985), The influence of microtopographic heterogeneity on carbon dioxide efflux from a subarctic bog, *Holarctic Ecology*, *8*, 306-312.

Luo, Y., and X. Zhou (2006), *Soil respiration and the environment*, 316 pp., Elsevier/Academic Press, Amsterdam.

Maberly, S. C. (1996), Diel, episodic and seasonal changes in pH and concentrations of inorganic carbon in a productive lake, *Freshwater Biology*, *35*, 579-598.

Mäkiranta, P., R. Laiho, H. Fritze, J. Hytönen, J. Laine, and K. Minkkinen (2009), Indirect regulation of heterotrophic peat soil respiration by water level via microbial community structure and temperature sensitivity, *Soil Biology & Biochemistry*, *41*(4), 695-703.

Mitsch, W. J., and J. G. Gosselink (2007), *Wetlands*, John Wiley & Sons, Inc., New York, NY, USA.

Moore, T. R., and M. Dalva (1993), The influence of temperature and water table position on carbon dioxide and methane emissions from laboratory columns of peatland soils, *Journal of Soil Science*, *44*, 651-664.

Moorhead, K. K., and M. M. Brinson (1995), Response of wetlands to rising sea level in the

lower coastal plain of North Carolina, *Ecological Applications, 5*(1), 261-271.

Morén, A.-S., and A. Lindroth (2000), CO_2 exchange at the floor of a boreal forest, *Agricultural and Forest Meteorology, 101*, 1-14.

Motulsky, H., and A. Christopoulos (2004), *Fitting models to biological data using linear and nonlinear regression: a practical guide to curve fitting*, Oxford University Press, New York, NY, USA.

Noormets, A., et al. (2008), Moisture sensitivity of ecosystem respiration: Comparison of 14 forest ecosystems in the Upper Great Lakes Region, USA, *Agricultural and Forest Meteorology, 148*, 216-230.

Pavelka, M., M. Acosta, M. V. Marek, W. Kutsch, and D. Janous (2007), Dependence of the Q_{10} values on the depth of the soil temperature measuring point, *Plant and Soil, 292*(1-2), 171-179.

Phillips, S. C., R. K. Varner, S. Frolking, J. W. Munger, J. L. Bubier, S. C. Wofsy, and P. M. Crill (2010), Interannual, seasonal, and diel variation in soil respiration relative to ecosystem respiration at a wetland to upland slope at Harvard Forest, *Journal of Geophysical Research-Biogeosciences, 115*, G02019.

Reichstein, M., J. D. Tenhunen, O. Roupsard, J.-M. Ourcival, S. Rambal, S. Dore, and R. Valentini (2002), Ecosystem respiration in two Mediterranean evergreen Holm Oak forests: drought effects and decomposition dynamics, *Functional Ecology, 16*, 27-39.

Riveros-Iregui, D. A., R. E. Emanuel, D. J. Muth, B. L. McGlynn, H. E. Epstein, D. L. Welsch, V. J. Pacific, and J. M. Wraith (2007), Diurnal hysteresis between soil CO_2 and soil temperature is controlled by soil water content, *Geophysical Research Letters, 34*, L17404, doi: 10.1029/2007GL030938.

Ruehr, N., A. Knohl, and N. Buchmann (2010), Environmental variables controlling soil respiration on diurnal, seasonal and annual time-scales in a mixed mountain forest in Switzerland, *Biogeochemistry, 98*(1), 153-170.

Sampson, D. A., I. A. Janssens, J. C. Yuste, and R. Ceulemans (2007), Basal rates of soil respiration are correlated with photosynthesis in a mixed temperate forest, *Global Change Biology*, *13*(9), 2008-2017.

Savage, K. E., and E. A. Davidson (2001), Interannual variation of soil respiration in two New England forests, *Global Biogeochemical Cycles*, *15*(2), 337-350.

Savage, K. E., and E. A. Davidson (2003), A comparison of manual and automated systems for soil CO_2 flux measurements: trade-offs between spatial and temporal resolution, *Journal of Experimental Botany*, *54*(384), 891-899.

Silvola, J., J. Alm, U. Ahlholm, H. Nykanen, and P. J. Martikainen (1996), CO_2 fluxes from peat in boreal mires under varying temperature and moisture conditions, *Journal of Ecology*, *84*, 219-228.

Smith, C. J., R. D. Delaune, and J. W. H. Patrick (1983), Carbon dioxide emission and carbon accumulation in coastal wetlands, *Estuarine, Coastal and Shelf Science*, *17*, 21-29.

Subke, J.-A., and M. Bahn (2010), On the 'temperature sensitivity' of soil respiration: Can we use the immeasurable to predict the unknown?, *Soil Biology & Biochemistry*, *42*, 1653-1656.

Tang, J. W., D. D. Baldocchi, and L. Xu (2005a), Tree photosynthesis modulates soil respiration on a diurnal time scale, *Global Change Biology*, *11*(8), 1298-1304.

Tang, J. W., L. Misson, A. Gershenson, W. X. Cheng, and A. H. Goldstein (2005b), Continuous measurements of soil respiration with and without roots in a ponderosa pine plantation in the Sierra Nevada Mountains, *Agricultural and Forest Meteorology*, *132*(3-4), 212-227.

Tjoelker, M. G., J. Oleksyn, and P. B. Reich (2001), Modelling respiration of vegetation: evidence for a general temperature-dependent Q10, *Global Change Biology*, *7*(2), 223-230.

Trettin, C. C., and M. F. Jurgensen (2003), Carbon cycling in wetland forest soils, in *The Potential of U.S. Forest Soils to Sequester Carbon and Mitigate the Greenhouse Effect*,

edited by J. M. Kimble, L. S. Heath, R. A. Birdsey and R. Lal, CRC Press, Boca Raton.

Vargas, R., and M. F. Allen (2008), Environmental controls and the influence of vegetation type, fine roots and rhizomorphs on diel and seasonal variation in soil respiration, *New Phytologist*, *179*(2), 460-471.

Vicca, S., I. A. Janssens, H. Flessa, S. Fiedler, and H. F. Jungkunst (2009), Temperature dependence of greenhouse gas emissions from three hydromorphic soils at different groundwater levels, *Geobiology*, *7*(4), 465-476.

Vincent, G., A. R. Shahriari, E. Lucot, P.-M. Badot, and D. Epron (2006), Spatial and seasonal variations in soil respiration in a temperate deciduous forest with fluctuating water table, *Soil Biology & Biochemistry*, *38*, 2527-2535.

Wang, X., S. Piao, P. Ciais, I. A. Janssens, M. Reichstein, S. Peng, and T. Wang (2010), Are ecological gradients in seasonal Q_{10} of soil respiration explained by climate or by vegetation seasonality?, *Soil Biology & Biochemistry*, *42*, 1728-1734.

Wheeler, B. D. (1999), Water and plants in freshwater wetlands, in *Eco-Hydrology*, edited by A. J. Baird and R. L. Wilby, Routledge, London, UK.

Zhou, X., Y. Luo, C. Gao, P. S. J. Verburg, J. A. I. Arnone, A. Darrouzet-Nardi, and D. S. Schimel (2010), Concurrent and lagged impacts of an anomalously warm year on autotrophic and heterotrophic components of soil respiration: a deconcolution analysis, *New Phytologist*, *187*, 184-198.

Tables and Figures

Table 2-1 Comparison of Q_{10} (mean±SE) estimated from two methods for soil respiration (R_s) with different water table depth (WTD) at HIGH microsite. At each WTD class, it was assumed that soil temperature (T_s) was the primary driver of R_s.

WTD range (cm)	Mean WTD (cm)	Observed T_s range (˚C)	Method (i)*			Method (ii)**		
			R_b	Q_{10}	RMSE	R_b	Q_{10}	RMSE
-45 - -30	-34.5	22.2-25.4	9.12	0.49±0.08	2.99	10.80±0.09	1.51±0.20	2.57
-30 - -25	-27.2	15.1-25.5	8.93	1.96±0.12	2.64	8.33±0.08	1.55±0.10	2.59
-25 - -20	-22.4	15.1-24.8	8.75	2.13±0.07	3.03	8.64±0.10	2.07±0.09	3.03
-20 - -15	-17.7	11.7-25.5	8.49	2.07±0.04	2.61	9.56±0.09	2.54±0.07	2.55
-15 - -10	-12.7	6.7-24.4	8.05	3.82±0.05	1.29	9.76±0.09	4.66±0.07	1.21
-10 - -5	-7.5	3.3-24.1	7.14	5.20±0.16	0.76	8.36±0.04	6.37±0.23	0.65

*: R_b was calculated first with $f_{R_b}(WTD) = \frac{V_{\max} WTD}{K_m + WTD}$, and then Q_{10} was estimated from conventional Q_{10} model: $R_s = R_b Q_{10}^{\frac{T_s - 24}{10}}$. When estimating Q_{10}, R_b was set as constants.

**: Both R_b and Q_{10} were estimated from conventional Q_{10} model.

Table 2-2 Quadratic models for modeling soil CO_2 effluxes (R_s) with soil temperature (T_s) during flooded periods.

	Model	R^2	p-value	Sample size
HIGH	$R_s = -0.48 + 0.16T_s - 0.0047T_s^2$	0.0213	<0.001	1252
MID	$R_s = -0.06 + 0.06T_s - 0.0013T_s^2$	0.1669	<0.001	6090
LOW	$R_s = -1.02 + 0.19T_s - 0.0052T_s^2$	0.0152	<0.001	2858

Table 2-3a Model parameters (mean±SE) of soil respiration under non-flooded conditions from regression with 30-min data.

Model	**unit**	**Microsite**			
Parameters		HIGH	MID	MID-2*	LOW
Conventional Q_{10}					
R_b	μmol CO_2 m^{-2} s^{-1}	10.02 ± 0.05	6.97 ± 0.05		4.94 ± 0.03
Q_{10}		5.14 ± 0.10	11.48 ± 0.55		11.03 ± 0.47
R^2		0.6225	0.5195		0.6243
MSE		7.5435	5.4522		2.0875
AIC		21819	8967		620
Multiplicative					
R_b	μmol CO_2 m^{-2} s^{-1}	7.33 ± 0.06	5.12 ± 0.05		4.49 ± 0.02
Q_{10}		3.09 ± 0.05	4.57 ± 0.18		5.27 ± 0.16
β		-0.0217 ± 0.0004	-0.0447 ± 0.0008		-0.0425 ± 0.0006
R^2		0.7187	0.7452		0.8590
MSE		5.6211	2.8923		0.4500
AIC		18644	5617		-2718
Nested Q_{10}					
V_{max}	μmol CO_2 m^{-2} s^{-1}	13.58 ± 0.13	19.59 ± 0.53	11*	7.63 ± 0.08
K_m	cm	-7.2 ± 0.3	-26.5 ± 1.23	-8.1 ± 0.1	-5.4 ± 0.2
β_1		3.63 ± 0.08	5.27 ± 0.21	6.07 ± 0.23	3.91 ± 0.12
β_2	m^{-1}	0.0533 ± 0.0022	0.1651 ± 0.0060	0.06*	0.0673 ± 0.0058
R^2		0.8219	0.8360	0.7819	0.9135
MSE		3.5597	1.8612	2.4750	0.2761
AIC		13713	3288	4793	-4381
Sample Size		10797	5286		3407

Table 2-3b Model parameters (mean±SE) of soil respiration under non-flooded conditions from regression with daily data.

Model	**unit**	**Microsite**			
Parameters**		HIGH	MID	MID-2*	LOW
Conventional Q_{10}					
R_b	g CO_2-C m^{-2} d^{-1}	10.58 ± 0.38	7.55 ± 0.37		4.77 ± 0.30
Q_{10}		3.65 ± 0.57	12.94 ± 4.31		9.06 ± 3.64
R^2		0.6905	0.6928		0.5918
MSE		4.9281	3.2008		1.0448
AIC		139.14	70.61		3.520
Multiplicative					
R_b	g CO_2-C m^{-2} d^{-1}	8.13 ± 0.53	5.47 ± 0.36		4.82 ± 0.17
Q_{10}		2.57 ± 0.37	4.79 ± 1.27		5.62 ± 1.41
β		-0.0162 ± 0.0032	-0.0389 ± 0.0055		-0.0500 ± 0.0055
R^2		0.7731	0.8633		0.8900
MSE		3.6569	1.4502		0.2900
AIC		114.45	24.85		-41.69
Nested Q_{10}					
V_{max}	g CO_2-C m^{-2} d^{-1}	13.11 ± 0.91	19.97 ± 2.26	11*	8.21 ± 0.68
K_m	cm	-6.1 ± 1.9	-26.4 ± 5.2	-7.4 ± 0.6	-5.9 ± 1.1
β_1		3.64 ± 0.76	5.10 ± 0.79	6.39 ± 1.30	4.33 ± 1.04
β_2	m^{-1}	0.0601 ± 0.0197	0.2007 ± 0.0250	0.065*	0.0690 ± 0.0473
R^2		0.8672	0.9701	0.9099	0.9577
MSE		2.1656	0.3229	0.9384	0.1151
AIC		70.36	-62.83	-1.79	-74.09
Sample Size		86	59		36

*: In nested Q_{10} model, the values of V_{max} and β_2 were manually set.

**: See the meaning of each parameter at Equations 1, 5 and 6.

Table 2-4 Estimates of total annual soil carbon emission (mean and 95% confidence interval, g CO_2-C m^{-2}) from a lower coastal plain forested wetland in North Carolina in 2009 and 2010.

Estimated carbon emission ($g\ m^{-2}$)	2009 Jul.-Dec.			2010 Jan.-Jun.			2010 Jul.-Dec.			2010 Total		
	HIGH	MID	LOW	HIGH	MID	LOW	HIGH	MID	LOW	HIGH	MID	LOW
Non-flooded												
Percentage of days (%)	50.8	0	0	77.4	37.6	26.8	84.8	27.8	25.1	81.1	21.7	17.2
Gap-filled mean	308	0	0	579	187	106	704	326	204	1283	513	311
95% CI-Lower	303	0	0	578	186	106	701	326	203	1279	512	309
95% CI-Upper	314	0	0	581	187	107	706	326	205	1287	513	312
Flooded												
Percentage of days (%)	49.2	100	100	22.6	62.4	73.2	15.2	72.2	74.9	18.9	78.3	82.8
Gap-filled mean	65	102	109	19	39	47	23	68	72	42	108	119
95% CI-Lower	31	37	32	4	15	8	9	29	2	12	43	10
95% CI-Upper	102	172	246	40	83	175	38	113	207	77	196	382
Total												
Mean	374	102	109	598	226	154	727	394	276	1325	621	430
95% CI-Lower	333	37	32	582	201	114	710	355	205	1291	555	319
95% CI-Upper	416	172	246	620	270	282	744	440	412	1365	710	694

Table 2-5 Comparison of carbon emission predictions (mean and 95% confidence interval, g CO_2-C m^{-2}) in a lower coastal plain forested wetland in North Carolina during non-flooded periods in 2009 and 2010.

Models	2009 Jul.-Dec.	2010 Jan.-Jun.			2010 Jul.-Dec.			2010 Total		
	HIGH	HIGH	MID	LOW	HIGH	MID	LOW	HIGH	MID	LOW
Percentage of data in the whole dataset (%)	13.0	40.9	57.1	55.3	46.1	42.9	44.7	87.0	100	100
Conventional Q_{10}										
Mean	651	460	202	115	832	331	185	1292	533	300
95% CI-Lower	644	451	196	112	821	326	182	1272	522	294
95% CI-Upper	659	469	208	119	843	336	188	1312	543	306
Multiplicative										
Mean	468	525	205	118	825	328	215	1350	532	333
95% CI-Lower	460	517	200	116	813	323	212	1330	523	329
95% CI-Upper	477	534	209	120	836	332	217	1371	542	337
Nested										
Mean	317	541	192	106	739	320	200	1279	513	307
95% CI-Lower	310	533	189	105	729	317	198	1262	506	303
95% CI-Upper	325	549	196	108	749	324	202	1297	520	310
Deviation from the nested model results										
Conventional Q_{10}	105.4%	-15.0%	5.2%	8.5%	12.6%	3.4%	-7.5%	1.0%	3.9%	-2.3%
Multiplicative	47.6%	-3.0%	6.8%	11.3%	11.6%	2.5%	7.5%	5.6%	3.7%	8.5%

Table 2-6 Contribution of dynamic R_b and Q_{10} to model performance by adding the water table depth effect into the conventional Q_{10} model separately (R_b-dynamic-only (A) versus Q_{10}-dynamic-only (B)) and in different order (A→the nested model versus B→ the nested model).

	R^2	R^2	Increase in R^2		Increase in R^2	
	A*	B**	Q_{10}→A	A→nested	Q_{10}→B	B→nested
HIGH	0.8083	0.7642	18.6%	1.4%	14.2%	5.8%
MID	0.8099	0.6101	29.0%	2.6%	9.1%	22.6%
LOW	0.9103	0.7401	28.6%	0.3%	11.6%	17.3%

* A: the R_b-dynamic-only model, $R_s = \frac{V_{\max} WTD}{K_m + WTD} Q_{10}^{\frac{T_s - 24}{10}}$

** B: the Q_{10}-dynamic-only model, $R_s = R_b \left\{ \beta_1 \exp\left[\beta_2 \left(WTD + 10 \right) \right] \right\}^{\frac{T_s - 24}{10}}$

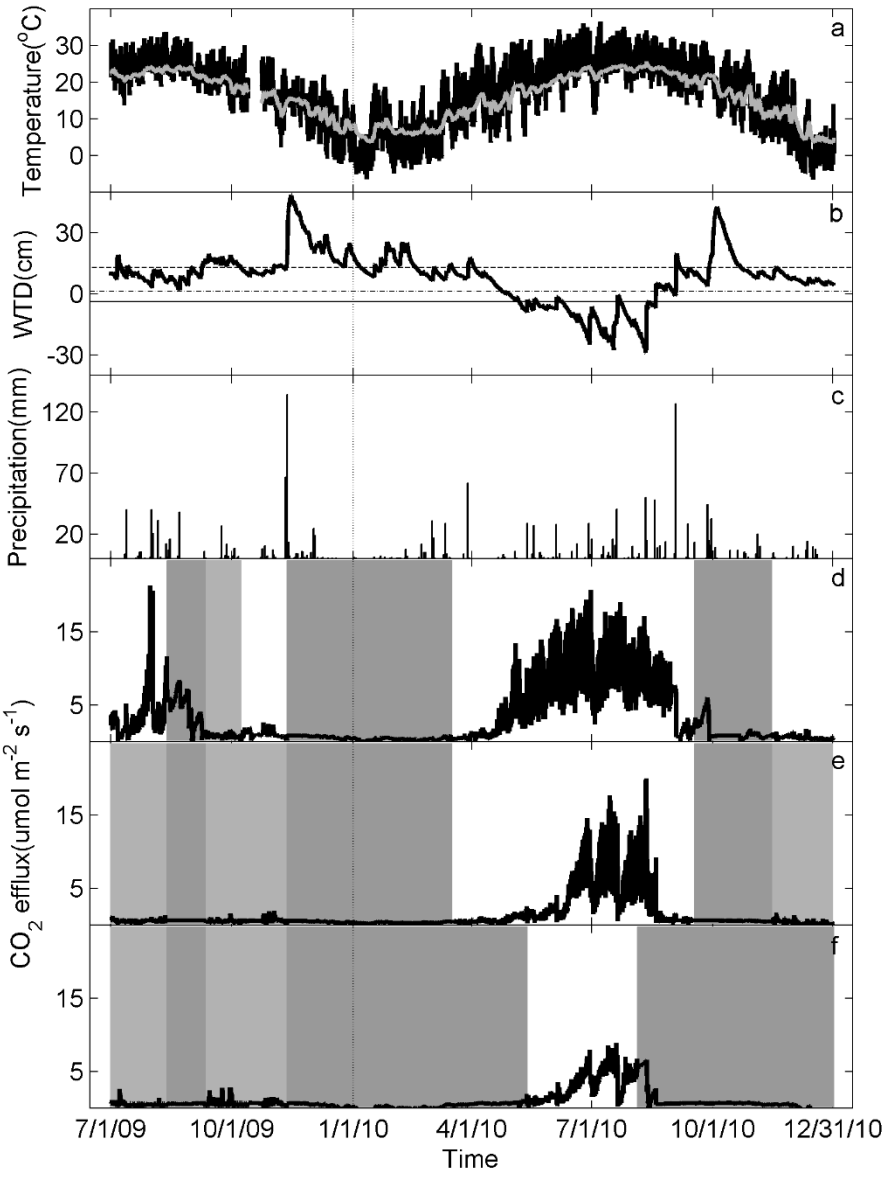

Figure 2-1 Seasonal variations observed in a lower coastal plain forested wetland in North Carolina, USA, during the period 7/1/2009-12/31/2010 in (a) Air temperature (grey line) and soil temperature at 5 cm depth (T_s, black line), (b) Water table depth (WTD) at three microsites of varying elevation (HIGH: dashed line; MID: dash dot line; LOW: solid line), (c) Precipitation, and (d, e, f) CO_2 efflux (R_s) at HIGH, MID and LOW microsites, respectively (Non-flooded records: white area; Flooded records: light grey area; No measurements: dark grey area, filled with model results).

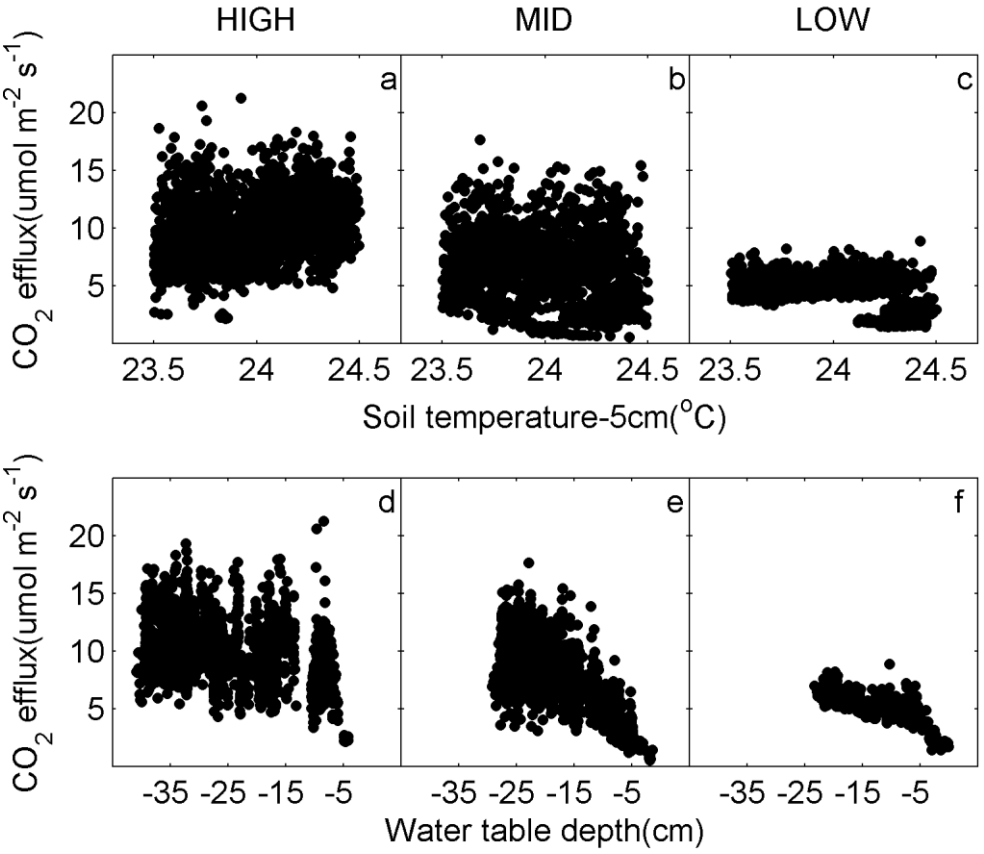

Figure 2-2 Relationship between basal respiration (R_b) and soil temperature (T_s) at 5 cm depth (a-c), between R_b and water table depth (d-f) at HIGH (a, d), MID (b, e), and LOW (c, f) microsites. R_b in this study was defined as respiration rate at 24˚C. R_s data during non-flooded periods with the range of T_s constrained to within ±0.5˚C, i.e. 23.5-24.5˚C was separated out as R_b data.

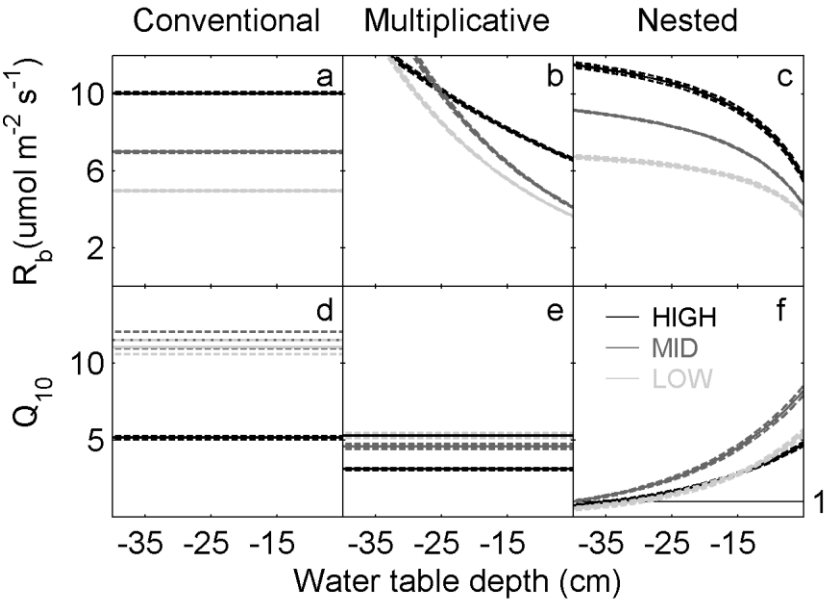

Figure 2-3 Comparison of water table depth (WTD)-R_b (a-c) and WTD-Q_{10} (d-f) relationships simulated by the three models: the conventional Q_{10} model (a,d); multiplicative model (b,e); the nested model (c,f). Solid line is mean value and dashed line is standard error of the parameters.

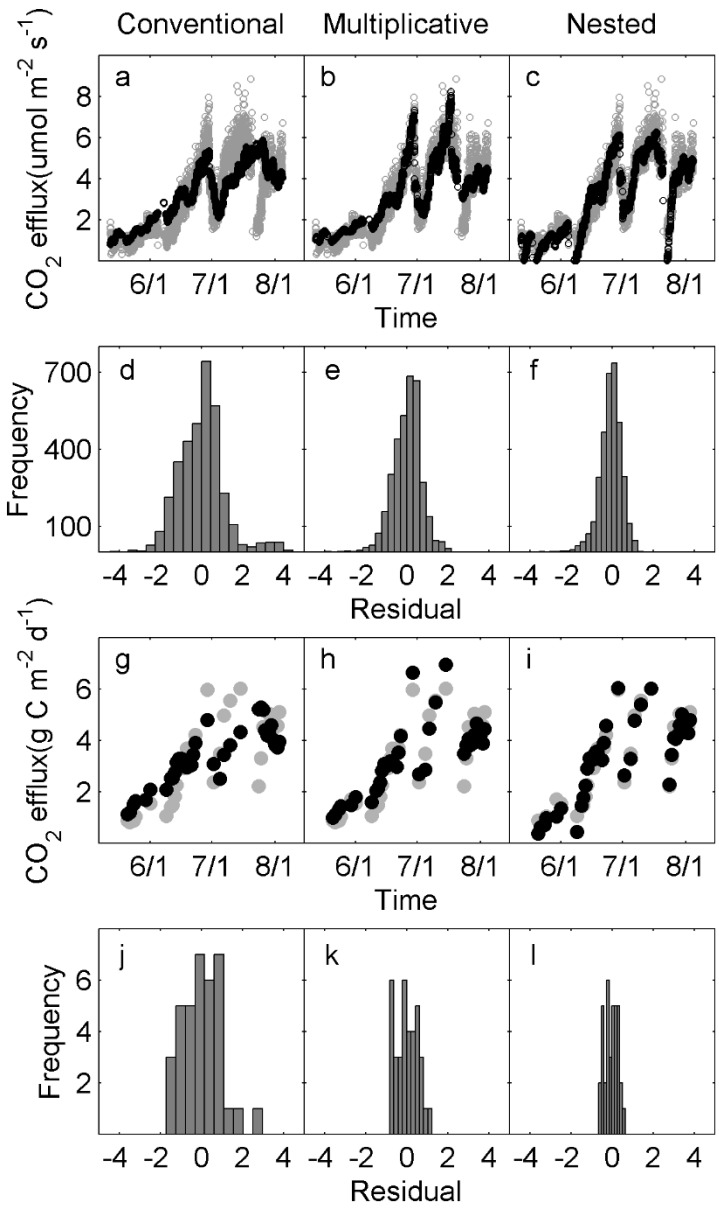

Figure 2-4 Comparison of modeled (black dots) and measured (grey dots) soil respiration between the models using 30-min dataset (a-c: time series; d-f: residual distribution) and daily dataset (g-i: time series; j-l: residual distribution) from LOW microsite. Models include: the conventional Q_{10} model (a,d,g,j), multiplicative model (b,e,h,k) and the nested model (c,f,i,l).

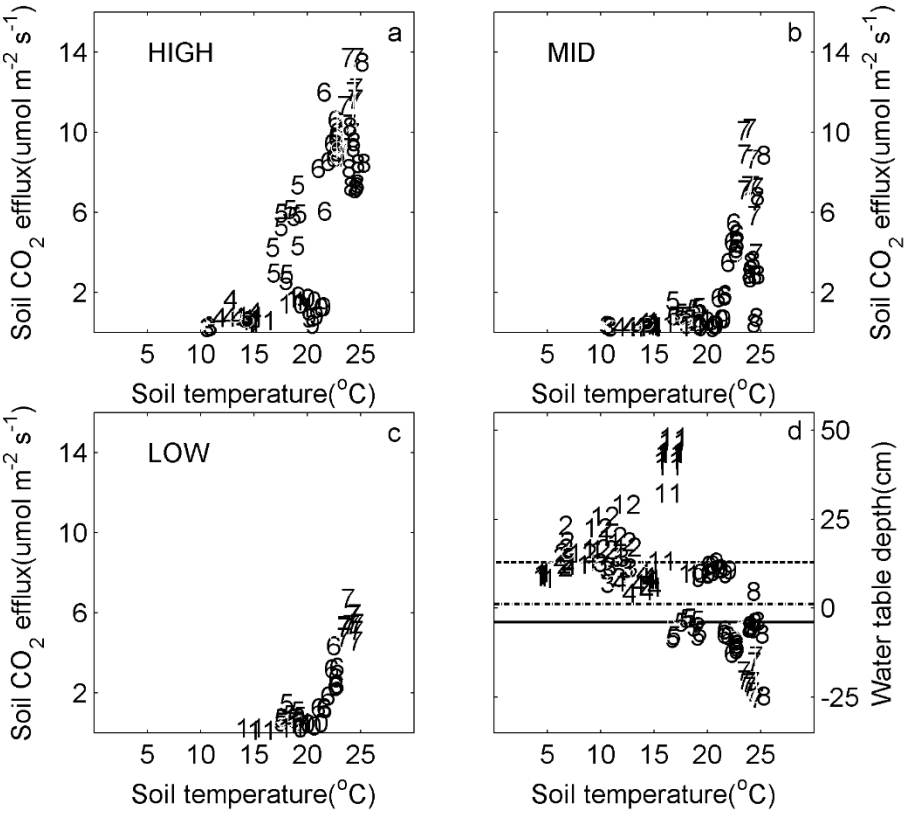

Figure 2-5 Relationship between soil CO_2 effluxes and drivers observed at HIGH, MID and LOW microsites during 10/1/2009-9/30/2010. Numbers in the figure represent month. (a) Seasonal pattern of interaction between soil temperature and water table depth. Lines represent the elevation of three microsites relative to water table probe location. (b) Soil CO_2 efflux at HIGH microsite exhibited a clear seasonal hysteresis: higher rate during spring/summer because of non-flooded condition versus lower rate during autumn under flooded condition. (c) and (d) Soil CO_2 efflux at MID and LOW microsites did not show the same seasonal pattern as HIGH microsite, because the two low-lying sites were flooded during both spring and autumn.

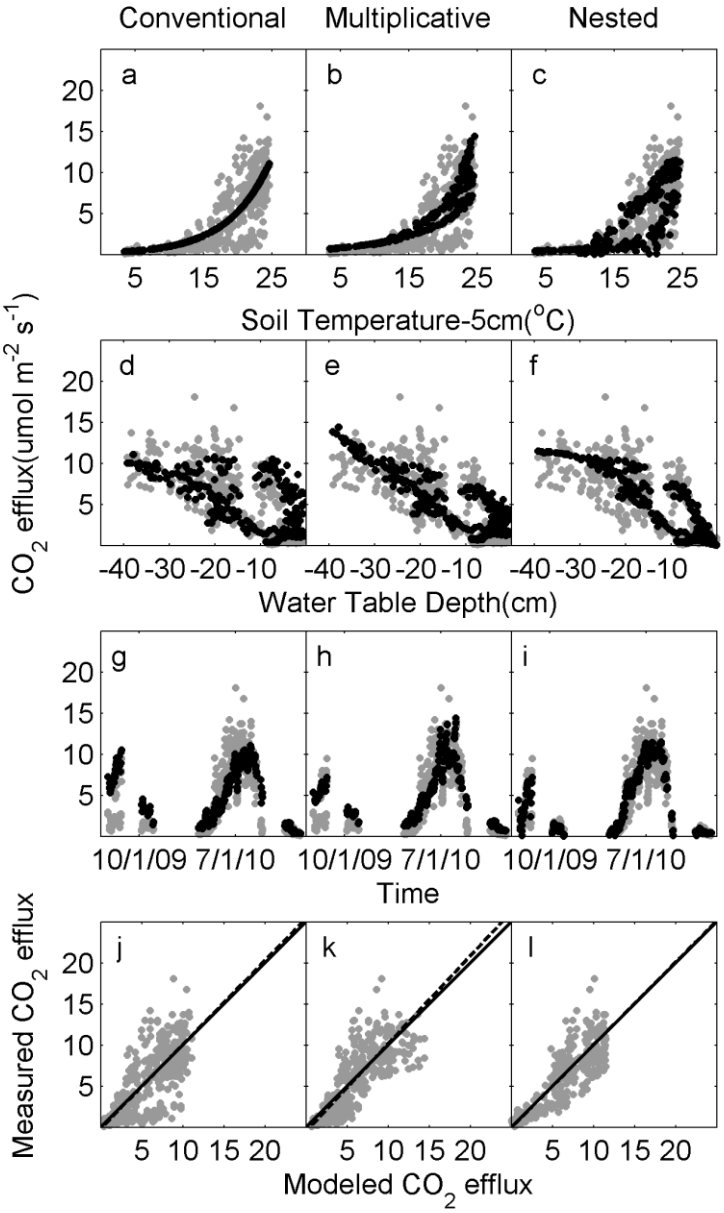

Figure 2-6 Comparison of modeled (black dots) and measured (grey dots) driver effects on soil respiration (R_s) at HIGH microsite by the conventional Q_{10} model (a,d,g,i), the multiplicative model (b,e,h,k) and the nested model (c,f,i,l). Only part of data was shown. a-c: Soil temperature effect on R_s; d-f: Water table depth effect on R_s; h-i: R_s time series; j-l: modeled R_s versus measured R_s with solid 1:1 line and dotted regression line.

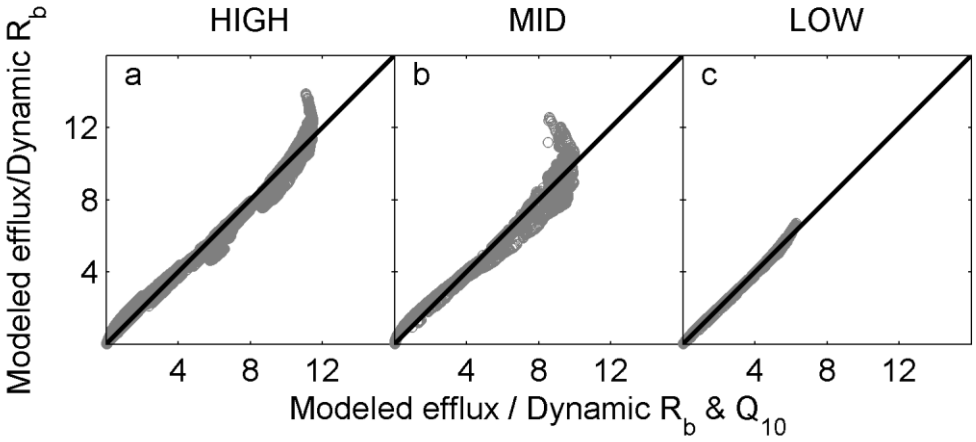

Figure 2-7 Comparison of modeled effluxes (μmol CO_2 m^{-2} s^{-1}) between R_b-dynamic-only model (see Table 6; y-axis) and the R_b-Q_{10}-both-dynamic model (i.e. the nested model; x-axis). The performance of the two models differed significantly at the higher efflux levels, indicating that the overall contribution of Q_{10} to improving model performance was smaller than that of R_b, but influenced the simulation at the higher level of soil respiration range.

CHAPTER 3. PARTITIONING ECOSYSTEM RESPIRATION IN A COASTAL PLAIN FORESTED WETLAND IN THE SOUTHEASTERN USA: CONTRASTING TEMPERATURE AND HYDROLOGIC SENSITIVITY AND INFLUENCES ON ECOSYSTEM RESPIRATION

Abstract

Carbon cycling in wetlands, especially soil dynamics, is an important component of carbon budgets in terrestrial ecosystems. Environmental change and land conversion for agricultural use have been affecting wetlands in recent decades and might change their role from carbon sinks to sources. However, carbon dynamics in wetlands are less-well investigated than in upland systems and still absent in regional- or global-scale studies. We established an eddy covariance flux tower in a coastal plain forested wetland in North Carolina, USA, and conducted measurements on ecosystem respiration (R_e), soil respiration (R_s) and decomposition of coarse wood debris (R_{CWD}) from 2009 to 2011. R_e and R_s were separately quantified for flooded and non-flooded periods considering the different mechanisms, and R_{CWD} was separated by decay class. R_s responded rapidly to water table fluctuation whereas the R_e responded slowly due to buffering from flood-tolerant plants in the ecosystem. R_s contributed most to R_e during non-flooded periods but much less during flooded periods with the R_s:R_e ratio of 0.67±0.11 (mean±SD) and 0.24±0.06, respectively. Aboveground plant respiration (R_p) may have been the main contributor to R_e during flooded periods. The contribution from R_{CWD} was relatively small but with great uncertainty related to the CWD biomass estimate. Seasonal variation of the R_s:R_e ratio exhibited a linear relationship with the water table fluctuation. Overall, this forested wetland released more than 1000 g CO_2-C m^{-2} y^{-1} annually, comparable to many upland forests. The temperature sensitivity of respiratory components under non-flooded conditions was also similar to upland forests. However, the hydrologic regimes resulted in unique characteristics of carbon dynamics in this forested

wetland, transiting between R_s:R_e ratio similar to boreal and temperate upland forests under non-flooded conditions and one similar to some tropical rainforests when flooded.

Abbreviations

Ecosystem respiration	R_e
Ecosystem respiration during flooded periods	$R_{e\text{-}FL}$
Ecosystem respiration during non-flooded periods	$R_{e\text{-}NFL}$
Soil respiration	R_s
Soil respiration during flooded periods	$R_{s\text{-}FL}$
Soil respiration during non-flooded periods	$R_{s\text{-}NFL}$
Coarse woody debris	CWD
Decomposition of coarse woody debris	R_{CWD}
Aboveground live plant respiration	R_p
Soil temperature	T_s
Water table depth	WTD

1. Introduction

Carbon cycling in wetlands, especially soil dynamics, is an important component of carbon budgets in terrestrial ecosystems [*Chmura et al.*, 2003; *Gorham*, 1991]. Early studies estimated that the mean residence time of soil organic carbon in wetlands is about 500 years, much greater than a mean residence time of about 32 years for the global pool of soil organic carbon [*Raich and Schlesinger*, 1992]. The long residence time results from the low decomposition rate under the permanently or intermittently flooded conditions, which is also the main reason that wetlands are generally viewed as carbon sinks [*Bridgham et al.*, 2006; *Mitsch et al.*, 2013]. Recently, awareness is growing that changes in climate and land use may be altering wetland carbon source-sink relationships. Sea level rise, high-energy waves and flooding associated with extreme storm events accelerates wetland soil erosion, threatening these globally important stores of carbon [*Webb et al.*, 2013]. Further, the conversion of wetlands to agriculture and other land uses through drainage could also turn existing wetlands from carbon sinks to sources by aerating the large quantities of labile carbon stored in previously saturated soils [*Armentano*, 1980; *Armentano and Menges*, 1986; *Laiho*, 2006]. Unfortunately, the sensitivity of carbon dynamics in wetlands to environmental changes are much less well investigated than in uplands, which limits our ability to quantify their future role in the global carbon cycle. Due to the data scarcity, wetlands are still absent in most regional- or global-scale studies [*Battin et al.*, 2009; *Davidson*, 2010; *Luyssaert et al.*, 2007; *Mahecha et al.*, 2010].

Respiration is a key determinant affecting the role of an ecosystem as carbon source or

sink [*Valentini et al.*, 2000]. At the ecosystem scale, it integrates a variety of plant and microbial processes, and every component may exhibit different sensitivities to changes in environmental conditions [*Trumbore*, 2006]. Therefore, partitioning ecosystem respiration (R_e) and quantifying driver sensitivities for each component are crucial for predicting the long-term response of terrestrial ecosystems to climate change. Because of differences in carbon allocation and driver sensitivities, component processes may contribute to R_e differently depending on ecosystem type [*Aerts*, 1997; *Davidson et al.*, 2006; *Harmon et al.*, 2004]. For example, decomposition of coarse woody debris (CWD, R_{CWD}) in some loblolly pine plantations in the Southeast U.S. was reported to be approximately 20% of total ecosystem respiration [*Noormets et al.*, 2012], whereas in a central Amazon forest it was predicted to be only 6% [*Chambers et al.*, 2004].

Soil respiration has been the most widely investigated among R_e components due to its large magnitude and sensitivity to a variety of controlling factors [*Davidson and Janssens*, 2006; *Kirschbaum*, 2010]. Its contribution to R_e, i.e. the ratio of R_s to R_e, could be potentially used as an indicator to characterize carbon sequestration and ecosystem type. Boreal and temperate upland ecosystems generally store large amounts of carbon in both plants and soils, of which the R_s contributes to R_e comparably to plant respiration, with the ratio reported at 0.4-0.8 [*Janssens et al.*, 2001; *Lavigne et al.*, 1997; *Law et al.*, 1999]. Tropical rainforests have much higher carbon storage in plants and low in soils compared to higher latitude forests, resulting lower contribution of R_s to R_e with a ratio of 0.3-0.4 [*Chambers et al.*, 2004; *Saleska et al.*, 2003]. In contrast, wetlands have much larger amounts of carbon stored in

soils than in plants, and permanently or intermittently flooded conditions change the driver sensitivity of both R_s and plant respiration. As a result, the ratio could be different from other types of terrestrial ecosystems, but has not specifically investigated in previous wetland studies. In addition, the seasonal variation of the ratio and its driver sensitivity are receiving more attention and may provide useful information for constraining carbon cycle modeling [*Davidson et al.*, 2006].

Eddy covariance (EC) methodology has been deployed worldwide to measure the CO_2 exchange of terrestrial ecosystems and estimate R_e [*Baldocchi*, 2003]. Within the global FLUXNET network, 25 of the 547 sites are located in wetlands (as determined by searching the words 'wetland, peatland, mire, bog, fen, and marsh' and by IGBP-Land-Use defined 'permanent wetlands'; information updated to Oct. 2011). 8 of the 25 sites are classified as forested wetlands, 5 are shrub land, 4 are woody savanna and rest are grassland, cropland or barren. In 2008, we established an EC flux tower in a forested wetland in the lower coastal plain of North Carolina, USA, and started continuous measurements from 2009 to 2011. We also conducted measurements on R_s and R_{CWD} across the study area for partitioning R_e. In this paper, we report data on R_e, R_s and R_{CWD}, and present a comprehensive partitioning of these respiratory processes in this forested wetland through (1) characterizing the seasonal variation of R_e, R_s and R_{CWD}; (2) contrasting the temperature and hydrologic sensitivities of each component; (3) characterizing the seasonal pattern of R_s:R_e ratio. We hypothesized that the R_s:R_e ratio in wetlands would exhibit different patterns from other ecosystems and be significantly affected by hydrologic factors. By comparing our results with previous studies

in upland ecosystems, we attempted to disclose some special characteristics of this forested wetland and proposed several mechanistic hypothesis for future studies.

2. Methods

2.1 Site description

The study site is located at the Alligator River National Wildlife Refuge (ARNWR), on the Albemarle-Pamlico peninsula of North Carolina, USA ($35^0$47′N, $75^0$54′W). The mean annual temperature and precipitation, from climate records of an adjacent meteorological station (Manteo AP, NC, $35^0$55′N, $75^0$42′W) for the period 1981-2010, are 16.9°C and 1270 mm, respectively. The forest type is mixed hardwood swamp forest; the overstory is predominantly composed of black gum (*Nyssa sylvatica*), swamp tupelo (*Nyssa biflora*) and bald cypress (*Taxodium distichum*), with occasional red maple (*Acer rubrum*) and white cedar (*Chamaecyparis thyoides*); the understory is predominantly fetterbush (*Lyonic lucida*), bitter gallberry (*Ilex galbra*), and red bay (*Persea borbonia*). The canopy height ranges at 15-20 m, the leaf area index peaks at 3.5±0.3; and aboveground live biomass was estimated allometrically at 37.5±12.5 Mg C ha^{-1}. Major soil series are poorly drained Pungo and Belhaven mucks. The average carbon content of soil profile (50 cm deep) ranges from 60-120 Mg C ha^{-1}. The study site was established in November 2008, including the 35-meter instrumented tower for EC measurements, micrometeorological station, and 13 vegetation plots spread over a 4 km^2 area (Figure 3-1).

2.2 Micrometeorological measurements

A micrometeorological station was established at the center of the study area in November

2008. The measurements included air temperature (T_a) and relative humidity (RH, HMP45AC, Vaisala, Finland), and photosynthetically active radiation (PAR, PARLITE, Kipp & Zonen, Delft, Netherlands (KZ)), soil temperature (T_s) at 5 and 20 cm (CS 107, Campbell Scientific Inc., UT, USA (CSI)), volumetric soil water content (CS 616, CSI), soil surface heat flux (HFP01, KZ), and water table depth (WTD, Infinities, Orange, FL). Parameters measured above the canopy (at 30 m) included T_a and RH (HMP45, Vaisala), PAR (PARLITE), net radiation (R_n, NRLITE, KZ), and precipitation (P, TE525, Texas Instruments). Water table depth was also monitored at the central 5 of 13 vegetation survey plots (WL 16, Global Water Instrumentation, TX).

The meteorological data from the adjacent meteorological station (Manteo AP, NC) was also analyzed through the observation period (2009-2011), and the monthly patterns in the three years were compared with the 30-year (1981-2010) normals to characterize the local climatic variation in recent decades.

2.3 Microtopography measurements

There is a distinct difference at the site in local hydrologic conditions between different microtopographic positions – mounds around tree bases are mostly above water table, and non-vegetated low-lying sites are submerged for more than 70% of a year. As these positions may have contrasting vegetation distribution, which is likely to have a direct influence on carbon cycling, we quantified the frequency distribution of different positions in the landscape. Three 30-m transects originating from the center of the plots towards 0°, 120° and 240° from due north were established in the 5 central vegetation survey plots (Figure 3-1). A

tripod-mounted laser level (RoboLaser Green RT-7210-1G, RoboToolz Inc., CA, USA) provided a horizontal reference line from which the distance to ground was measured every 40 cm along each transect. The elevation of different plots was normalized in relation to water table during a high water stage when over 90% of the study area was submerged.

The distribution of height-normalized elevation data across the 5 central plots approximated a gamma distribution (Figure 3-2). The mean value of this gamma distribution was calculated as the site average elevation, i.e. 8.7 cm relative to the water table probe location at the micrometeorological station. We then adjusted the WTDs to site average values and applied them to modeling R_e and site average R_s. The site average microtopography was also used to separate data into flooded and non-flooded cases (i.e. when the WTD at the central water table probe exceeded 8.7 cm, the site was defined as flooded).

2.4 Automated and survey soil CO_2 efflux measurements

Soil CO_2 efflux was measured with both automated and manual survey systems. The automated system was deployed next to the micrometeorological station in the center of the study area, and handheld survey measurements were made in the 5 central plots (Figure 3-1). The automated system, consisting of a portable infrared gas analyzer (IRGA, LI-8100, Licor Inc.), multiplexer (LI-8150, Licor Inc.), and permanently installed 20 cm diameter PVC collars, monitored three micro-topographic locations with elevations relative to the water table probe of +12.9, +1.2 and -3.8 cm (named as HIGH, MID and LOW, the elevations shown as solid lines in Figure 3-2) from summer 2009 to 2010. Further details of the

automated R_s measurements were described earlier [*Miao et al.*, in review].

The survey R_s system consisted of LI-8100 and a portable survey chamber (LI 8100-103, Licor Inc.). The survey measurements were conducted from early spring of 2010 to summer 2011. At each plot, six microsites were positioned in a 7 m diameter circle and installed with 20 cm diameter PVC collars. The collars were moved in early 2011 to minimize the artificial disturbance on soil. Thus 60 microsites in total were involved in survey measurements. Soil temperature at 5 and 10 cm depth and volumetric water content at top 12 cm were recorded at each measurement.

Elevation of each survey microsite was also measured relative to the local water table well. The WTD of each microsite at each measurement date was estimated based on their elevations and the WTD readings from respective plot probes. All the survey microsites were also classified into three groups which corresponded to the HIGH, MID and LOW microsites in the automated measurements. The cutoff points (the dashed lines 'L' and 'H' in Figure 3-2) were derived from the gamma microtopographic distribution and the assumption that R_s is linearly related to the microtopography. The elevation of the two cutoff points was -1 and 5 cm.

2.5 Coarse woody debris CO_2 efflux measurements

Coarse woody debris CO_2 efflux was measured on four downed trees on each of the 5 central survey plots during the same periods as survey R_s measurements. Some collars were replaced in early 2011 due to damage by severe flooding and animals. In all, 22 CWD sections were sampled, with 3, 6, 10 and 3 pieces in decay classes 1, 2, 3 and 4, respectively. The decay

classes were defined according to Harmon et al. [2004]. CWD CO_2 effluxes were measured with an EGM-4 environmental CO_2 monitor and SRC-1 closed system chambers (PP Systems International Inc., MA, USA) concurrently with the survey R_S measurements. The temperature of the woody substrate at 5 cm depth was recorded at each measurement. Moisture was assessed qualitatively by the appearance of the substrate as submerged, saturated, moist, dry or very dry. Most of the CWDs were elevated above the surface and out of direct flooding. As CWD moisture was inversely correlated with temperature and assessed only in qualitative terms, it was not considered as an explicit driver when modeling the CO_2 efflux. Coarse woody debris biomass was measured at the end of 2010 and 2011 for scaling up R_{CWD}. The respective total CWD biomass was 163±104 and 306±204 g C m^{-2} in 2010 and 2011.

2.6 Eddy covariance flux measurements

The EC flux system started from March 2009 and ran through the end of 2011. The net ecosystem CO_2 exchange (NEE) between forest canopy and atmosphere was calculated as the sum of turbulent exchange (measured using EC) and storage flux (measured with a 5-level CO_2 profile system). The instruments, mounted at 30 m, were about 16.7 m above the displacement height. The EC flux system consisted of LI-7500 open-path infrared gas analyzer (Licor Inc.), CSAT3 3-dimensional sonic anemometer (CSI), and CR1000 data logger (CSI). The 30-minute mean fluxes of CO_2 were computed as the covariance of vertical wind speed and the concentration of CO_2, using the EC_PROCESSOR software package (http://www4.ncsu.edu/~anoorme/ECP) [*Noormets et al.*, 2010]. The CO_2 profile system

consisted of a LI-820 infrared gas analyzer and a multiport system. CO_2 concentrations at each level were recorded as 30-second averages every 5 minutes [*Yang et al.*, 2007].

Nighttime NEE was assumed to represent R_e, and used for developing R_e models (see section 2.9). The data were first screened for low wind speed by applying the friction velocity threshold filter of 0.25 m/s when air temperature was lower than 20°C and 0.27 m/s when air temperature was higher than 20°C. Approximately 40-45% of nighttime data were excluded. After further data reductions due to atmospheric stability, power problems and extreme weather, the final percentage of nighttime NEE data of good quality were 18.0%, 18.8%, and 15.8% in 2009, 2010, and 2011, respectively. Despite the low percentage, the range of driver data covered by the good quality data was still representative for different seasons (Figure 3-3 a-d).

2.7 Upscaling of soil respiration

The automated and survey R_s data were used together to constrain the estimate of site average R_s because of their different representation of temporal and spatial variations. Automated R_s from the three microtopographic locations was gap filled first and then integrated [*Miao et al.*, in review]. The site average R_s was derived based on the areal representativeness (A_i) of each microsite given the frequency distribution of ground elevation.

$$R_s = \sum_{i=LOW,MID,HIGH} A_i R_{s,i} \quad (1)$$

where i is the index for individual microtopographic locations. The A_i was 60%, 23% and 17% for the HIGH, MID and LOW microsites, respectively.

To upscale from survey measurements, a response model of R_s to T_s and WTD was developed. We assumed that the microtopography information was contained in the spatial variation of survey measurements and the T_s-R_s and WTD-R_s relationship reflected in the survey data represented the response at the ecosystem scale. Therefore the survey R_s was used as a whole without microtopographic classification and only separated to flooded ($R_{s\text{-}FL}$) and non-flooded ($R_{s\text{-}NFL}$) cases for deriving respective response models. The nested Q_{10} model (model D in Table 3-1) developed in a previous study was adopted for $R_{s\text{-}NFL}$ [*Miao et al.*, in review]; and a simple quadratic equation (Equation 2, R^2=0.31, p<0.001) was used for $R_{s\text{-}FL}$ which we assumed was controlled by physical diffusion [*Miao et al.*, in review]. The site average R_s was then estimated with the models and daily site average T_s and WTD.

$$R_{s-FL} = 0.0032T_s^2 - 0.040T_s + 0.39 \quad (2)$$

The temperature and hydrologic sensitivity of site average R_s was also calculated from both automated and survey measurements. For automated measurements, the raw measurements of $R_{s,i}$ (without gap-filling) were used and also integrated with Equation 1. The integrated R_s was subsequently regressed with the nested Q_{10} model to obtain the T_s and WTD sensitivity of R_s. Because the available data at each microsite was not synchronous, combination of raw data resulted in the narrower coverage of site average R_s, and the derived parameters were limited at certain conditions (Figure 3-3 e-f). In contrast, the data coverage from survey measurements was better (Figure 3-3 g-h), from which we assumed the driver sensitivity from survey measurements would better represent site average R_s.

2.8 Upscaling coarse woody debris respiration

Annual site R_{CWD} was estimated as reported previously [*Noormets et al.*, 2012]. The temperature response of R_{CWD} was evaluated separately for each decay class based on chamber measurements, except for classes 1 and 2, which were combined because of similar efflux rates. R_{CWD} was scaled up based on Q_{10} function (model A in Table 3-1) with continuous daily CWD temperature, which was estimated based on the observed relationship between CWD CO_2 efflux measurements and soil temperature at the micrometeorological station. Site average R_{CWD} per unit ground area was estimated as the product of areal coverage of CWD ($A_{CWD,i}$) and upscaled R_{CWD} for each class ($R_{CWD,i}$). The $A_{CWD,i}$ was the ratio of CWD projected area to plot area and positively related with the CWD biomass.

$$R_{CWD} = \sum_{i=2}^{4} A_{CWD,i} R_{CWD,i} \quad (3)$$

2.9 Data gap filling for ecosystem respiration

To fill the data gaps in R_e, models were developed based on T_s and WTD, separately for flooded ($R_{e\text{-}FL}$) and non-flooded ($R_{e\text{-}NFL}$) cases. To allow comparison of driver effects on R_e with those on R_s, T_s was used instead of T_a. Different from $R_{s\text{-}FL}$, $R_{e\text{-}FL}$ contains the aboveground live plant respiration (R_p) which is still active under flooded conditions. We therefore evaluated the T_s and WTD effects on $R_{e\text{-}FL}$ with the same framework as on $R_{e\text{-}NFL}$, but used the reciprocal of WTD (i.e. 1/WTD) because the $R_{e\text{-}FL}$ responded negatively to the increase of WTD.

The conceptual framework was previously described [*Miao et al.* in review]. In short, the

main steps included: (i) defining base temperature (T_b) with the broadest range of WTD; (ii) evaluating WTD-dependence of R_e at T_b, and determining whether base respiration (R_b) is dynamic or constant; (iii) evaluating temperature sensitivity (Q_{10}) in WTD bins, and determining Q_{10} dynamic or constant; and (iv) combining R_b and Q_{10} to form the full model. There are 4 possible combinations with dynamic or constant R_b and Q_{10}, corresponding to 4 models, i.e. conventional Q_{10} model, R_b-dynamic-only model, Q_{10}-dynamic model and nested Q_{10} model (Table 3-1). The data collected in 2009 and 2010 were used for regression analysis and the data of 2011 for validation. To evaluate model performance, both the coefficient of determination (R^2) and Akaike's information criterion (AIC) were evaluated to assess the explanatory power of model parameters [*Miao et al.* in review]. Due to year-to-year differences in data coverage, the performance of the same model differed in regression performance and validation. The full model was chosen by optimizing model performance.

2.10 Component comparison and partitioning

Overall, we classified 7 respiratory components in this study: $R_{s\text{-}NFL}$, $R_{s\text{-}FL}$, $R_{e\text{-}NFL}$, $R_{e\text{-}FL}$ and R_{CWD} with 3 decay classes. Modeled parameters were compared to elucidate differences in temperature and hydrologic sensitivities between respiratory components. The comparison of seasonal variation of components and partitioning of R_e was mainly based on the data in 2010 when the records for all the components were relatively complete. The 30-min gap-filled automated data (R_e and R_s) were used to calculate daily and monthly variation. The survey data in daily scale were also transformed to monthly scale. Respiration partitioning were performed at both daily and monthly scales.

It has been suggested that the deviation of the total flux estimate is usually less in spite of the divergence between individual model results and measurements [*Desai et al.*, 2008; *Janssens et al.*, 2003]. We therefore analyzed the prediction of total carbon emissions for 2009 and 2011 by the respective models and compared them with the results of 2010 for preliminary quantification of inter-annual variation.

3. Results

3.1 Local climate and hydrologic regimes

The hydroperiod, which is the seasonal pattern of WTD in a wetland, is distinct in this forested wetland and varies with inter-annual variation in precipitation (Figure 3-4 b-c). WTD in this wetland generally started significant decreasing from the end of spring through summer, and then rapidly increased after autumn storms. The percentage of flooded and non-flooded ground area changed correspondingly (Figure 3-4 d). During the 3-year study period, 2009 was a relatively wet year while 2010 and 2011 were dry years. The WTD was shallower during summer of 2009 with an adjusted site average WTD = -3 cm (negative values mean water table was below soil surface), compared to 2010 and 2011 (WTD = -20 cm in both years). The amount of time with more than half of the area not flooded was 42%, 51% and 81% in 2009 (starting from 3/19), 2010 and 2011, respectively, illustrating that 2011 was by far the driest of the three years.

Data from the adjacent station indicated that the temperature during the 3-year study period was similar to the 30-year normal, but precipitation appeared to decrease over time. The average maximum air temperature was 20.8, 22.0 and 22.3°C in 2009, 2010 and 2011,

respectively, bracketing the 30-year normal of 21.2°C. The average minimum temperature was 12.2, 12.9 and 12.4°C in 2009, 2010 and 2011, respectively. The difference in minimum temperature between years and from the 30-year normal was smaller than that of maximum temperature (Figure 3-5 a). Annual precipitation was 1002, 758 and 960 mm in 2009, 2010 and 2011, respectively, and was lower than the recorded 30-year normal of 1270 mm (Figure 3-5 b).

3.2 Seasonal variation of soil, coarse woody debris and ecosystem respiration

Seasonality of R_s from survey and automated measurements was consistent between years in terms of the average magnitude at different microtopographic categories although the spatial variation resulted in marked deviation within each category (Figure 3-6 a-c). In spring and autumn, when MID and LOW microsites were submerged, R_s was lower than those at HIGH microsites under non-flooded conditions. Pronounced differences between microsites were present throughout the year in automated measurements, but decreased in magnitude during summer months in the survey measurements, when WTD<0 at all microsites. The approach of classifying microsites by two oversimplified cutoff points was also one of the causes of the decreased differences.

In 2010, the site average R_s in spring (Mar.-May) and autumn (Sep.-Nov.) was 2.2±1.6 (mean±SD) g CO_2-C m^{-2} d^{-1} and 1.0±0.6 g CO_2-C m^{-2} d^{-1}, respectively. Highest R_s occurred in summer (Jun.-Aug.) with a 3-year average of 6.4±2.8 g CO_2-C m^{-2} d^{-1} and lowest in winter (Dec.-Feb.) at 0.6±0.4 g CO_2-C m^{-2} d^{-1}. The wet summer of 2009 resulted in the low rate of R_s of 2.8±1.4 g CO_2-C m^{-2} d^{-1}, and the coldest winter of 2010 corresponded to the extremely

low R_s of 0.3±0.1 g CO_2-C m^{-2} d^{-1} (Figure 3-6 d).

Coarse woody debris also released highest amount of CO_2 during summer, and R_{CWD} decreased with increasing CWD decay class (Figure 3-7 a-c). The unit rates was similar between 2010 and 2011, but the site average R_{CWD} determined by scaling CWD biomass was significantly different between the two years. The 2-year average R_{CWD} was 0.5±0.4 (mean±SD), 1.1±0.6, 0.7±0.5 and 0.2±0.2 g CO_2-C m^{-2} d^{-1} from spring to summer, autumn and winter, respectively (Figure 3-7 d).

Summer R_e averaged 8.2±1.4 (mean±SD) g CO_2-C m^{-2} d^{-1} across all three years. Winter R_e averaged 1.5±0.7 g CO_2-C m^{-2} d^{-1}, and spring fluxes were higher than those in autumn with R_e of 4.3±2.0 and 3.3±1.2 g CO_2-C m^{-2} d^{-1}, respectively. These seasonal differences in R_e were related to dynamics of WTD. Similarly, the inter-annual differences in summer fluxes correlated with dynamics of WTD, with the wettest summer in 2009 having lower R_e (7.0±1.4 g CO_2-C m^{-2} d^{-1}) compared to drier years in 2010 (8.8±0.6 g CO_2-C m^{-2} d^{-1}) and 2011 (8.8±1.2 g CO_2-C m^{-2} d^{-1}). The coldest winter of 2010 experienced the lowest R_e at 1.1±0.3 g CO_2-C m^{-2} d^{-1} (Figure 3-8).

3.3 Temperature and hydrologic sensitivity of soil, coarse woody debris and ecosystem respiration

Relationships between T_s, WTD and R_s differed significantly between flooded and non-flooded periods (Figure 3-9), and the magnitude of $R_{s\text{-}FL}$ was much lower than that of $R_{s\text{-}NFL}$, indicating different controlling mechanisms and the necessity of separating them for modeling. T_s and WTD explained 60% of the variation in site average $R_{s\text{-}NFL}$ with automated

data, but only about 35% in the survey R_s data (Table 3-2). With WTD in the model, the improved performance of modeling the variance in T_s-R_s and WTD-R_s relationships indicated that T_s and WTD both had significant influences on R_s. In the Q_{10}-related parameters, β_1 (the Q_{10} at WTD = -10 cm) was not statistically different between the automated data (3.16±0.12) and survey data (3.69±1.02), whereas β_2 (the WTD-sensitivity of Q_{10}) was much greater in the survey data. When WTD varied between -30 and -5 cm, the Q_{10} of $R_{s\text{-}NFL}$ ranged at 2.2-3.5 from the automated data and 0.7-5.7 from the survey data.

Temperature explained 25-45% of R_{CWD} variation across decay classes. The tremendous variance in class 1-2 resulted in the greatest uncertainty and lowest performance when modeling with temperature (Table 3-2, Figure 3-10). R_b decreased with increasing of decay class. Although the mean of Q_{10} itself exhibited an opposite pattern to R_b, which might partly result from the interdependence between the two parameters, Q_{10} was not significantly different between decay classes with the uncertainty involved and averaged at 2.5±0.1 (Table 3-2).

Similar to R_s, the response of R_e to T_s and WTD also differed between flooded and non-flooded periods (Figure 3-11). Temperature and WTD explained approximately 50% of $R_{e\text{-}NFL}$ variation and 40% of $R_{e\text{-}FL}$ variation. Based on the current data coverage and the models with best performance, the R_b of $R_{e\text{-}NFL}$ did not exhibit a significant relationship with WTD (Model C in Table 3-2), whereas that of $R_{e\text{-}FL}$ did (Model B in Table 3-2). The constant R_b of $R_{e\text{-}NFL}$, 8.8±0.3 μmol CO_2-C m^{-2} s^{-1}, was higher than the maximum R_b of $R_{e\text{-}FL}$, 6.1±0.2 μmol CO_2-C m^{-2} s^{-1}. In contrast, the Q_{10} of $R_{e\text{-}NFL}$ was to some extent exponentially related with

WTD, whereas that of $R_{e\text{-}FL}$ was not. The Q_{10} of $R_{e\text{-}FL}$ averaged 2.5, similar to that of R_{CWD} and smaller than the maximum values of $R_{e\text{-}NFL}$ and $R_{s\text{-}NFL}$. The β_1 of $R_{e\text{-}NFL}$ was 2.20±0.12 and smaller than that of $R_{s\text{-}NFL}$. The β_2 of 0.059±0.006 was in the medium range of values of $R_{s\text{-}NFL}$ from both survey and automated data. The modeled dynamic Q_{10} of $R_{e\text{-}NFL}$ varied between 0.7 and 3.0 when WTD ranged from -30 to -5 cm, of which the high level was smaller than that of $R_{s\text{-}NFL}$. (Table 3-2).

3.4 Relative contributions to ecosystem respiration

The annual R_s:R_e ratio was calculated to be 0.65 in 2010; it was 0.76 and 0.25 for flooded and non-flooded periods, respectively. The R_s:R_e ratio also exhibited distinct seasonal variation. It started increasing in April from 0.38 to 0.64 in May, and reached peaked in June and July at 0.96 and 0.90, respectively. It began decreasing in August to 0.78. In September of 2010, while the site was flooded from Hurricane Irene, the R_s:R_e ratio dropped to 0.34. Similarly, during late autumn and winter, the ratio was low at 0.27±0.05 (mean±SD, Figure 3-12).

The daily variation differed between R_s and R_e. R_s responded sharply to the WTD change, decreasing with increasing WTD, whereas R_e did not show significant short-term response to WTD change but decreased when WTD reached a certain threshold above the soil surface (Figure 3-12). During summer, the drying-flooding cycle caused by rainfall events resulted in significant daily variation of R_s:R_e ratio. For example, in July of 2010, several precipitation events caused rapid rise in WTD and the R_s:R_e ratio varied between 0.5 and 1.0 with some values even above 1.0 (possibly due to the measurement error and estimate uncertainty).

After mid-August in 2010, frequent heavy rainfall events occurred and shifting the system into a flooded condition. Daily R_s decreased gradually with the increasing WTD and associated flooded area (Figure 3-2 d). During the same period, R_e also started decreasing but more slowly than R_s. Correspondingly, the R_s:R_e ratio decreased from 0.9-1.0 to 0.5 after mid-August. After Hurricane Irene, both R_s and R_e decreased significantly and the R_s:R_e ratio averaged at 0.2 (Figure 3-10).

Model predictions of R_s:R_e ratio were 0.45 in 2009 and 0.63 in 2011. Despite the distinct inter-annual difference in R_s:R_e, the respective ratios for flooded and non-flooded periods were similar between years. Through the 3-year study period, the average ratio was 0.24±0.06 (mean±SD) and 0.67±0.11 for flooded and non-flooded periods, respectively. The contribution of R_{CWD} to R_e was small compared to R_s, but with large inter-annual variability and upscaling uncertainties. Annual R_{CWD}:R_e ratio was 0.06 and 0.21 in 2010 and 2011, respectively.

3.5 Total carbon emission estimate

Annual R_e ranged 1331 to 1731 g CO_2-C m^{-2} y^{-1} through the 3-year study period. Annual R_s was estimated at 593-1082 g CO_2-C m^{-2} y^{-1}, with the smallest soil CO_2 efflux occurring in the wet year of 2009. Estimate of R_{CWD} differed tremendously between years, with totals of 94 (95% CI: 70-117) and 359 (261-458) g CO_2-C m^{-2} y^{-1} in 2010 and 2011, respectively (Table 3-3).

For each component, carbon emissions during the non-flooded period were much greater than during flooded period, although the difference varied inter-annually depending on the

length of the respective periods (Table 3-3). However, the residual between R_e and the other two components (R_s and R_{CWD}), which we equated to R_p, was much smaller between flooded and non-flooded periods in all three years. The percentage of non-flooded days during the growing season (April to October) was 57%, 72% and 71% in 2009, 2010 and 2011, respectively. Mean R_p in 2010 was 228 g CO_2-C m^{-2} for both flooded (95% CI: 172-261) and non-flooded (95% CI: 197-245) periods, respectively, and in 2011 was 129 (91-163) and 160 (118-179) g CO_2-C m^{-2}. CWD biomass was not measured in 2009 and therefore we could not estimate total R_{CWD}, but the difference between R_s and R_e were similar between flooded and non-flooded periods, with values of 356 (306-393) and 382 (360-397) g CO_2-C m^{-2}, respectively. Because 2009 was a wet year (during summer there were a number of flooded days), it is reasonable to think that R_{CWD} during flooded and non-flooded periods might have been similar, implying that the aboveground live plant respiration was similar (Table 3-4).

4. Discussion

4.1 Seasonal hysteresis of respiratory processes

In wetlands, it is thought that hydroperiod exerts strong regulation on seasonal variation of carbon cycling in addition to temperature. At our site, we observed a seasonal hysteresis of R_s at HIGH microsites but not at MID and LOW microsites, which was related to the effect of microtopography and surface soil immersion [*Miao et al.* in review]. In the current study, our survey of microtopography indicates the higher percentage of HIGH microsites in this wetland relative to MID and LOW microsites. As a result, the site average R_s exhibited a similar hysteresis to that at the HIGH microsites. A hysteresis pattern was also observed in

R_e, but with a magnitude different from R_s. The clockwise hysteresis pattern in R_e and R_s corresponded to the counter-clockwise pattern in WTD (Figure 3-13).

Difference in seasonal hysteresis was marked between R_s and R_e in 2010. In September when temperature was similar to June, R_s responded immediately to flooding and decreased to 1.8±1.2 (mean±SD) g CO_2-C m^{-2} d^{-1}, whereas the rate was 8.1±1.8 g CO_2-C m^{-2} d^{-1} in June. In contrast, R_e responded slowly and decreased to 5.2±1.1 g CO_2-C m^{-2} d^{-1} in September, compared to the rate of 8.5±0.8 g CO_2-C m^{-2} d^{-1} in June. Because the contribution from R_{CWD} was small, the slower response of R_e to WTD change was more likely attributed to change in R_p. Measuring R_p directly is beyond the scope of this study, but most of the species in this forested wetland have been characterized as tolerant to very tolerant of flooding [*Angelov et al.*, 1996; *Hook*, 1984]. Gravatt and Kirby [*Gravatt and Kirby*, 1998] evaluated the flood-tolerance of several tree species and suggested that short-term (<32 days) flooding events did not significantly decrease leaf and stem growth rates in tolerant species. During the fall, the effects of rising WTD may be combined with the commencement of the dormant season (e.g. decreasing temperature and day length), resulting in the significant reduction of R_p [*Gill*, 1970]. As a result, the magnitude of R_e decreased 3.8±0.9 (mean±SD) g CO_2-C m^{-2} d^{-1}, from the rate of 6.7±0.6 in May to 2.9±0.4 g CO_2-C m^{-2} d^{-1} in October. This magnitude was similar to that in R_s (3.5±1.0 g CO_2-C m^{-2} d^{-1}), from 4.3±1.0 in May to 0.8±0.2 g CO_2-C m^{-2} d^{-1} in October. The R_s and R_e were both consistently low from November to the following April (Figure 3-13).

While R_s and R_e are the focus of the current study and the aboveground processes are

beyond the scope, it has been studied in upland ecosystems that respiratory processes are affected by photosynthesis [*Davidson and Holbrook*, 2009; *Janssens et al.*, 2001], and photosynthesis responds differently to temperature early and late in the growing season [*Niu et al.*, 2011; *Piao et al.*, 2008; *Vesala et al.*, 2010]. To our knowledge, there are still no studies investigating the response of photosynthesis at different stages of the growing season in wetland ecosystems. The hydroperiod and plant adaptation to flooding conditions might result in remarkable difference between wetland and upland ecosystems. This question is also important for quantifying the fraction of autotrophic respiration in R_s and R_e and will be addressed in our future studies.

4.2 Temperature and hydrologic sensitivity of respiratory processes

Among the 7 components we classified, the $R_{s\text{-}FL}$ was most likely diffusion-limited [*Greenway et al.*, 2006], which is a different mechanism from the main focus of the current study. The other 6 components were controlled mainly by autotrophic or heterotrophic respiration, and Q_{10} or modified Q_{10} models were developed to quantify the environmental controls. Because the best fitting models differed between components, it was difficult to make direct comparisons of temperature and hydrologic sensitivity of each component. Briefly, the R_b of each component ranked as $R_{s\text{-}NFL} \sim R_{e\text{-}NFL} > R_{CWD}$ (class 1-2) $> R_{e\text{-}FL} > R_{CWD}$ (class 3) $> R_{CWD}$ (class 4), whereas the Q_{10} ranked as $R_{s\text{-}NFL} \sim R_{e\text{-}NFL} > R_{e\text{-}FL} \sim R_{CWD}$ (all classes).

Estimates of R_e had great uncertainty due to limited data coverage, but the difference in the R_b and Q_{10} patterns between $R_{e\text{-}NFL}$ and $R_{e\text{-}FL}$ provides some insight into differences in the

main sources of variation. The $R_{s\text{-}NFL}$ contributed 75-90% to the $R_{e\text{-}NFL}$, which likely explains the similarity in Q_{10} between $R_{e\text{-}NFL}$ and $R_{s\text{-}NFL}$. The $R_{s\text{-}FL}$ only contributed 20-25% to the variation in $R_{e\text{-}FL}$, and the $R_{CWD\text{-}FL}$ contributed about 8%, implying that R_p would be the main contributor to $R_{e\text{-}FL}$ (accounting for 67-72% of the variation). Therefore the driver sensitivity of $R_{e\text{-}FL}$, i.e. the constant Q_{10}, perhaps reflected the sensitivity of R_p during flooded periods. In contrast to R_s, on which the water table fluctuation had direct influence through the amount of available substrate, the carbon sources for R_p are essentially from plant carbon storage and current photosynthate [*Chapin et al.*, 1990]. The WTD effect on temperature sensitivity of R_p, as a result, might be relatively buffered. Previous studies have also found that flooding did not change leaf size and patchy stomatal opening of swamp tupelo seedlings [*Angelov et al.*, 1996]. In addition, we classified flooded periods based on a statistical average elevation, meaning that we integrated a certain proportion of HIGH and LOW microsites. Trees growing on HIGH microsites are less affected by flooding compared to MID and LOW microsites, and causing a less insignificant response to variation in WTD. There was no apparent pattern for R_b of $R_{e\text{-}NFL}$ and $R_{e\text{-}FL}$ in the current study. The performance of models with dynamic R_b (model B and D in Table 3-2) for $R_{e\text{-}NFL}$ exhibited marked difference between the simulation and validation and needs further study.

In the current study, modeled driver sensitivities of R_e and R_s were derived from a wet year (2009) and a dry year (2010), making results representative of various environmental conditions. Nevertheless, because the modified Q_{10} models for R_s and R_e are different from conventional Q_{10} models, we could not compare the temperature sensitivity of respiratory

components explicitly between this forested wetland and other types of ecosystems. In addition, the selection of T_a or T_s at different depth could affect the Q_{10} value, also limiting the comparison between ecosystems [*Lasslop et al.*, 2012]. However, the Q_{10} of R_e in this forested wetland, 0.7-3.0 of $R_{e\text{-}NFL}$ and 2.5 of $R_{e\text{-}FL}$, was within the range of responses to T_s published for other forests. For example, a Q_{10} of 2.5 was reported for a black spruce forest [*Jarvis et al.*, 1997], of 2.2 for a northern hardwood forest in Massachusetts [*Goulden et al.*, 1996], and at 2.3 for a pine ecosystem in Florida, USA [*Clark et al.*, 1999]. Compared with other wetlands, our Q_{10} was similar to that of a temperate bog (2.8) with a low density tree cover in Sweden [*Lund et al.*, 2007], and a reed coastal wetland (2.5) in China [*Han et al.*, 2013].

Environmental driver sensitivity of site average $R_{s\text{-}NFL}$ from the survey data was comparable to that for $R_{s\text{-}NFL}$ from automated measurements [*Miao et al.* in review]. This suggests the automated measurements are representative of each type of microsite and shows the value of comparison with replicated measurements. Compared with the Q_{10} values reported from the global soil respiration database (SRDB version 20100517), the Q_{10} of 2.2-3.5 of $R_{s\text{-}NFL}$ (temperature range: 15-25°C and WTD range: -30 - -5 cm) was within the range of 2.6±1.1 over the temperature range of 10-20°C [*Bond-Lamberty and Thomson*, 2010]. The wider range of 0.7-5.7 from survey data (temperature range: 5-25°C) was also similar to the reported range of 3.0±1.1 over the temperature range of 0-20°C in SRDB.

The temperature sensitivity of R_{CWD} was of the same order of magnitude as that of R_e and R_s (Table 3-2). The R_{CWD} Q_{10} of 2.5 in this forested wetland was slightly higher than that

from an adjacent loblolly pine plantation, with the value of 1.7 for decay class 2 and 2.0 for decay class 3 [*unpublished data*]. Our values of R_{CWD} Q_{10} were also similar to the values reported in some ecosystems from warmer climate zones, such as 2.4 in tropical forests of the central Amazon [*Chambers et al.*, 2001] and 2.5 in Austrian forests [*Mackensen et al.*, 2003].

4.3 Hydrologic control on R_s:R_e ratio

With the daily data derived from the gap-filled 30-min data, we analyzed environmental driver effects on the R_s:R_e ratio. Under non-flooded conditions, the R_s:R_e was positively related to T_s and maintained the hysteresis pattern similar to that of R_s and R_e. Interestingly, the ratio was linearly related to WTD (Figure 3-14). The intercept of the linear regression, 0.33±0.01 (mean±SE), represented the $R_{s\text{-}NFL}$ contribution to $R_{e\text{-}NFL}$ at WTD = 0 cm; the slope of -0.026±0.000 indicated that $R_{s\text{-}NFL}$ contribution increased 0.026 when WTD decreased 1 cm. The relationship under flooded conditions was not as clear as that under non-flooded conditions because of the greater uncertainties at the low level of CO_2 efflux and different mechanisms (e.g. diffusion limitation), which needs different experimental designs to elucidate. $R_{s\text{-}FL}$:$R_{e\text{-}FL}$ was approximately constant at 0.25±0.08 (mean±SD).

Furthermore, for R_s or R_e individually, there were additional T_s or WTD effects that could not be explained by the interaction between T_s or WTD, e.g. the independent WTD effect reflected in the T_s-R_s and T_s-R_e relationship (Figure 3-9 a, 3-11 a) and the T_s effect in the WTD-R_s and WTD-R_e relationship (Figure 3-9 b, 3-11 b). Nevertheless, the R_s:R_e ratio seemed exhibiting different pattern. The additional WTD effect still appeared in the T_s-(R_s:R_e) relationship, but the T_s effect was not significant in the WTD-(R_s:R_e) relationship. It implied

that only WTD effect seemed sufficient to interpret the variations of the R_s:R_e ratio, while T_s effect was the reflection of the interaction between T_s and WTD. This hypothesis would be useful to quantify the impact of climate change on carbon cycling in wetlands and needs further study to test.

Previous studies on upland forests found the negative relationship between the R_s:R_e ratio and T_s or T_a [*Davidson et al.*, 2006; *Jassal et al.*, 2007]. Several mechanisms were attributed to this pattern, such as the lag between soil temperature and air temperature resulting in the difference between the aboveground and belowground processes. Also, water stress on plants at upland areas may have different effects on autotrophic and heterotrophic respiration [*Davidson et al.,* 2006]. In contrast to upland forests where temperature is a main driver of R_s:R_e ratio, our results indicates that R_s:R_e ratio in this type of forested wetland is highly responsive to WTD. This might be due to a large contribution from heterotrophic respiration which iss controlled by the WTD-induced availability of substrates [*Freeman et al.,* 2001; *Freeman et al.,* 2004; *Jaatinen et al.,* 2007], whereas the autotrophic respiration of flood-tolerant species was not affected by WTD within a certain range.

As mentioned, the impacts from photosynthesis on the respiratory processes at our site are still unquantified. The conclusion that the WTD is the main driver to the R_s:R_e ratio needs to be qualified by the recognition that there is still uncertainty from other confounding or unaccounted factors. In addition, if this wetland had a severe drought, WTD might decrease beyond the range reported here. It is likely that the relationship between R_s:R_e ratio and WTD changes because soil processes might respond differently from the current situation and

plants might have drought stress as well [*Lugo et al.*, 1990; *Alm et al.*, 1999; *Sonnentag et al.*, 2010].

4.4 Uncertainties and implication of partitioning respiration in a forested wetland

Two sources of uncertainty specifically related to wetland ecosystems became apparent in the current study. In the first, accounting for variation in microtopography decreased unexplained variation of estimating site average R_s by explicitly quantifying the percentage of individual microsites, and therefore the fraction of the soil surface in flooded vs. non-flooded condition. Our assumption of a linear relationship between R_s and microtopographic position, however, is arbitrary and needs to be tested. CWD biomass and decay classes introduce uncertainty into estimates of R_{CWD}, which resulted in the marked differences between years in this study. Although most of CWDs was elevated above the soil surface, flooding in the LOW microtopographic positions still affected our CWD biomass survey in a wet year or season. An analysis on CWD spatial distribution would be useful to estimate the percentage of flooded and non-flooded CWDs and refine the R_{CWD} estimate.

This study has illustrated how periodic flooding may complicate estimation of sources of respiration in forested wetlands. By adjusting respiration models to account for flooded and non-flooded conditions as influenced by variation in microtopography and WTD, we were able to estimate an annual R_e of more than 1000 g C m^{-2} y^{-1}, similar in magnitude to that of many upland forests [*Valentini et al.*, 2000]. Temperature sensitivity of respiratory components (R_e, R_s and R_{CWD}) was also similar to upland forests, demonstrating common environmental control over respiratory processes. On the other hand, the transition between

flooded and non-flooded conditions resulted in unique responses as well. R_s was the main contributor to R_e during non-flooded periods and the R_s:R_e ratio was similar to that reported for boreal and temperate upland forests, while R_p was likely the main contributor to R_e during flooded periods, similar to many tropical rainforests.

R_p, which was assumed as residual between R_e and R_s, was similar between non-flooded and flooded periods, even though the respective length of the two periods was different year to year (Table 3-4). It has been broadly acknowledged that the plants in wetlands have physiologically adapted to flooding conditions, but the question that how these adaptations affect carbon cycling is still less addressed. This requires long term studies and direct observations on plant growth as the current speculation was based on R_s and R_e, each of which embedded uncertainties from the data gap filling and upscaling. Sensitivity of R_p needs to be confirmed with direct measurements.

R_s in the wet year of 2009 showed lower CO_2 efflux than in the dry years of 2010 and 2011, demonstrating that the wetter conditions acted as a negative feedback to the atmosphere. Whether such a response would acclimate at the ecosystem level over time requires further study. However, the decreasing precipitation of the three years relative to the 30-year climate normal (Figure 3-5 b) suggested that atmospheric CO_2-forcing may have been increasing in recent years due to the accelerated turnover of carbon stored in this system, which has serious implications for carbon storage in wetland ecosystems if drought-severity increases over most of the global land surface as projected [*King et al.*, 2013]. Further study of this forested wetland is needed to fully determine net ecosystem exchange under future

climate conditions, accounting for effects on photosynthesis and methane production, as well as respiration.

References

Aerts, R. (1997), Climate, Leaf litter chemistry and leaf litter decomposition in terrestrial ecosystems: A triangular relationship, *Oikos*, *79*(3), 439-449.

Alm, J., L. Schulman, J. Walden, H. Nykanen, P. J. Martikainen, and J. Silvola (1999), Carbon balance of a boreal bog during a year with an exceptionally dry summer, *Ecology*, *80*(1), 161-174.

Angelov, M. N., S.-J. S. Sung, R. L. Doong, W. R. Harms, P. P. Kormanik, and C. C. Black (1996), Long- and short-term flooding effects on survival and sink–source relationships of swamp-adapted tree species, *Tree Physiology*, *16*(5), 477-484.

Armentano, T. V. (1980), Drainage of organic soils as a factor in the world carbon cycle, *BioScience*, *30*(12), 825-830.

Armentano, T. V., and E. S. Menges (1986), Patterns of change in the carbon balance of organic soil-wetlands of the temperate zone, *Journal of Ecology*, *74*(3), 755-774.

Baldocchi, D. D. (2003), Assessing the eddy covariance technique for evaluating carbon dioxide exchange rates of ecosystems: past, present and future, *Global Change Biology*, *9*(4), 479-492.

Battin, T. J., S. Luyssaert, L. A. Kaplan, A. K. Aufdenkampe, A. Richter, and L. J. Tranvik (2009), The boundless carbon cycle, *Nature Geosci*, *2*(9), 598-600.

Bond-Lamberty, B., and A. Thomson (2010), A global database of soil respiration data, *Biogeosciences*, *7*, 1915-1926.

Bridgham, S., J. P. Megonigal, J. Keller, N. Bliss, and C. Trettin (2006), The carbon balance of North American wetlands, *Wetlands*, *26*(4), 889-916.

Chambers, J. Q., J. P. Schimel, and A. D. Nobre (2001), Respiration from coarse wood litter in central Amazon forests, *Biogeochemistry*, *52*(2), 115-131.

Chambers, J. Q., E. S. Tribuzy, L. C. Toledo, B. F. Crispim, N. Higuchi, J. d. Santos, A. C. Araújo, B. Kruijt, A. D. Nobre, and S. E. Trumbore (2004), Respiration from a tropical forest ecosystem: Partitioning of sources and low carbon use efficiency, *Ecological Applications*, *14*(4), S72-S88.

Chapin III, F. S., E.-D. Schulze, and H. A. Mooney (1990), The ecology and economics of storage in plants, *Annual Review of Ecology and Systematics*, *21*, 423-447.

Chmura, G. L., S. C. Anisfeld, D. R. Cahoon, and J. C. Lynch (2003), Global carbon sequestration in tidal, saline wetland soils, *Global Biogeochemical Cycles*, *17*(4), 1111.

Clark, K. L., H. L. Gholz, J. B. Moncrieff, F. Cropley, and H. W. Loescher (1999), Environmental controls over net exchanges of carbon dioxide from contrasting Florida ecosystems, *Ecological Applications*, *9*(3), 936-948.

Davidson, E. A. (2010), Permafrost and wetland carbon stocks, *Science*, *330*(6008), 1176-1177.

Davidson, E. A., and I. A. Janssens (2006), Temperature sensitivity of soil carbon decomposition and feedbacks to climate change, *Nature*, *440*(7081), 165-173.

Davidson, E. A., and N. M. Holbrook (2009), Is temporal variation of soil respiration linked to the phenology of photosynthesis?, in *Phenology of Ecosystem Processes*, edited by A. Noormets, pp. 187-199, Springer New York.

Davidson, E. A., A. D. Richardson, K. E. Savage, and D. Y. Hollinger (2006), A distinct seasonal pattern of the ratio of soil respiration to total ecosystem respiration in a spruce-dominated forest, *Global Change Biology*, *12*(2), 230-239.

Desai, A. R., et al. (2008), Cross-site evaluation of eddy covariance GPP and RE decomposition techniques, *Agricultural and Forest Meteorology*, *148*(6-7), 821-838.

Freeman, C., N. Ostle, and K. H. (2001), An enzymic 'latch' on a global carbon store, *Nature*, *409*, 149.

Freeman, C., N. J. Ostle, N. Fenner, and H. Kang (2004), A regulatory role for phenol oxidase during decomposition in peatlands, *Soil Biology & Biochemistry*, *36*, 1663-1667.

Gill, C. J. (1970), The flooding tolerance of woody species - a review, *Forestry Abstracts*, *31*(4), 671-688.

Gorham, E. (1991), Northern peatlands: Role in the carbon cycle and probable responses to climatic warming, *Ecological Applications*, *1*(2), 182-195.

Goulden, M. L., J. W. Munger, S. M. Fan, B. C. Daube, and S. C. Wofsy (1996), Measurements of carbon sequestration by long-term eddy covariance: methods and a critical evaluation of accuracy, *Global Change Biology*, *2*(3), 169-182.

Gravatt, D. A., and C. J. Kirby (1998), Patterns of photosynthesis and starch allocation in seedlings of four bottomland hardwood tree species subjected to flooding, *Tree Physiology*, *18*(6), 411-417.

Greenway, H., W. Armstrong, and T. D. Colmer (2006), Conditions leading to high CO_2 (>5 kPa) in waterlogged–flooded soils and possible effects on root growth and metabolism, *Annals of Botany*, *98*(1), 9-32.

Han, G., L. Yang, J. Yu, G. Wang, P. Mao, and Y. Gao (2013), Environmental controls on net ecosystem CO_2 exchange over a reed (*Phragmites australis*) wetland in the Yellow River Delta, China, *Estuaries and Coasts*, *36*(2), 401-413.

Harmon, M. E., et al. (2004), Ecology of coarse woody debris in temperate ecosystems, in *Advances in Ecological Research*, edited by H. Caswell, pp. 59-234, Academic Press.

Hook, D. D. (1984), Waterlogging tolerance of lowland tree species of the south, *Southern Journal of Applied Forestry*, *8*(3), 136-149.

Jaatinen, K., H. Fritze, J. Laine, and R. Laiho (2007), Effects of short- and long-term water-level drawdown on the populations and activity of aerobic decomposers in a boreal peatland, *Global Change Biology*, *13*, 491-510.

Janssens, I. A., S. Dore, D. Epron, H. Lankreijer, N. Buchmann, B. Longdoz, J. Brossaud, and L. Montagnani (2003), Climatic influences on seasonal and spatial differences in soil CO_2 efflux, in *Fluxes of carbon, water, and energy of European forests*, edited by R. Valentini, Springer, Berlin; New York.

Janssens, I. A., et al. (2001), Productivity overshadows temperature in determining soil and ecosystem respiration across European forests, *Global Change Biology*, *7*(3), 269-278.

Jarvis, P. G., J. M. Massheder, S. E. Hale, J. B. Moncrieff, M. Rayment, and S. L. Scott (1997), Seasonal variation of carbon dioxide, water vapor, and energy exchanges of a boreal black spruce forest, *Journal of Geophysical Research: Atmospheres*, *102*(D24), 28953-28966.

Jassal, R. S., T. A. Black, T. Cai, K. Morgenstern, Z. Li, D. Gaumont-Guay, and Z. Nesic (2007), Components of ecosystem respiration and an estimate of net primary productivity of an intermediate-aged Douglas-fir stand, *Agricultural and Forest Meteorology*, *144*(1–2), 44-57.

King, J. S., R. Ceulemans, J. M. Albaugh, S. Y. Dillen, J.-C. Domec, R. Fichot, M. Fischer, Z. Leggett, E. Sucre, M. Trnka, and T. Zenone (2013), The challenge of lignocellulosic bioenergy in a water-limited world. *BioScience*, 63, 102-117.

Kirschbaum, M. U. F. (2010), The temperature dependence of organic matter decomposition: seasonal temperature variations turn a sharp short-term temperature response into a more moderate annually averaged response, *Global Change Biology*, *16*(7), 2117-2129.

Laiho, R. (2006), Decomposition in peatlands: Reconciling seemingly contrasting results on the impacts of lowered water levels, *Soil Biology and Biochemistry*, *38*(8), 2011-2024.

Lasslop, G., et al. (2012), On the choice of the driving temperature for eddy-covariance carbon dioxide flux partitioning, *Biogeosciences*, *9*(12), 5243-5259.

Lavigne, M. B., et al. (1997), Comparing nocturnal eddy covariance measurements to estimates of ecosystem respiration made by scaling chamber measurements at six coniferous boreal sites, *Journal of Geophysical Research: Atmospheres*, *102*(D24), 28977-28985.

Law, B. E., M. G. Ryan, and P. M. Anthoni (1999), Seasonal and annual respiration of a ponderosa pine ecosystem, *Global Change Biology*, *5*(2), 169-182.

Lugo, A. E., S. Brown, and M. Brinson (1990), *Forested wetlands*, Elsevier, Amsterdam, Netherlands.

Lund, M., A. Lindroth, T. R. Christensen, and L. StrÖM (2007), Annual CO_2 balance of a temperate bog, *Tellus B*, *59*(5), 804-811.

Luyssaert, S., et al. (2007), CO_2 balance of boreal, temperate, and tropical forests derived from a global database, *Global Change Biology*, *13*(12), 2509-2537.

Mackensen, J., J. Bauhus, and E. Webber (2003), Decomposition rates of coarse woody debris: a review with particular emphasis on Australian tree species, *Australian Journal of Botany*, *51*(1), 27-37.

Mahecha, M. D., et al. (2010), Global convergence in the temperature sensitivity of respiration at ecosystem level, *Science*, *329*(5993), 838-840.

Miao, G., A. Noormets, J.-C. Domec, C. Trettin, S. G. McNulty, G. Sun, and J. S. King (in review), The effect of water table fluctuation on soil respiration in a lower coastal plain forested wetland in southeastern USA, *Journal of Geophysical Research: Biogeosciences*.

Mitsch, W., B. Bernal, A. Nahlik, Ü. Mander, L. Zhang, C. Anderson, S. Jørgensen, and H. Brix (2013), Wetlands, carbon, and climate change, *Landscape Ecol*, *28*(4), 583-597.

Niu, S., Y. Luo, S. Fei, L. Montagnani, G. I. L. Bohrer, I. A. Janssens, B. Gielen, S. Rambal, E. Moors, and G. Matteucci (2011), Seasonal hysteresis of net ecosystem exchange in response to temperature change: patterns and causes, *Global Change Biology*, *17*(10), 3102-3114.

Noormets, A., S. G. McNulty, J.-C. Domec, M. Gavazzi, G. Sun, and J. S. King (2012), The role of harvest residue in rotation cycle carbon balance in loblolly pine plantations. Respiration partitioning approach, *Global Change Biology*, *18*(10), 3186-3201.

Noormets, A., M. J. Gavazzi, S. G. McNulty, J.-C. Domec, G. E. Sun, J. S. King, and J. Chen (2010), Response of carbon fluxes to drought in a coastal plain loblolly pine forest, *Global Change Biology*, *16*(1), 272-287.

Piao, S., et al. (2008), Net carbon dioxide losses of northern ecosystems in response to autumn warming, *Nature*, *451*(7174), 49-52.

Raich, J. W., and W. H. Schlesinger (1992), The global carbon dioxide flux in soil respiration and its relationship to vegetation and climate, *Tellus B*, *44*(2), 81-99.

Saleska, S. R., et al. (2003), Carbon in Amazon forests: Unexpected seasonal fluxes and disturbance-induced losses, *Science*, *302*(5650), 1554-1557.

Sonnentag, O., G. Kamp, A. G. Barr, and J. M. Chen (2010), On the relationship between water table depth and water vapor and carbon dioxide fluxes in a minerotrophic fen, *Global Change Biology*, 16, 1762-1776. DOI: 10.1111/j.1365-2486.2009.02032.x

Trumbore, S. (2006), Carbon respired by terrestrial ecosystems – recent progress and challenges, *Global Change Biology*, *12*(2), 141-153.

Valentini, R., et al. (2000), Respiration as the main determinant of carbon balance in European forests, *Nature*, *404*(6780), 861-865.

Vesala, T., et al. (2010), Autumn temperature and carbon balance of a boreal Scots pine forest in Southern Finland, *Biogeosciences*, *7*(1), 163-176.

Webb, E. L., D. A. Friess, K. W. Krauss, D. R. Cahoon, G. R. Guntenspergen, and J. Phelps (2013), A global standard for monitoring coastal wetland vulnerability to accelerated sea-level rise, *Nature Clim. Change*, *3*(5), 458-465.

Yang, B., P. J. Hanson, J. S. Riggs, S. G. Pallardy, M. Heuer, K. P. Hosman, T. P. Meyers, S. D. Wullschleger, and L.-H. Gu (2007), Biases of CO_2 storage in eddy flux measurements in a forest pertinent to vertical configurations of a profile system and CO_2 density averaging, *Journal of Geophysical Research: Atmospheres*, *112*(D20), D20123.

Tables and Figures

Table 3-1 Performance comparison of models used for simulating ecosystem respiration (R_e) during non-flooded periods and flooded periods with soil temperature (T_s) and water table depth (WTD) in a lower coastal plain forested wetland in North Carolina, USA.

	Models*	Number of Parameter	Non-flooded ($w = WTD$; $w_0 = -10$)					Flooded ($w = 1/WTD$; $w_0 = 0.1$)				
			Simulation		Validation			Simulation		Validation		
			R^2	AIC	R^2	AIC		R^2	AIC	R^2	AIC	
A	Conventional Q_{10} model $R = R_b Q_{10}^{\frac{T_S - T_b}{10}}$	2	0.5000	1964	0.5281	1903		0.3864	1418	0.2163	132	
B	R_b-dynamic-only model $R = \frac{V_{max} w}{K_m + w} Q_{10}^{\frac{T_S - T_b}{10}}$	3	0.5556	1806	0.4949	1976		0.3973	1394	0.2423	129	√
C	Q_{10}-dynamic-only model $R = R_b \left\{ \beta_1 \exp\left[\beta_2 \left(w - w_0 \right) \right] \right\}^{\frac{T_S - T_b}{10}}$	3	0.5250	1872	0.5335	1893	√	0.3865	1419	0.2203	133	
D	Nested Q_{10} model $R = \frac{V_{max} w}{K_m + w} \left\{ \beta_1 \exp\left[\beta_2 \left(w - w_0 \right) \right] \right\}^{\frac{T_S - T_b}{10}}$	4	0.5556	1808	0.4959	1976		0.3889	1416	0.2159	136	
	Sample size		982		1451			1043		120		

*: The meaning of parameters in these models:

R - respiration rate; R_b - basal respiration; T_b - basal temperature; Q_{10} - temperature response parameter.

V_{max} - maximum R_b rate at T_b; K_m - the water table depth at half V_{max}; β_1 - the Q_{10} at $w=w_0$; β_2 - WTD response parameter.

Table 3-2 Parameters of nonlinear regression for modeling ecosystem respiration (flooded $R_{e\text{-}FL}$ and non-flooded $R_{e\text{-}NFL}$ separately), soil respiration under non-flooded conditions ($R_{s\text{-}NFL}$) with soil temperature (T_s) and water table depth (WTD), and modeling decomposition of coarse woody debris (R_{CWD}) with T_s.

(mean±SE)	R_b (μmol m^{-2} s^{-1})	Q_{10}	R_b-related parameters		Q_{10}-related parameters		R^2
			V_{max} (μmol m^{-2} s^{-1})	K_m (m^{-1})	β_1	β_2 (m^{-1})	
$R_{s\text{-}NFL}$			(Nested Q_{10} model)				
Automated	9.7 - 5.6 [a]	2.2 - 3.5 [a]	11.3±0.2	-5.1±0.3	3.16±0.12	0.018±0.006	0.6427
Manual	13.2 - 4.7 [a]	0.7 - 5.7 [a]	20.6±4.0	-16.9±6.6	3.69±1.02	0.087±0.026	0.3569
R_{CWD}			(Conventional Q_{10} model)				
Decay class 1-2	6.5±0.7	2.40±0.49					0.2681
Decay class 3	2.9±0.2	2.51±0.39					0.3256
Decay class 4	2.2±0.3	2.61±0.82					0.4566
$R_{e\text{-}NFL}$			(Q_{10}-dynamic-only model)				
	8.8±0.3	0.7 - 3.0 [a]			2.20±0.12	0.059±0.006	0.5250
$R_{e\text{-}FL}$			(R_b-dynamic-only model)				
	5.7 - 4.2 [b]	2.50±0.09	6.1±0.2	0.015±0.004			0.3973

a: The dynamic basal respiration (R_b) and Q_{10} during non-flooded period were derived based on WTD in the range of -30 - -5 cm, decreasing with the WTD rise.

b: The dynamic R_b during flooded period were derived based on WTD in the range of 5 - 30 cm, decreasing with the WTD rise.

Table 3-3 Estimated annual carbon emission of ecosystem respiration (R_e), soil respiration (R_s) and decomposition of coarse woody debris (R_{CWD}) (g CO_2-C m^{-2} yr^{-1}) in a lower coastal plain forested wetland in 2010, with 95% confidence interval in parenthesis.

	Data gap filled	Predicted		
	2010 [1/1-12/31]	2009 [3/19-12/31]	2010 [1/1-12/31]	2011 [1/1-12/31]
R_e	1560 (1471-1650)	1331 (1256-1406)	1559 (1464-1654)	1731 (1615-1846)
Flooded	341 (321-361)	503 (477-529)	342 (320-365)	260 (248-272)
Non-flooded	1219 (1150-1288)	828 (779-877)	1217 (1144-1289)	1470 (1367-1574)
Automated R_s	1015 (960-1103)	593 (503-702)	1010 (936-1120)	1082 (1012-1179)
Flooded	86 (45-150)	147 (84-223)	86 (40-155)	47 (17-80)
Non-flooded	928 (915-953)	446 (419-479)	924 (896-965)	1035 (995-1099)
Manual R_s	NA	499 (266-856)	1179 (914-1600)	1318 (930-1751)
Flooded	NA	90 (0-304)	64 (0-284)	49 (0-139)
Non-flooded	NA	409 (266-553)	1114 (914-1317)	1268 (930-1613)
R_{CWD}	NA	NA	94 (70-117)	359 (261-458)
Flooded	NA	NA	28 (19-38)	84 (68-101)
Non-flooded	NA	NA	65 (52-79)	275 (193-357)

Table 3-4 Comparison of the residual between ecosystem respiration (R_e), soil respiration (R_s) and decomposition of coarse woody debris (R_{CWD}) in a lower coastal plain forested wetland.

	Data gap filled	Predicted		
	2010 [1/1-12/31]	2009 [3/19-12/31]	2010 [1/1-12/31]	2011 [1/1-12/31]
Residual	(R_e - R_s)	(R_e - R_s)	(R_e - R_s - R_{CWD})	(R_e - R_s - R_{CWD})
	546 (510-547)	738 (703-753)	455 (417-458)	289 (210-342)
Flooded	255 (212-275)	356 (306-393)	228 (172-261)	129 (91-163)
Non-flooded	291 (235-336)	382 (360-397)	228 (197-245)	160 (118-179)
Days within a year		288	365	365
Flooded		152	155	64
Non-flooded		136	210	301
Percentage of non-flooded days		47%	58%	82%
Days in growing season (Apr.-Oct.)		214	214	214
Flooded		91	61	62
Non-flooded		123	153	152
Percentage of non-flooded days		57%	72%	71%

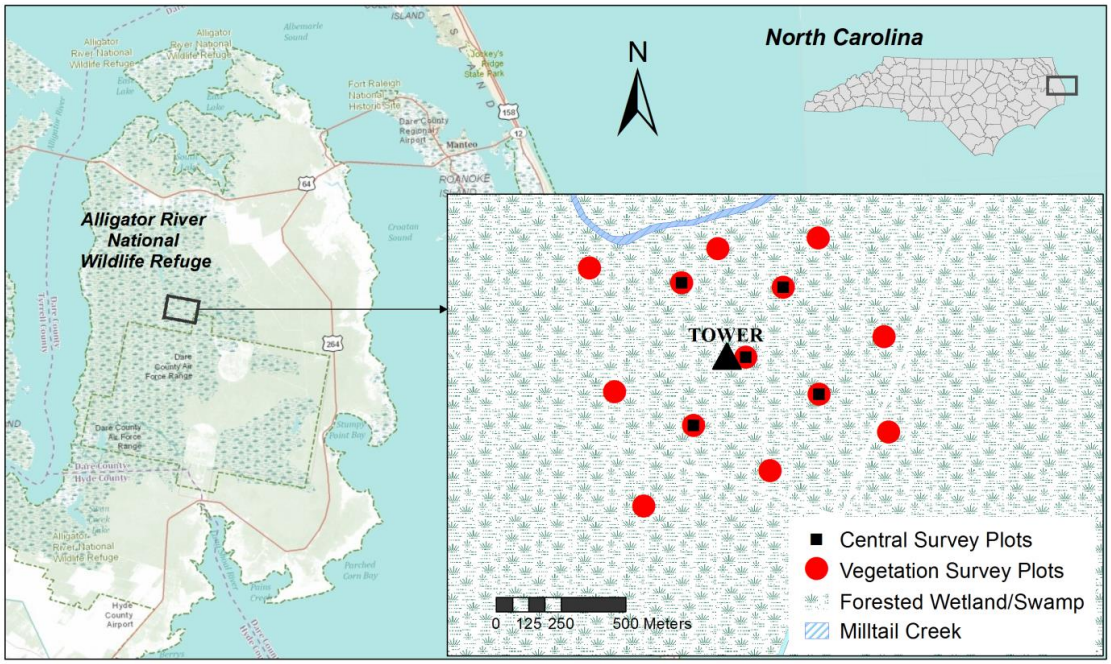

Figure 3-1 Location and field settings of study site at the Alligator River National Wildlife Refuge (ARNWR) (35^{0}47′N, 75^{0}54′W) in eastern North Carolina, USA.

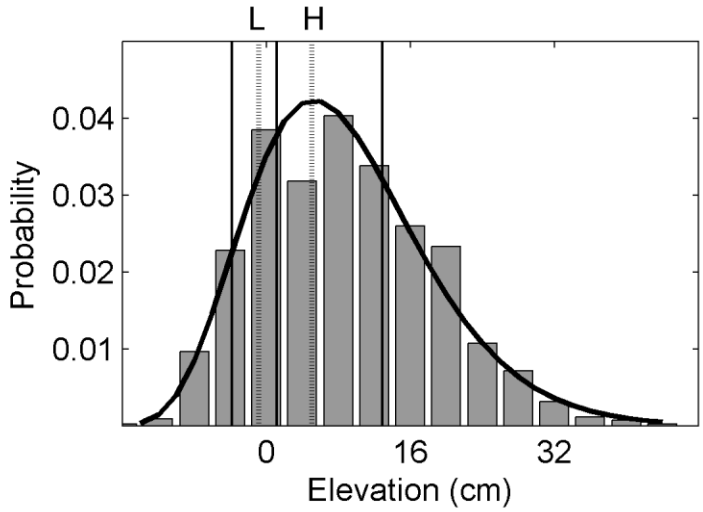

Figure 3-2 Histogram and fitted gamma distribution of microtopography in a lower coastal plain forested wetland. The three solid straight lines represent the elevations of the three microsites (LOW, MID, and HIGH from left to right) where the automated soil respiration (R_s) measurements were conducted. The two dotted straight lines represent the cutoff points used to calculate the areal representativeness of each microsite. Based on the assumption that R_s is linearly related to the micro-topography, the average R_s of microtopographic positions lower than 'L', where half is lower than LOW microsite and half is higher, equals to the R_s of the LOW microsite. A similar definition was applied to point 'H', i.e. the average R_s of positions higher than 'H' equals to the R_s of the HIGH microsite. The positions between 'L' and 'H' were assumed to respire equally to the MID microsite.

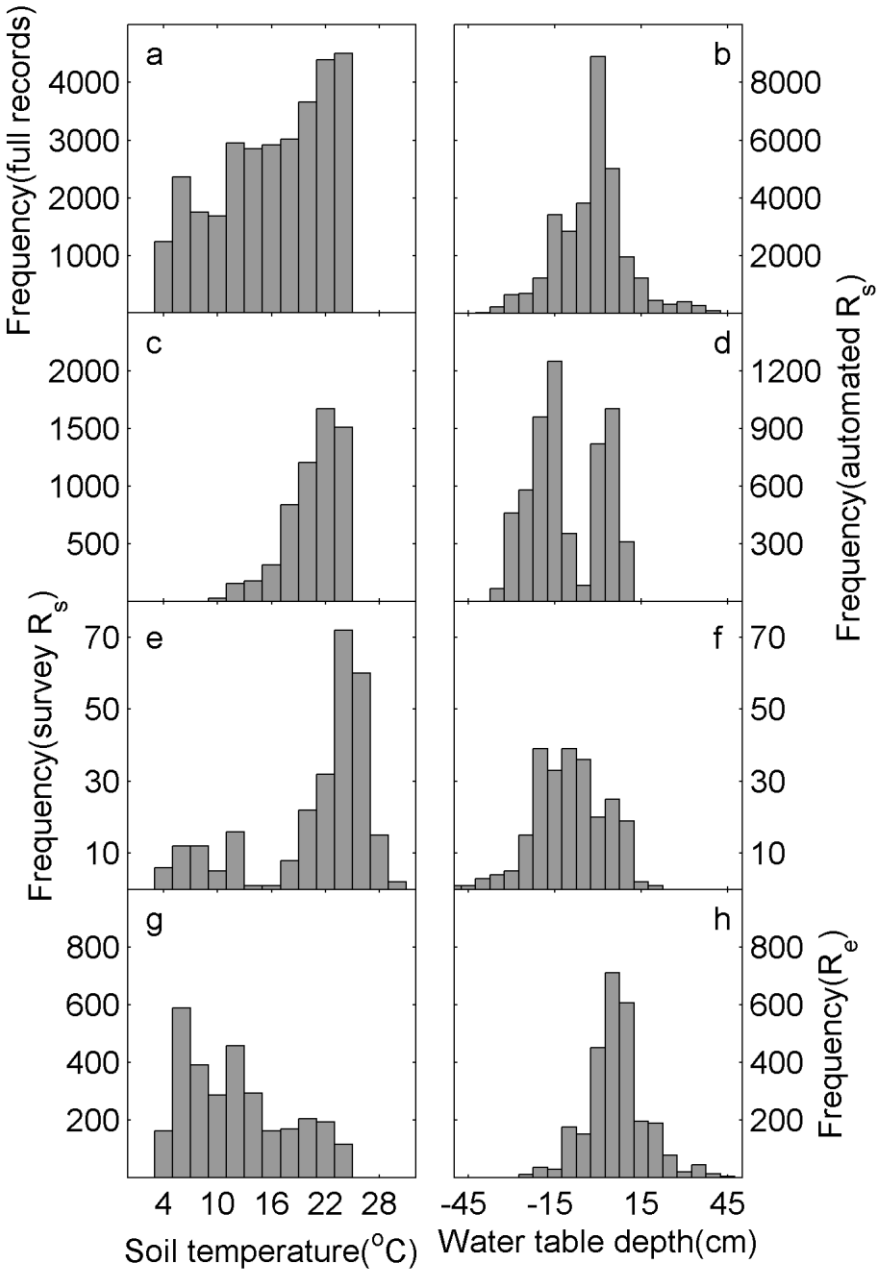

Figure 3-3 Comparison of histogram between soil temperature (T_s) and water table depth (WTD) in full records (a, b) and those corresponding to available ecosystem respiration (R_e) data records (c, d), automated soil respiration (R_s) measurements (e, f), and survey R_s (g, h).

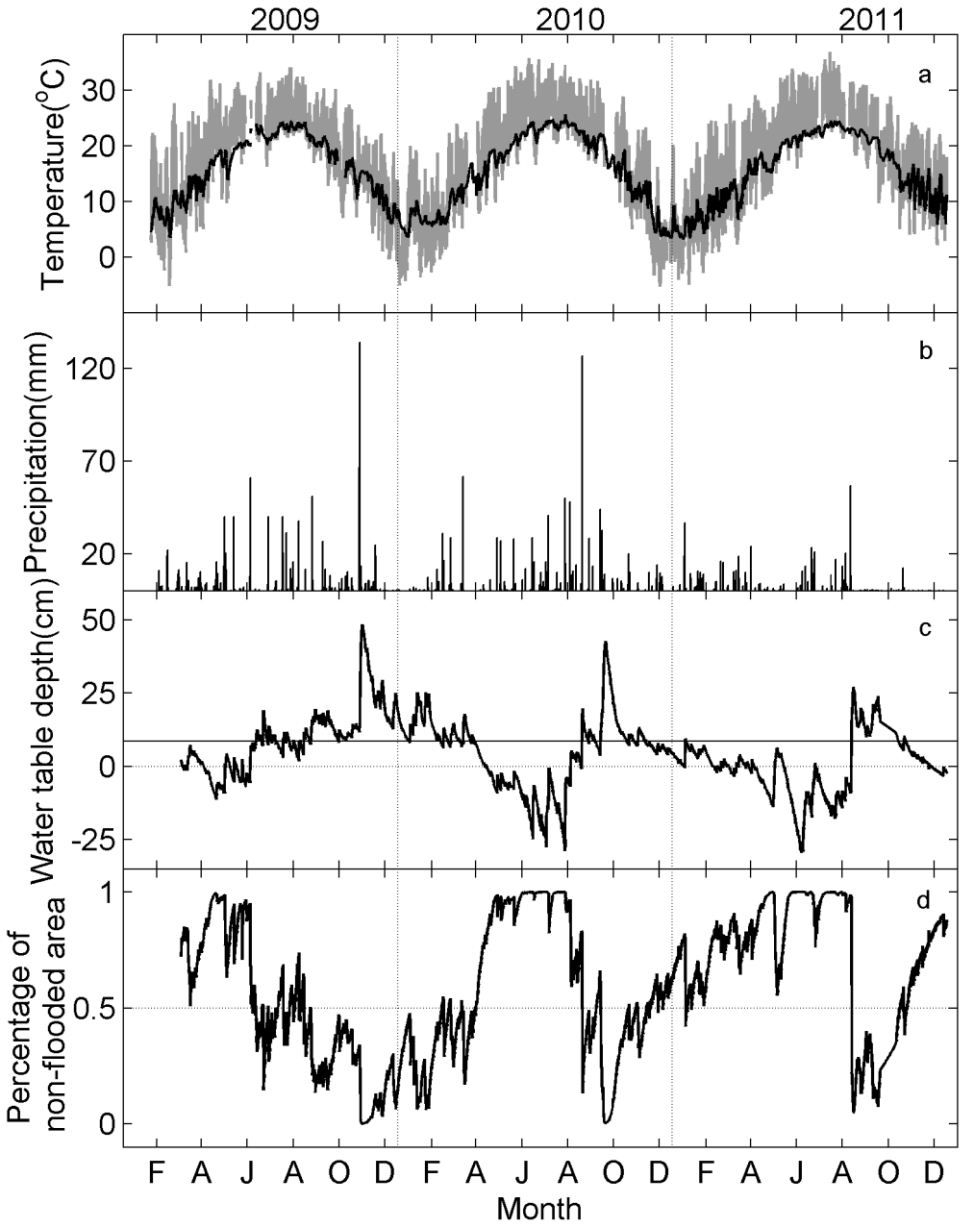

Figure 3-4 Seasonal variations observed in a lower coastal plain forested wetland in North Carolina, USA, during the period 3/19/2009-12/31/2011 in (a) Air temperature (grey) and soil temperature at 5 cm depth (T_s, black), (b) Precipitation, (c) Water table depth (WTD) with the site average elevation (solid line) relative to ground water probe location at ground meteorological station (dotted line), and (d) Percentage of non-flooded area calculated based on gamma distribution of micro-topography across the study area.

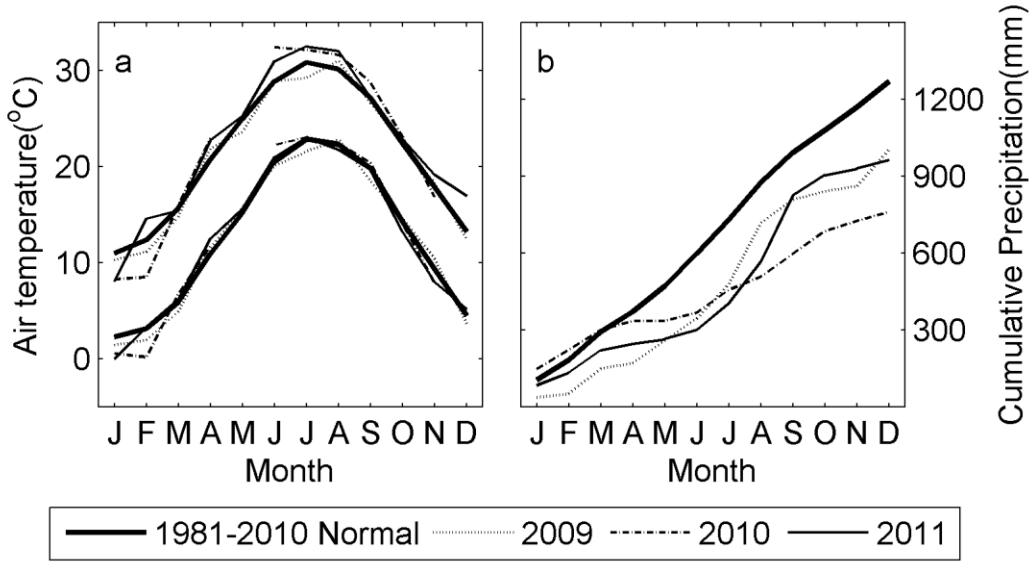

Figure 3-5 Comparison of (a) monthly air temperature (maximum and minimum), and (b) cumulative precipitation between the 30-year normal and the study periods (2009-2011) at Manteo, AP meteorological station in North Carolina, USA.

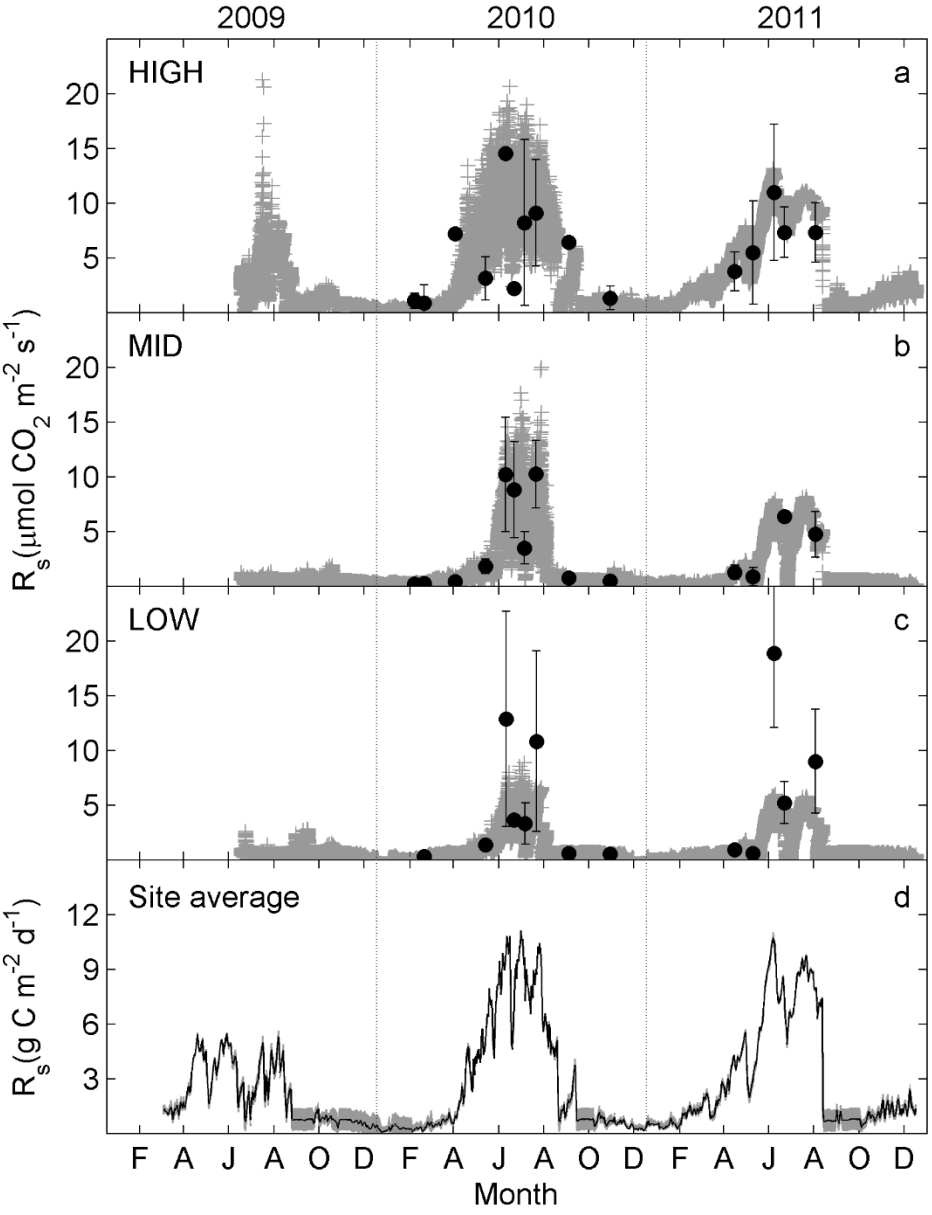

Figure 3-6 Time series of soil respiration (R_s) in a lower coastal plain forested wetland from 2009 to 2011. The data in 2009 and 2010 were gap-filled, and the data in 2011 were the results predicted by the nested Q_{10} model we developed in a previous study [*Miao et al.* in review]. (a)-(c): Comparison between 30-minute automated (grey '+') and monthly survey (black dots – mean values; error bar – standard deviation) measurements at (a) HIGH, (b) MID and (c) LOW microsites; (d): The daily mean (black line) and 95% confidence interval (shaded area) of site average R_s (g CO_2-C m^{-2} d^{-1}).

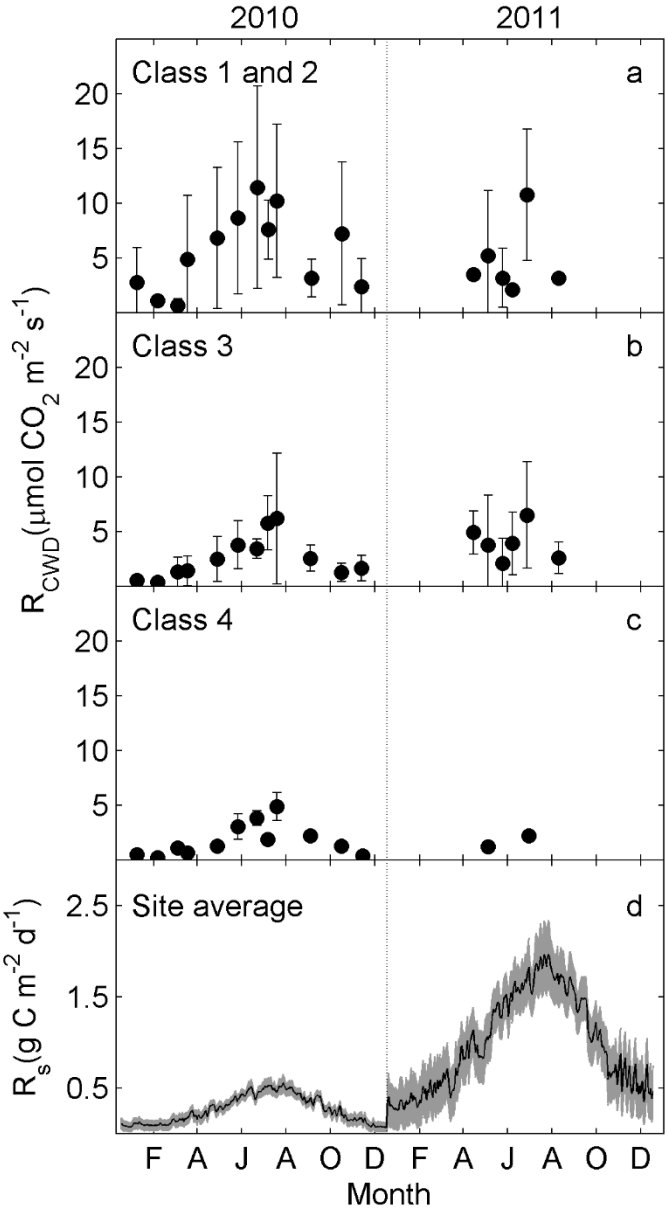

Figure 3-7 Time series of decomposition of coarse woody debris (CWD) in a lower coastal plain forested wetland from 2010 to 2011. (a)-(c): Monthly measurements (black dots – mean values; error bar – standard deviation) at (a) decay class 1-2, (b) class 3 and (c) class 4; (d): The daily mean (black line) and 95% confidence interval (shaded area) of site average decomposition of coarse woody debris (R_{CWD}, g CO_2-C m^{-2} d^{-1}).

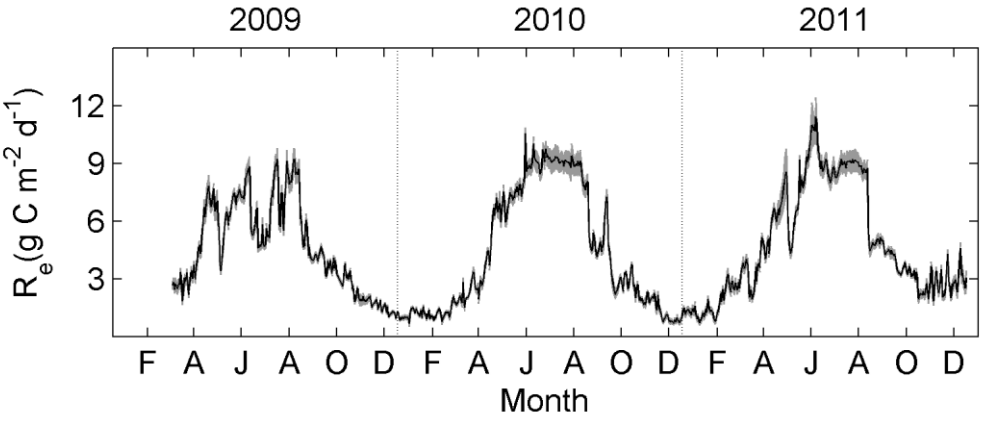

Figure 3-8 Time series of ecosystem respiration (R_e, gap filled) in a lower coastal plain forested wetland from 2010 to 2011, the daily mean (g CO_2-C m^{-2} d^{-1}, black line) and 95% confidence interval (shaded area).

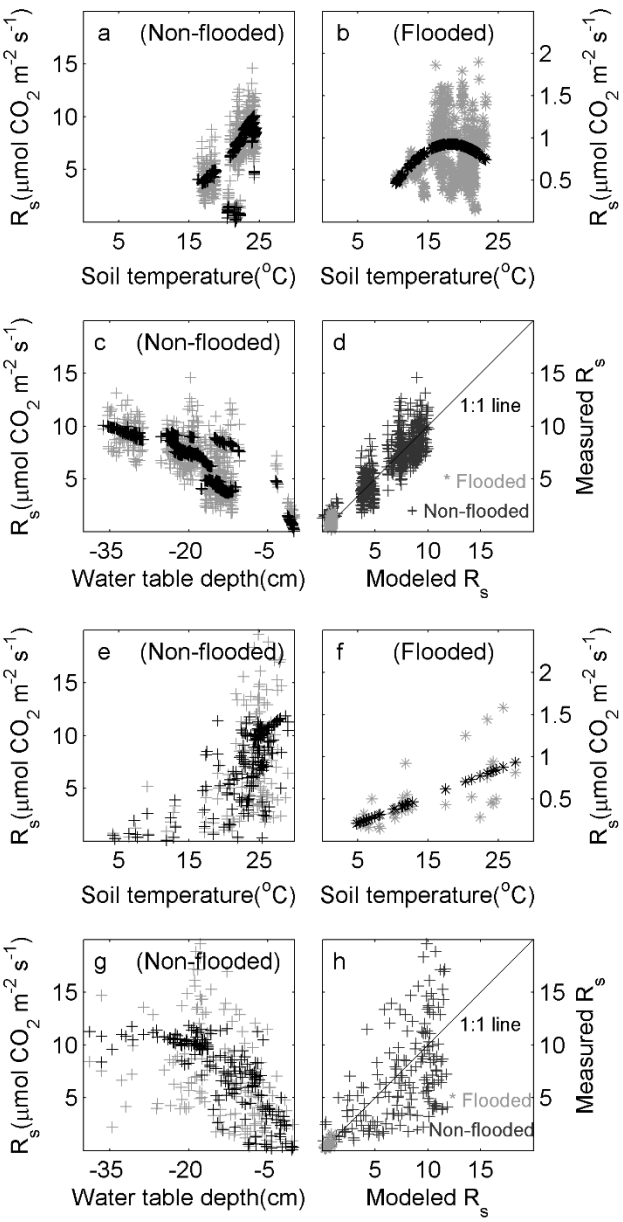

Figure 3-9 Soil temperature (T_s) and water table depth (WTD) effects on soil respiration (R_s) observed by both automated (a-d) and survey (e-h) measurements. The R_s under non-flooded conditions was modeled by the nested Q_{10} model with T_s and WTD; the R_s under flooded conditions modeled by a quadratic equation with only T_s involved. In a, b, c, e, f, and g, grey symbols represent for observations and black symbols for modeled results; d and h illustrate model performance.

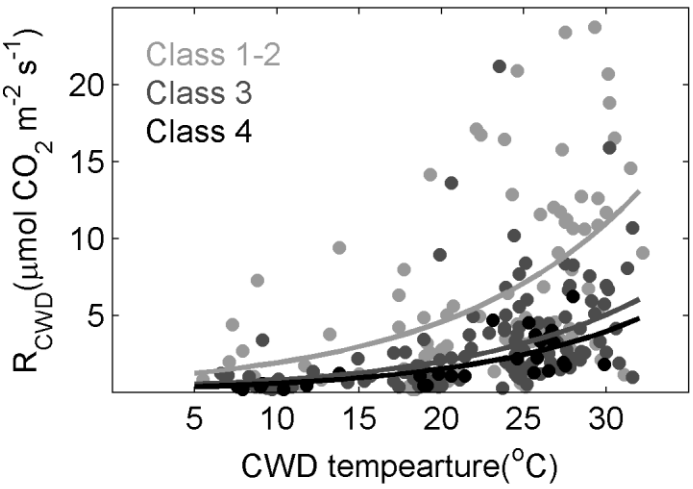

Figure 3-10 Observed (dots) and modeled (lines) temperature effect on the decomposition of coarse woody debris (R_{CWD}) in a lower coastal plain forested wetland. Coarse woody debris is classified by decay class, with the smaller number representing newer debris.

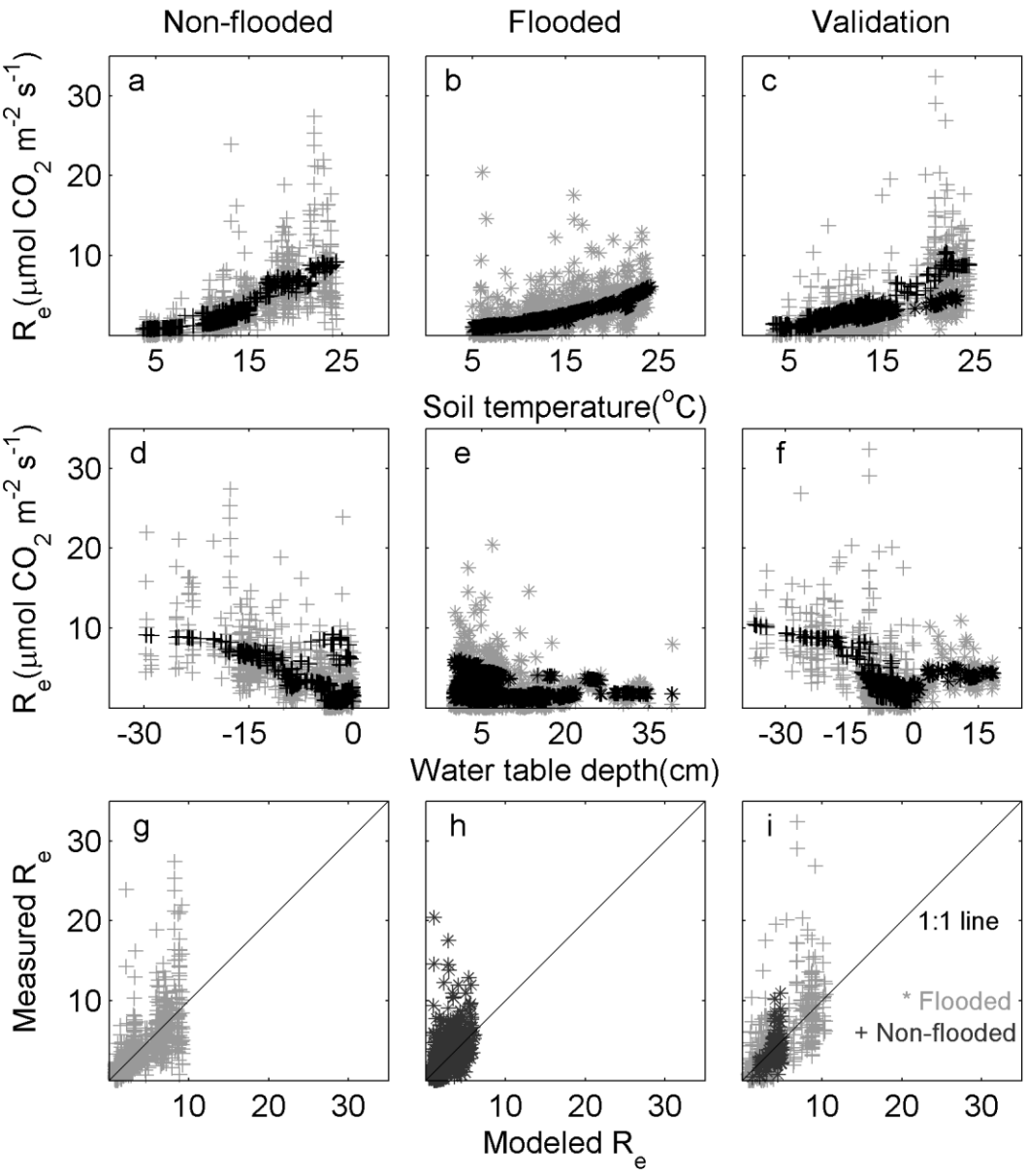

Figure 3-11 Observed (grey symbols) and modeled (black symbols) soil temperature (T_s) and water table depth (WTD) effects on ecosystem respiration (R_e) in a lower coastal plain forested wetland. In a, b, d, e, g and h were the data collected in 2009 and 2010 and used for model regression. In c, f and i were the data in 2011 and used for validation.

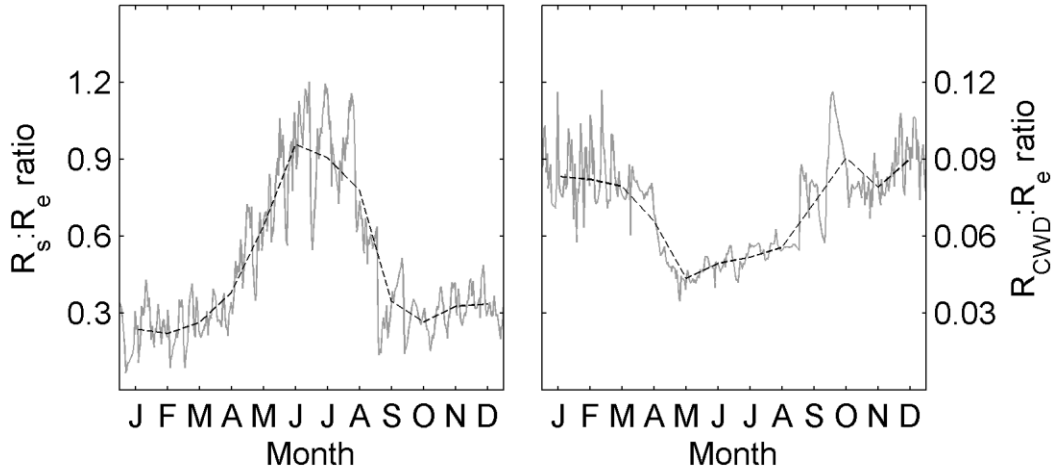

Figure 3-12 The daily (grey solid line) and monthly (black dotted line) (a) the ratio between soil respiration (R_s) and ecosystem respiration (R_e); (b) the ratio between the decomposition of coarse woody debris (R_{CWD}) and R_e, in a lower coastal plain forested wetland.

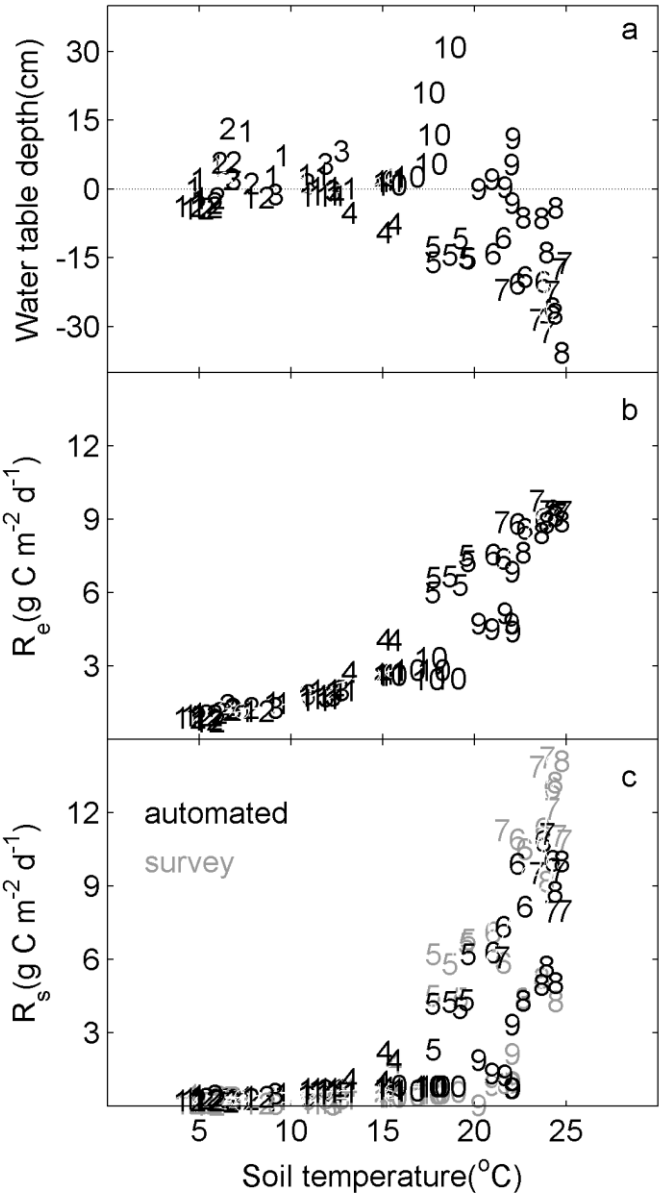

Figure 3-13 The relationship between daily (a) soil temperature (T_s) and water table depth (WTD), (b) T_s and ecosystem respiration (R_e) and (c) T_s and site average soil respiration (R_s) in 2010, showing the seasonal hysteresis of R_e and site average R_s, both of which was related to WTD but in a different magnitude. In (c), both automated and survey R_s measurements were presented.

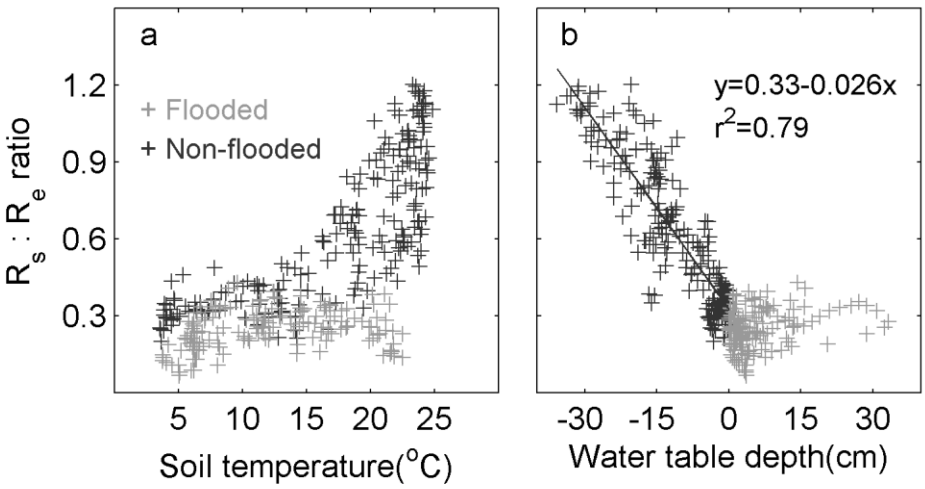

Figure 3-14 Soil temperature (T_s) and water table depth (WTD) effects on the ratio between soil respiration (R_s) and ecosystem respiration (R_e) in a lower coastal plain forested wetland.

CHAPTER 4. HYDROLOGIC CONTROL ON ^{13}C COMPOSITION OF SOIL-RESPIRED CO_2 IN A FORESTED WETLAND: METHODOLOGICAL CONSIDERATIONS FOR SOIL RESPIRATION PARTITIONING

Abstract

Two years of study on natural $\delta^{13}C$ of soil-respired CO_2 ($\delta^{13}C_{Rs}$) was conducted in a coastal plain forested wetland, of which the carbon dynamics are less-well investigated compared to upland forests, in southeastern USA. The study accounted for site microtopography, in which HIGH microsites where trees grow and the water table is below ground most of the time and non-vegetated LOW microsites which are flooded frequently after rainfall events. Seasonal variation of $\delta^{13}C_{Rs}$ was determined by microtopography and hydrologic effects jointly, differentiating the dominant component. The $\delta^{13}C_{Rs}$ at HIGH microsites was depleted during summer and enriched in spring and autumn, whereas the $\delta^{13}C_{Rs}$ at LOW microsites exhibited the opposite pattern ($\delta^{13}C_{Rs}$ was enriched during summer and depleted in spring). The more depleted $\delta^{13}C_{Rs}$ at HIGH microsites under drier conditions (-28.0±0.2‰, mean±SE) was similar to that at LOW microsites under near-saturated conditions (-28.3±0.3‰), which may be attributed to the increased relative contribution of root respiration (R_{root}, f_{root}) and litter decomposition (R_{litter}, f_{litter}) at those microsites, respectively. Conversely, the more enriched $\delta^{13}C_{Rs}$ at LOW microsites under drier conditions (-27.2±0.4‰) may result from the stimulation of soil organic carbon decomposition (R_{SOC}), similar to the $\delta^{13}C_{Rs}$ at HIGH microsites under near-saturated conditions (-27.1±0.2‰) due to the inhibition of water on R_{root}. Through the spatial difference in $\delta^{13}C_{Rs}$, we estimated the ratio of relative contribution of R_{SOC} to R_s (f_{SOC}) between HIGH and LOW microsites, i.e. $f_{SOC,HIGH}$:$f_{SOC,LOW}$ was 0.77±0.10 (mean±SE) under drier conditions and 1.56±0.23 under near-saturated conditions. Accounting for spatial (microtopographic) differences and hydrologic effects will improve

the stable isotope method for partitioning soil respiration between autotrophic and heterotrophic sources by decreasing uncertainty from the $\delta^{13}C$ of C_{SOC} and the ^{13}C fractionation of R_{SOC}, providing more information to solve the unknown terms in traditional end-member mixing models.

Abbreviations

Stable carbon isotope	^{13}C
^{13}C signature or ^{13}C composition	$\delta^{13}C$
Soil respiration (soil CO_2 efflux)	R_s
^{13}C composition of soil-respired CO_2	$\delta^{13}C_{Rs}$
Root respiration	R_{root}
Relative contribution of root respiration to soil respiration	f_{root}
Litter decomposition	R_{litter}
Relative contribution of litter respiration to soil respiration	f_{litter}
Soil organic carbon decomposition	R_{SOC}
Soil organic carbon content	C_{SOC}
^{13}C signature of soil organic carbon	$\delta^{13}C_{SOC}$
Relative contribution of soil organic carbon decomposition to soil respiration	f_{SOC}

1. Introduction

Wetlands store large amount of soil organic carbon (SOC) with the highest density of 72 kg C/m^2 (1 m deep) among all types of ecosystems due to the low decomposition rate [*Lugo et al.*, 1990]. This carbon pool is vulnerable to global warming, with potentially positive atmospheric feedbacks [*Ise et al.*, 2008]. Previous studies have found that soil respiration (R_s, defined as the soil CO_2 efflux from the ground surface) of wetlands has the potential of releasing an amount of CO_2 into the atmosphere comparable to upland ecosystems of similar climate zones [*Chimner*, 2004; *Miao et al.*, in review; *Raich and Schlesinger*, 1992]. Because R_s is a mixture of various carbon sources with differing sensitivities to environmental drivers and turnover rates, partitioning R_s is necessary to improve understanding of mechanisms controlling SOC mean residence times and their feedbacks to climate change [*Bird et al.*, 1996; *Knorr et al.*, 2005; *Liski et al.*, 1999].

Partitioning R_s has been broadly investigated by invasive methods such as direct root-exclusion, trenching, shading and clipping or tree girdling etc, but artifacts are associated with these methods due to altered environmental conditions affecting interactions between roots and microbes. Partitioning R_s under natural conditions with noninvasive methods, however, is still a current research challenge [*Hanson et al.*, 2000; *Kuzyakov*, 2006]. Stable carbon isotope (^{13}C) have been recognized for their value as tracers of ecological and physiological processes, with great potential for elucidating SOC cycling with minimal disturbance to the soil system [*Ehleringer et al.*, 2000; *Staddon*, 2004].

Several ^{13}C approaches have been broadly adopted in recent years. Using ^{13}C-labeled

sources (e.g. Högberg and Ekblad, 1996; Ekblad and Högberg, 2000) or growing C4-plants on C3-plant residue dominated soils or vice versa (e.g. Robinson and Scrimgeour 1995; Rochette et al. 1999) to obtain distinct ^{13}C signatures ($\delta^{13}C$) of carbon sources for partitioning R_s with end member mixing model are artificial. The former is limited for long-term investigation and the latter is restricted to extrapolate the study results to broader scales due to its unnatural system. Some studies used natural $\delta^{13}C$ to partition R_s by incubating roots, litter and soils separately, which also changes natural conditions, usually can only experiment for a short period, and the conclusion or implications differed greatly from each other [*Formánek and Ambus*, 2004; *Millard et al.*, 2010]. Many studies also examine the soil carbon content (C_{SOC}) and $\delta^{13}C$ of SOC ($\delta^{13}C_{SOC}$) in depth profiles, and use the C_{SOC}-$\delta^{13}C_{SOC}$ relationship to demonstrate the long-term decomposition rate of SOC [*Accoe et al.*, 2002; *Garten Jr*, 2006]. This method generally provides limited information on the response of dynamic processes to environmental changes.

The seasonal variation of $\delta^{13}C_{Rs}$ in a natural ecosystem has been investigated as a component of ecosystem respiration to help interpret the isotopic variation of ecosystem-respired CO_2, i.e. the ^{13}C exchange between atmosphere and biosphere [*Bowling et al.*, 2008; *Fung et al.*, 1997; *Marron et al.*, 2009; *Maunoury-Danger et al.*, 2013]. However, R_s in these studies is usually regarded as a source to ecosystem respiration, not a product from different sources. Currently the component contributions to R_s is still not the main objective in these studies. To date, still few studies on natural $\delta^{13}C_{Rs}$ investigated the seasonal variation of component contributions under natural conditions [*Risk et al.*, 2012; *Taneva and Gonzalez-*

Meler, 2011]. For comparison, there have been a number of studies on this issue with radiocarbon isotope method [*Gaudinski et al.*, 2000; *Schuur et al.*, 2009; *Trumbore*, 2000].

Application of the natural $\delta^{13}C_{Rs}$ is limited by several difficulties and uncertainties. The continuum of belowground carbon pools obscures to obtain distinguished ^{13}C signature of sources [*Dungait et al.*, 2012; *Phillips and Gregg*, 2001]. The ^{13}C fractionation of each respiration component is still uncertain and would bias the fraction estimation by end-member mixing model [*Dawson et al.*, 2002; *Werth and Kuzyakov*, 2010]. However, it is not convinced yet without sufficient studies that whether the information in $\delta^{13}C_{Rs}$ variation is confounded by these uncertainties or it could be useful for designing relevant field or modeling experiments to partition R_s.

Our previous studies in a forested wetland in North Carolina, USA, found that the spatial variation in aerobic R_s related to differences in microtopography and therefore hydrologic status, and related to plant distributions and the contributions from SOC decomposition (R_{SOC}) and plant-derived respiration (R_{plant}, including root respiration - R_{root} and litter decomposition - R_{litter}) [*Miao et al.*, in review]. The high mound microsites (HIGH) around tree bases may have higher contribution from R_{root} than the non-vegetated low-lying (LOW) microsites. Accordingly, in the current study we hypothesized that the $\delta^{13}C_{Rs}$ at HIGH microsites would be more depleted than at LOW microsites due to the higher contribution from R_{root} (with more depleted $\delta^{13}C$). In addition, we hypothesized the $\delta^{13}C_{Rs}$ would increase under warm and non-flooded conditions because of increased decomposition of the large stores of SOC in the organic soil.

The objectives of the current study were to provide baseline data on SOC dynamics in a forested wetland through natural $\delta^{13}C$ and to explore the potentials of using natural $\delta^{13}C$ to partitioning sources of R_s. We collected soil-respired CO_2 for ^{13}C analysis and quantified the seasonal and spatial dynamics of $\delta^{13}C_{Rs}$, and attempted to partition the component contributions to R_s reflected by $\delta^{13}C_{Rs}$, mainly focusing on the aerobic R_s. We also analyzed the C_{SOC}-$\delta^{13}C_{SOC}$ relationship for a preliminary estimate on long-term decomposition of SOC, which results from the cumulative effect of aerobic and anaerobic respiration in this intermittently flooded wetland.

2. Methods

2.1 Site description and field measurement design

This study was conducted in a lower coastal plain forested wetland in eastern North Carolina, USA ($35^0$47′N, $75^0$54′W) in the Alligator River National Wildlife Refuge. Mean annual temperature and precipitation from an adjacent meteorological station (Manteo AP, NC, $35^0$55′N, $75^0$42′W) for the period 1981-2010 were 16.9°C and 1270 mm, respectively. The forest type is mixed hardwood swamp forest. The overstory is predominantly composed of black gum (*Nyssa sylvatica*), swamp tupelo (*Nyssa biflora*) and bald cypress (*Taxodium distichum*), with occasional red maple (*Acer rubrum*) and white cedar (*Chamaecyparis thyoides*); the understory is predominantly fetterbush (*Lyonic lucida*), bitter gallberry (*Ilex galbra*), and red bay (*Persea borbonia*).

Aboveground carbon storage in live biomass was estimated allometrically at 37.5±12.5 Mg C ha^{-1}. Average carbon storage in live fine root biomass to a depth of 30 cm was 3.1±1.0

Mg C ha^{-1} and annual leaf litter fall was estimated at 1.9±0.2 Mg C ha^{-1} yr^{-1}. The soil types are poorly drained Pungo and Belhaven mucks. The soils are acidic with pH of 4.2-4.8 in surface horizons and the average carbon content of the soil profile (30 cm deep) ranges at 45-90 Mg C ha^{-1}.

Five 7-m-diameter survey plots in a 25-hectare square area centered on an eddy covariance tower were installed at the end of 2009, with one plot in the center and four plots at the four corners of the square. Six microsites were randomly selected within each 7-m-diameter plot, installed with 20-cm-diameter PVC static chambers to collect soil gas. We classified microsites as HIGH, where trees grew and the water table was below the soil surface most time of the year, and LOW, which were located in relatively non-vegetated areas that flooded frequently after rainfall events. Ten cm-tall chambers were installed at HIGH microsites and 25-cm-tall chambers at LOW microsites to avoid being submerged.

Soil CO_2 efflux was measured at all microsites. Gas samples for $\delta^{13}C_{Rs}$ analysis were collected from only one HIGH microsite and one LOW microsite at each plot, both of which were randomly selected at each sampling date. Sampling was conducted monthly from January 2010 to August 2011, covering two growing seasons. Chambers were moved to new microsites after 1-year of measurement to decrease bias caused by the disturbance to the soil. In total, 62 microsites were involved in R_s measurement, of which 22 were classified as HIGH and 40 were LOW.

2.2 Micrometeorology, water table depth and microtopography measurements

A ground meteorological station was built at the center plot where air temperature and

relative humidity (HMP45AC, Vaisala, Finland) at 2 m aboveground, soil temperature (T_s, CS 107, Campbell Scientific Inc. (CSI), UT, USA) at 5 and 20 cm belowground and volumetric soil water content (CS 616, CSI) at 20 cm belowground were recorded every 30 minutes. In each plot we installed a groundwater probe at the distance of 15-30 m away from the soil chambers to record water table depth (WTD) every 30 minutes. The microtopography of each microsite was measured with a tripod-mounted laser level (RoboLaser Green RT-7210-1G, RoboToolz Inc., CA, USA) providing a horizontal reference line. We then normalized the microtopography relative to the elevation of groundwater probe location at each plot. Water table depth of each microsite at each measuring date was calculated from the relative microtopography and the probe WTD readings (see Appendix B for details). The adjusted WTD was used to identify non-flooded and flooded conditions, defined as WTD<0 cm and WTD≥0 cm, respectively.

2.3 Gas sampling and $\delta^{13}C$ analysis of soil-respired CO_2

The design of gas sampling method to obtain $\delta^{13}C_{Rs}$ was based on the Keeling plot method which was developed from conservation of mass and is also an application of two-end member mixing models [*Keeling*, 1958; *Pataki et al.*, 2003]. The mass in this method refers to the concentration and $\delta^{13}C$ of CO_2 in soil chamber headspace, and the two end members are the soil-respired CO_2 and the CO_2 in the background air.

The static chamber at each sampling microsite was sealed for approximately-16.5 minutes and gas samples were collected with a gas tight syringe (50 ml Luer-lock syringe, SGE Analytical Science Pty Ltd, Australia) every 5.5 minutes (Figure 4-1). Samples were

stored in evacuated 12-ml glass vials fitted with rubber septa (12-ml Exetainer® vials, Labco Limited, UK). Soil temperature at 5 and 10 cm depth and volumetric water content were recorded during sampling. Gas samples were sent to Cornell University Stable Isotope Lab (COIL, New York, USA) for CO_2 concentration and $\delta^{13}C$ analysis. The $\delta^{13}C$ values were corrected against Vienna Pee Dee Belemnite standard.

In the sealed chambers, the change in CO_2 concentration and $\delta^{13}C$ can be simulated by Equation 1, in which C_a is the CO_2 concentration in the closed system at each sampling time; C_0 is the initial CO_2 concentration; $\delta^{13}C_a$ and $\delta^{13}C_0$ are the corresponding $\delta^{13}C$ of C_a and C_0. C_0 and $\delta^{13}C_0$ are constants. We assumed that C_{Rs} originated from proportionally stable, integrated carbon sources over a short time periods (e.g. 15-20 minutes), and therefore the $\delta^{13}C_{Rs}$ during the sampling period was also stable. C_a, C_{Rs} and $\delta^{13}C_a$ were assumed to vary during the sampling period. By combining the two sub-equations in Equation 1, we could derive a linear equation (Equation 2) in which the left side is the varying $\delta^{13}C_a$; the right side includes the reciprocal of C_a, the slope term consisting of constants, and the $\delta^{13}C_{Rs}$ (the intercept). Therefore, to obtain the value of $\delta^{13}C_{Rs}$, the C_a and $\delta^{13}C_a$ of the gas samples collected every 5.5 minutes were used for linear regression.

$$\begin{cases} C_a = C_0 + C_{Rs} \\ \left(\delta^{13}C_a\right)C_a = \left(\delta^{13}C_0\right)C_0 + \left(\delta^{13}C_{Rs}\right)C_{Rs} \end{cases} \quad (1)$$

$$\left(\delta^{13}C_a\right) = \left\{C_0\left[\left(\delta^{13}C_0\right) - \left(\delta^{13}C_{Rs}\right)\right]\right\}\frac{1}{C_a} + \left(\delta^{13}C_{Rs}\right) \quad (2)$$

The uncertainty of intercept, i.e. $\delta^{13}C_{Rs}$, is affected by the magnitude of soil CO_2 efflux

and the regression fitting [*Phillips and Gregg*, 2001]. To minimize the uncertainty, the data records whose regression R^2 was lower than 0.99 were excluded in our analysis (Figure 4-2). There were 89 (71%) acceptable data points of the total 125 collected.

2.4 Soil CO_2 efflux measurements

Soil CO_2 efflux at all microsites was manually measured with a portable IRGA (LI-8100, Licor Inc.) and a portable survey chamber (LI 8100-103, Licor Inc.). Soil temperature at 5 and 10 cm depth and volumetric soil water content at top 12 cm were recorded at each measurement. The data for which the deviation from the mean R_s was greater than three standard deviations were considered as outliers. Only 5 data were excluded of the total 342 collected.

For both $\delta^{13}C_{Rs}$ and R_s survey measurements, we combined the survey data collected from all microsites at the same day statistically to evaluate seasonal variation. When analyzing the effect of environmental drivers (T_s at 5 cm and WTD), we used the raw data and inherent spatial variation.

2.5 Ancillary measurements

The long-term SOC decomposition rate was estimated through the C_{SOC}-$\delta^{13}C_{SOC}$ relationship. Soil cores were collected from three of the five survey plots with a peat sampler (Eijkelkamp Agrisearch Equipment, Giesbeek, NL). Due to the spatial differences in the soil profile, we distinguished soil layers by color instead of arbitrary, fixed depth. The black top-layer was identified as organic soil texture and the brown sub-layer as the mixture of organic and mineral (clay) texture. At each plot, several cores were collected, separated into the two

layers by color, and aggregated. The density (d)-fractionation method, adapted from Baisden et al. [2002] and Tu et al. [2006], was used to physically separate soil samples into three fractions (F1: d<1.0, F2: 1.0<d<1.6, and F3: d>1.6 g cm^{-3}). Each fraction of samples was grounded and analyzed for $\delta^{13}C_{SOC}$ and C_{SOC}.

The $\delta^{13}C_{SOC}$ and $\ln(C_{SOC}/C_{SOC,0})$ were then regressed based on the Rayleigh equation (Equation 3), which describes the gradual enrichment in $\delta^{13}C_{SOC}$ during long-term decomposition, to calculate the slope ε defined as enrichment factor [*Balesdent and Mariotti*, 1996]. $C_{SOC,0}$ and $\delta^{13}C_{SOC,0}$ represents the initial values of C_{SOC} and $\delta^{13}C_{SOC}$. $C_{SOC,0}$ was approximated by the highest value of C_{SOC} in all the SOC samples, which was from the F1 of the top-layer. Modified from the fixed-depth profile method used in literature in which bulk SOC was analyzed [*Accoe et al.*, 2002; *Diochon and Kellman*, 2008], this fractionation method attempts to account for both the soil structure and depth effects [*McFarlane et al.*, 2013; *Trumbore*, 2000].

$$\delta^{13}C_{SOC} = \delta^{13}C_{SOC,0} + \varepsilon \ln \frac{C_{SOC}}{C_{SOC,0}} \quad (3)$$

3. Results

3.1 Site meteorology

The meteorological conditions were similar between the two years of the study period (Figure 4-3). The annual mean air temperature was 16.4 and 17.1°C in 2010 and 2011, respectively, which was close to the 30-year normal of 16.9°C. Mean annual T_s was 15.0 and 15.5 °C in 2010 and 2011, respectively. Precipitation from January to August was similar

between the two years with the respective amounts of 614 and 547 mm. Mean WTD from water table probe from April to August, when most of the ^{13}C data were collected, was also similar between 2010 and 2011, at -10.6 cm and -11.4 cm, respectively. Seasonal pattern of soil temperature from the survey microsites was consistent with the data from the ground meteorological station (Figure 4-3 a), indicating that the spatial difference in T_s was small.

3.2 Seasonal and spatial variation of $\delta^{13}C$ of soil-respired CO_2

The range of seasonal variation in $\delta^{13}C_{Rs}$ was approximately at 7.8‰, with significant differences between non-flooded ($\delta^{13}C_{Rs\text{-}NFL}$) and flooded ($\delta^{13}C_{Rs\text{-}FL}$) periods. The $\delta^{13}C_{Rs\text{-}NFL}$ was more depleted than $\delta^{13}C_{Rs\text{-}FL}$ (Table 4-1). The $\delta^{13}C_{Rs\text{-}NFL}$ was -27.8±1.5‰ (mean±SD), with a range of -30.6 to -25.9‰ (i.e. 4.7‰). The $\delta^{13}C_{Rs\text{-}FL}$ was -24.0±2.8‰, with a range of -28.2 to -22.8‰ (i.e. 5.4‰). Both HIGH and LOW microsites had $\delta^{13}C_{Rs\text{-}NFL}$ records, and only LOW microsites recorded $\delta^{13}C_{Rs\text{-}FL}$ after September.

The $\delta^{13}C_{Rs}$ exhibited different seasonal variation between microsites (Figure 4-4). At HIGH microsites, the $\delta^{13}C_{Rs}$ decreased gradually from January to August, whereas R_s increased gradually. The $\delta^{13}C_{Rs}$ increased after September while the R_s decreased. This seasonal pattern was consistent for 2010 and 2011. The $\delta^{13}C_{Rs}$ was depleted during summer with the $\delta^{13}C_{Rs}$ ranging -28.5 to -27.7‰ in 2010 and -28.4 to -28.0‰ in 2011, and was more enriched during other seasons with the $\delta^{13}C_{Rs}$ of -27.4 to -25.9‰. The magnitude of $\delta^{13}C_{Rs}$ values was also consistent for 2010 and 2011, although the overall R_s was lower in 2011 than in 2010.

There were no available $\delta^{13}C_{Rs}$ data at LOW microsites in winter and early spring until

May, when the soil surface at LOW microsites became exposed to the air. In both 2010 and 2011, the $\delta^{13}C_{Rs}$ exhibited increased from May to August when R_s increased as well (Figure 4-4). The range of $\delta^{13}C_{Rs}$ during summer at LOW microsites was -28.8 to -27.5‰ and -28.2 to -27.0‰ in 2010 and 2011, respectively. The increasing pattern of $\delta^{13}C_{Rs}$ from May to August at LOW microsites was opposite to the decreasing pattern at HIGH microsites during the same period, but the range of $\delta^{13}C_{Rs}$ values was similar in magnitude between microsites.

3.3 Hydrological effect on $\delta^{13}C$ of soil-respired CO_2

Most of the acceptable data came from the middle of the growing season. As a result, T_s was limited to the range of 15-25°C. The range in WTD was 0 to -30 cm at HIGH microsites, and from -5 to -20 cm at LOW microsites under non-flooded conditions, and from 5 to 15 cm under flooded conditions (Figure 4-5). There was a clear divergence in the T_s-$\delta^{13}C_{Rs}$ relationship at HIGH microsites (Figure 4-5 a) when T_s was between 15 and 25°C, which could be related to the difference in WTD (Figure 4-5 b). Due to the narrow T_s range at LOW microsites, the T_s-$\delta^{13}C_{Rs}$ relationship did not exhibit a clear pattern. In contrast, the response to WTD was well defined at both HIGH and LOW microsites.

The hydrologic effect on $\delta^{13}C_{Rs}$ was remarkable between the flooded and non-flooded conditions. The $\delta^{13}C_{Rs\text{-}FL}$ was more enriched at -24.7±0.6‰ (mean±SE) than the $\delta^{13}C_{Rs\text{-}NFL}$ of -27.8±0.1‰ ($p=0.0002$). This effect also exhibited distinct pattern under non-flooded conditions with WTD=-13 cm marking the transition point. At HIGH microsites, the $\delta^{13}C_{Rs\text{-}NFL}$ was -27.1±0.2‰ when -13<WTD<0 cm (near-saturated conditions), and was -28.0±0.2‰ when WTD<-13 cm, the difference being statistically significant ($p=0.006$; Figure 4-6 a).

The difference at LOW microsites exhibited the opposite pattern. The $\delta^{13}C_{Rs\text{-}NFL}$ was -28.3±0.3‰ when -13<WTD<0 cm, and was -27.2±0.4‰ when WTD<-13 cm, in which the case of shallower WTD was significantly more depleted (p=0.02; Figure 4-6 b).

3.4 The content and $\delta^{13}C$ of soil organic carbon

With two layers and three fractions identified, the $\delta^{13}C_{SOC}$ at this forested wetland averaged -29.0±0.7‰ (mean±SD) and ranged from -30.1 to -27.7‰ (i.e. a range of 2.4‰). The C_{SOC} averaged 19.4±18.0% and ranged from 0.2 to 57.8% (Table 4-1). The C_{SOC} and $\delta^{13}C_{SOC}$ were not significantly different between F1 and F2; but F3, the fraction of highest density was significantly lower in C_{SOC} and more enriched in $\delta^{13}C_{SOC}$ than the two lighter fractions. This also implied that two fractions (i.e. d<1.6 g cm^{-3} and d>1.6 g cm^{-3}) could be sufficient to represent the fraction in this wetland soil. In F1 and F2, the sub-layer exhibited lower C_{SOC} and more enriched $\delta^{13}C_{SOC}$ than the top-layer (Figure 4-7). The relationship between C_{SOC} and $\delta^{13}C_{SOC}$ was well-fit by the Rayleigh equation (equation 3) across all the three fractions. The enrichment factor ε was -0.4±0.0‰ (mean±SE). The regression of the two lighter fractions derived the enrichment factor of -0.6±0.1‰.

4. Discussion

4.1 Overview of soil $\delta^{13}C$ data in a forested wetland relative to other ecosystems

The average values of $\delta^{13}C_{SOC}$ (-29.1±0.8‰) and $\delta^{13}C$ values of the three soil fractions in our forested wetland (Table 4-1) were more depleted than those reported in an earlier study for mid-latitude upland soils (-27.7±0.6‰, 20-40°N or S) and the average $\delta^{13}C$ for forest soils (-27.7±0.8‰) [*Bird et al.,* 1996]. Only two F3 samples from the sub-layer were similar to

values reported in the literature. This depleted trend could result from several causes. Firstly, the fractionation in photosynthesis and microbial decomposition may play roles in this difference between ecosystems [*Ehleringer et al.*, 2000; *Ehleringer et al.*, 2002]. Secondly, the $\delta^{13}C$ of atmospheric CO_2 has been decreasing since the beginning of the Industrial Revolution, reported as decreasing from -6.8‰ in 1940 to -7.8‰ in 1988 [*Fung et al.*, 1997], and recently about -8.3‰ [*GLOBALVIEW-CO2C13*, 2009]. The impact from atmospheric CO_2 on the decade scale of $\delta^{13}C_{SOC}$ variation is still uncertain. In the study of Bird et al. [1996], it was suggested that the top-layer of soil and lighter fractions were from recent plant residues which would decrease in parallel with the atmosphere.

The range of seasonal $\delta^{13}C_{Rs\text{-}NFL}$ variation in this forested wetland (4.7‰) was the same as reported for upland ecosystems (1-8‰) [*Andrews et al.*, 1999; *Kodama et al.*, 2008; *Risk et al.*, 2012]. The average $\delta^{13}C_{Rs\text{-}NFL}$ (-27.8±1.5‰) was slightly more depleted than the $\delta^{13}C_{Rs}$ from a hardwood forest (-26.2±0.8‰) and a loblolly pine plantation (-26.9±1.8‰) in an adjacent area in North Carolina [*Mortazavi et al.* 2005]. It was also more depleted than the $\delta^{13}C_{Rs}$ from some other temperate forests [*Kodama et al.*, 2008; *Maunoury-Danger et al.*, 2013], but similar to that from some boreal forests [*Risk et al.*, 2012]. As the product of R_{root} and R_{SOC}, the difference in $\delta^{13}C_{Rs}$ was also associated with the difference in $\delta^{13}C_{SOC}$ between ecosystems and associated uncertainties of fractionation processes.

The enrichment factor (-0.4‰ and -0.6‰) from this wetland soil was lower than that reported from the soil in some upland forests and agricultural systems, for example, a northern forest (-0.8‰) [*Natelhoffer and Fry*, 1988], and an agricultural station (-2.3‰)

[*Accoe et al.*, 2002]. 'Enrichment factor' concept is still being debated because of uncertainties of the enrichment mechanisms [*Ehleringer et al.*, 2000; *Werth and Kuzyakov*, 2010]. However, the differences between this forested wetland, an upland forest and an agricultural ecosystem are consistent with current theoretical understanding. The lower enrichment factor at the forested wetland, compared to upland forests and agricultural fields can be attributed to lower decomposition rates in the former.

4.2 Difference between $\delta^{13}C$ of soil-respired CO_2 and $\delta^{13}C$ of soil organic carbon

The range of $\delta^{13}C_{Rs\text{-}NFL}$ values was broader than for $\delta^{13}C_{SOC}$ (2.4‰). The minimum $\delta^{13}C_{Rs\text{-}NFL}$ was similar to the $\delta^{13}C$ of leaf litter (-30.6±0.6‰) in this wetland, whereas the maximum $\delta^{13}C_{Rs}$ (-25.9‰) was more enriched than the most enriched $\delta^{13}C_{SOC}$ (F3, -27.7‰). The average $\delta^{13}C_{Rs\text{-}NFL}$ was also more enriched than the average $\delta^{13}C_{SOC}$ (Table 4-1). If we assume that plant-derived carbon sources, i.e. plant litter and roots, were the new carbon source and SOC was the old carbon source, these differences demonstrate the potential limitation of end member mixing models on this system because the $\delta^{13}C$ of products was out of the $\delta^{13}C$ range of sources [*Dawson et al.*, 2002; *Phillips and Gregg*, 2001]. This marked difference might partly result from the ^{13}C fractionation of respiratory components. Previous studies have found that the $\delta^{13}C$ of R_{root} was more depleted (-2.1±2.2‰) than $\delta^{13}C$ of root tissue for C3-plants and the $\delta^{13}C$ of R_{SOC} was more enriched (+0.7±2.8‰) than $\delta^{13}C_{SOC}$ [*Werth and Kuzyakov*, 2010]. In order to explain the observed difference, the ^{13}C fractionation of R_{SOC} in the current study must have been an enrichment and at the higher level of the average range in literature (+0.7±2.8‰) [*Werth and Kuzyakov*, 2010]. For

example, if F1 were the main old carbon source, the average ^{13}C fractionation must be greater than +1.8‰, i.e. the difference between the average $\delta^{13}C_{Rs\text{-}NFL}$ and the average $\delta^{13}C_{SOC}$ of F1 (Table 4-1).

4.3 $\delta^{13}C$ of soil-respired CO_2 reflecting the contribution of respiratory components

The observed either temporal or spatial variations in $\delta^{13}C_{Rs}$ could be caused by any of several factors – heterogeneity of source material, proximity to source, chemical decomposition pathways, environmental conditions, and physical emission pathways of produced CO_2, to name a few. Earlier studies argued that gas transport is the main factor resulting in the more enriched $\delta^{13}C_{Rs}$ of dry soils than wet soils, rather than biological fractionation [*Nickerson and Risk*, 2009; *Phillips et al.*, 2010]. If that were the case in the current study, the relationship between WTD and $\delta^{13}C_{Rs\text{-}NFL}$ should be consistent between HIGH and LOW microsites. However, the contrasting response of $\delta^{13}C_{Rs\text{-}NFL}$ to WTD suggests the biological control. Thus, the spatial variation in plant distribution has a quantifiable effect on contributions from different respiratory components.

As the major objective of this study is to investigate the temporal and spatial variation of $\delta^{13}C_{Rs}$ in a wetland, and explore the possibility of $\delta^{13}C$ utility for tracing the variation of component contributions to R_s under natural conditions, directly monitoring the variation in contribution from each component is beyond the scope of the study. However, we compared our current results with previous studies and speculated possible mechanisms which would be useful for future experiment designs.

It is generally accepted that $\delta^{13}C_{Rs}$ reflects the contribution of belowground carbon pools

[*Kuzyakov*, 2006; *Søe et al.*, 2004]. In the current study, the increase of R_{root} or R_{litter} would correspond to a depleted $\delta^{13}C_{Rs\text{-}NFL}$ and the enhanced R_{SOC} would result in an enriched $\delta^{13}C_{Rs}$. $\delta^{13}C_{Rs\text{-}NFL}$ decreased during warm season at HIGH microsites, which did not support our hypothesis of increased $\delta^{13}C_{Rs\text{-}NFL}$ during summer due to more active soil microbial activities. This may suggest that R_{root} increased more than R_{SOC} and contributed more to R_s although both may increase during the warmer and drier season. This pattern was consistent with observations in a previous study at the Duke-FACE experiment [*Andrews et al.*, 1999]. In that study, the $\delta^{13}C_{Rs}$ from the elevated CO_2 treatment plots, where the atmosphere was labeled by δ^{13}C-depleted CO_2, became increasingly depleted through the growing season when R_s increased. In our study, when WTD was shallower (closer to soil surface), R_{root} was decreased due to the near-saturated condition, resulting in the less depleted $\delta^{13}C_{Rs}$. When the site became drier during summer, R_{root} increased following the increased soil aeration, and as a result, $\delta^{13}C_{Rs\text{-}NFL}$ was more depleted.

The increase in $\delta^{13}C_{Rs\text{-}NFL}$ at LOW microsites was consistent with our initial hypothesis and with mineralization of older soil carbon shown in other systems. Several studies with radiocarbon isotope method observed a drop of ^{14}C values resulting from an increase in the relative contribution of old soil carbon [*Gaudinski et al.*, 2000; *Schuur et al.*, 2009]. Corresponding to the drop of radioactive ^{14}C composition, the stable $\delta^{13}C$ would increase with the higher contribution of old carbon due to its enriched signature [*Balesdent and Mariotti*, 1996; *Ladyman and Harkness*, 1980], which is the pattern that we observed at LOW microsites, i.e. more enriched $\delta^{13}C_{Rs\text{-}NFL}$ when WTD dropped further below the soil

surface.

4.4 Implication of spatial difference in $\delta^{13}C$ of soil-respired CO_2

There was a significant interaction between microtopography and fluctuating WTD on $\delta^{13}C_{Rs}$. Without separating WTD to two levels (i.e. WTD<-13 and -13<WTD<0 cm), there was no significant difference in $\delta^{13}C_{Rs\text{-}NFL}$ between HIGH and LOW microsites (p=0.4), with the value of -27.9±0.2‰ (mean±SE) at HIGH microsites and -27.7±0.2‰ at LOW microsites. By separating the WTD levels, spatial differences between HIGH and LOW microsites imply different relative contributions of individual respiration components.

Based on the spatial difference in $\delta^{13}C_{Rs}$ and the fraction calculation with end member mixing models [*Dawson et al.*, 2002], we were able to directly quantify the difference in relative contribution from R_{SOC} between HIGH and LOW microsites without the $\delta^{13}C_{Rsoc}$ information, the most uncertain term in end member mixing models. Assuming the $\delta^{13}C$ of individual carbon sources and the ^{13}C fractionation of respiratory components are homogeneous spatially within the forest stand, we could derive Equation 4 from a two-end member mixing model. In this equation, f_{SOC} represents the fraction of R_{SOC} in R_s, and $\delta^{13}C_{Rplant}$ for the $\delta^{13}C$ of plant-derived respiration (the mixture of R_{root} and R_{litter} in this study). The subscript 1 and 2 represent different microsites (e.g. HIGH and LOW).

$$\left.\begin{aligned} f_{SOC,1} &= \frac{\delta^{13}C_{Rs,1} - \delta^{13}C_{Rplant}}{\delta^{13}C_{Rsoc} - \delta^{13}C_{Rplant}} \\ f_{SOC,2} &= \frac{\delta^{13}C_{Rs,2} - \delta^{13}C_{Rplant}}{\delta^{13}C_{Rsoc} - \delta^{13}C_{Rplant}} \end{aligned}\right\} \Rightarrow \frac{f_{SOC,1}}{f_{SOC,2}} = \frac{\delta^{13}C_{Rs,1} - \delta^{13}C_{Rplant}}{\delta^{13}C_{Rs,2} - \delta^{13}C_{Rplant}} \quad (4)$$

If we assume no fractionation in the plant-derived respiration, the ratio of f_{SOC} between HIGH and LOW microsites when WTD<-13cm was estimated at 0.77±0.10 (mean±SE). The ratio less than 1 indicated that under drier conditions f_{SOC} was lower at HIGH microsites than at LOW microsites. The ratio at -13<WTD<0cm was estimated at 1.56±0.23, implying the opposite pattern that under near-saturated conditions f_{SOC} was higher at HIGH microsites than LOW microsites. This equation can also be used to calculate the change of component contribution when WTD varies at a given microsite, for example, the ratio between the two hydrologic regimes, i.e. WTD<-13 cm and -13<WTD<0 cm.

It was unexpected that the $\delta^{13}C_{Rs\text{-}NFL}$ at HIGH microsites when WTD<-13 cm was similar to the $\delta^{13}C_{Rs\text{-}NFL}$ at LOW microsites when -13<WTD<0 cm (both were more depleted). The R_s was contrasting with the higher rate in the former case at drier condition than in the latter one at near-saturated condition. We attribute this more depleted $\delta^{13}C_{Rs\text{-}NFL}$ to higher relative contribution from R_{root} (f_{root}) at HIGH microsites, compared to higher relative contribution from R_{litter} (f_{litter}) at LOW microsites. In other words, f_{SOC} was the same at the two cases according to Equation 4, and the plant-derived respiration approximated to each other in both cases, both of which resulted in similar $\delta^{13}C_{Rs\text{-}NFL}$. Likewise, $\delta^{13}C_{Rs\text{-}NFL}$ at HIGH microsites when -13<WTD<0 cm and the $\delta^{13}C_{Rs\text{-}NFL}$ at LOW microsites when WTD<-13cm were similar to each other, which could be attributed to lower f_{root} and higher f_{SOC}, respectively.

In order to test this hypothesis, we quantified leaf litter biomass from both HIGH and LOW microsites, and found that the amount of leaf litter was greater at LOW microsites ($p=0.056$, $n=12$). This accumulation of litter at LOW microsites was due to the interaction of

microtopography, vegetation and hydrology in this forested wetland with rapidly fluctuating WTD [*Ehrenfeld*, 1995; *Hardin and Wistendahl*, 1983]. Although previous studies have not specifically investigated the effect of microtopography on the distribution of leaf litter biomass within a forest stand, it has been found that forested wetlands generally have the highest depression storage among different types of terrestrial ecosystems [*Richards et al.*, 2012]. This difference in leaf litter storage between microsites also helps explain the more depleted $\delta^{13}C_{Rs\text{-}NFL}$ at LOW microsites than at HIGH microsites when -13<WTD<0 cm at both microsites (Figure 4-6), and when both R_{root} and R_{SOC} decreased under near-saturated condition.

Due to the difficulties encountered in root sampling during the study period, we could not evaluate the effects of root distribution between HIGH and LOW microsites. However, several studies in other wetlands reported higher root biomass and annual fine root production in hummocks than in hollows [*Jones et al.*, 1996; *Sullivan et al.*, 2008], analogous to HIGH and LOW microsites of the current study. Future work will elucidate the role of root distributions on R_s and $\delta^{13}C_{Rs}$.

In addition to the spatial distribution of belowground carbon sources, the difference in data coverage and environmental conditions during the study period at the two types of microsites might be also related to the spatial differences and is one source of the uncertainties. For example, the WTD range at LOW microsites was rather narrow compared to that at HIGH microsites. The surface soil VWC at both WTD levels (i.e. WTD<-13 cm and -13<WTD<0 cm) was generally lower at HIGH microsites than at LOW (Figure 4-8).

This may partly resulted from the depression storage of leaf litter as well, which could have significant impacts on leaf litter decomposition [*Prescott*, 2010; *Richards et al.*, 2012], and subsequently cause the spatial difference in $\delta^{13}C_{Rs\text{-}NFL}$.

4.5 Importance of microtopography

Microtopography is increasingly recognized as a key source of variability of biogeochemical processes in wetland ecosystems [*Frei et al.*, 2012; *Van der Ploeg et al.*, 2012]. Although the mechanistic link between microtopography and carbon cycling is still poorly characterized, mechanisms proposed above qualitatively demonstrate the importance of microtopography. Without accounting for effects of microtopographic position and hydrologic conditions, the contrasting contributions from R_{root}, R_{litter} and R_{SOC}, and their sensitivity to environmental drivers, may well mask the signals in each other.

We have observed significant differences in environmental sensitivity of R_s at different microsites at this forested wetland [*Miao et al.*, in review], and ecosystem-level soil gas fluxes are integrate contributions from all microtopographic positions. The greater percentage of HIGH microsites where the total R_s is generally higher would result in large amount of site average CO_2 emission. If the total R_s were more attributed to R_{root} than to R_{SOC}, as shown by the depleted $\delta^{13}C_{Rs\text{-}NFL}$ during summer at HIGH microsites, the long-term positive feedback of soils in this system might be smaller than the trend reflected by the large amount of site average R_s because of the rapid carbon turnover in roots [*Norby et al.*, 2002; *Pendall et al.*, 2004]. However, the enriched $\delta^{13}C_{Rs\text{-}NFL}$ at LOW microsites still implies potential increase of net carbon release from SOC.

4.6 Methodological potentials and challenges

Seasonal variation of R_s at both HIGH and LOW microsites observed with the survey measurements of the current study was generally consistent with the pattern we observed with an automated R_s system on a spatially-restricted but continuously monitored subset of sampling locations [*Miao et al.*, in review]. Variation in microsite physical dimensions of the survey measurements may have introduced unexplained variation in R_s compared to automated R_s system. Therefore, the difference in the magnitude of total R_s between the two types of microsites shown in survey measurements was not as clear as that in continuous measurements (Figure 4-4) [*Miao et al.*, in review]. Despite this uncertainty in survey R_s measurements, the clear difference in $\delta^{13}C_{Rs}$ between microsites supported our hypothesis that (1) the spatial differences in R_s observed in continuous measurements at microsites in different microtopography are related to the contribution of component processes, and (2) R_{root} (i.e. autotrophic respiration) may contribute more to R_s at HIGH microsites, whereas the R_{SOC} and R_{litter} (i.e. heterotrophic respiration) contributes more at LOW microsites. These results also support the validity of using the spatial difference for partitioning R_s. With only the $\delta^{13}C$ information, the relative change of the component contributions can be quantified with less uncertainty related to the $\delta^{13}C_{Rsoc}$. This has important implications for ecosystems in which obtaining distinct $\delta^{13}C$ and ^{13}C fractionation rate of R_{SOC} is difficult. When designing experiments with consistent measurements of both R_s and $\delta^{13}C_{Rs}$ at representative microsites, it will be possible to quantify the absolute contributions of different respiration sources without disturbing the soil because spatial differences and hydrologic effects would

provide more information for solving the unknown terms in end member mixing models.

This methodology of using stable isotopes to distinguish component sources of R_s may have application beyond forested wetlands. Many studies observed seasonal hysteresis in R_s and suggested it may be related to the seasonal variation of component contributions. For example, higher R_s early in the growing season compared to late in the year was attributed to high rates of fine root production [*Gaumont-Guay et al.*, 2006; *Vargas and Allen*, 2008]. The opposite pattern has also been observed, higher R_s late in the growing season, and it was suggested that microbial activity was stimulated by the warming of deeper soil layers [*Drewitt et al.*, 2002; *Goulden et al.*, 1998; *Morén and Lindroth*, 2000; *S C Phillips et al.*, 2010]. These studies were unable to test these hypotheses, and few partitioning studies have explicitly discussed seasonal variation of contributions from different R_s components. For comparison, these two opposing patterns corresponded to the seasonal variations we observed at HIGH and LOW microsites, respectively. While there are no studies yet, to our knowledge, to evaluate the component contributions through the spatial variation in $\delta^{13}C_{Rs}$ within an ecosystem, we would suggest to test this method in other ecosystems. This type of spatial variation observed in our site would not be a specific characteristic in wetlands as the soil heterogeneity and corresponding plant distribution difference also clearly exists in upland or dryland ecosystems [*Gibson*, 1988; *Parker and Van Lear*, 1996; *Richards et al.*, 2012].

Because it is difficult to directly measure the $\delta^{13}C$ of components such as $\delta^{13}C_{Rroot}$ or $\delta^{13}C_{Rsoc}$, the use of stable carbon isotopes to partition sources of R_s described above is based

on the assumption that the $\delta^{13}C$ of respiratory components is stable over time, which is also an assumption of end member mixing models [*Taneva and Gonzalez-Meler*, 2011]. Further it has also been assumed that the ^{13}C fractionation of respiration processes is also constant when partitioning R_s based on the $\delta^{13}C$ of carbon sources [*Lin et al.*, 1999]. Both assumptions require further study/verification and remain challenge for the application of ^{13}C methods to understand soil carbon dynamics [*Kuptz et al.*, 2011].

5. Conclusions

The seasonal variation of ^{13}C composition ($\delta^{13}C$) of soil-respired CO_2 ($\delta^{13}C_{Rs}$) was investigated in a coastal plain forested wetland in southeastern USA from early 2010 to summer 2011, with the objective to provide insights on partitioning the varying contribution of individual respiratory components to total soil respiration. This study accounted for effects of microtopography by quantifying R_s and $\delta^{13}C_{Rs}$ separately at HIGH and LOW microsites as affected by rapidly fluctuating WTD. Microtopography and hydrology interacted to significantly affect seasonal variation of $\delta^{13}C_{Rs}$, indicative of the contributions of different source components. The $\delta^{13}C_{Rs}$ at a given microsite was significantly different between drier conditions (WTD<-13 cm) and near-saturated conditions (-13<WTD<0 cm). Under a certain hydrologic regime, the $\delta^{13}C_{Rs}$ also differed significantly between the two types of microsites. The more depleted $\delta^{13}C_{Rs}$ at HIGH microsites under drier conditions was similar to that at LOW microsites under near-saturated conditions, which may attribute to the increased relative contribution of root respiration and litter decomposition, respectively. On contrary, the more enriched $\delta^{13}C_{Rs}$ at LOW microsites under drier conditions may have resulted from

the stimulation of soil organic carbon decomposition, similar to the $\delta^{13}C_{Rs}$ at HIGH microsites under wet conditions due to the inhibition from water on root respiration. This spatial difference and hydrologic effects would improve the stable isotope method to partition soil respiration by providing more information to solve the unknown terms in traditional end member mixing models and reducing the uncertainty from the $\delta^{13}C$ of soil organic carbon decomposition.

References

Accoe, F., P. Boeckx, O. Van Cleemput, G. Hofman, Y. Zhang, R. H. Li, and G. X. Chen (2002), Evolution of the delta C-13 signature related to total carbon contents and carbon decomposition rate constants in a soil profile under grassland, *Rapid Commun. Mass Spectrom.*, *16*(23), 2184-2189.

Andrews, J. A., K. G. Harrison, R. Matamala, and W. H. Schlesinger (1999), Separation of root respiration from total soil respiration using carbon-13 labeling during Free-Air Carbon Dioxide Enrichment (FACE), *Soil Sci. Soc. Am. J.*, *63*(5), 1429-1435.

Balesdent, J., and A. Mariotti (1996), Measurement of soil organic matter turnover using 13C natural abundance, in *Mass spectrometry of soils*, edited by T. W. Boutton and S.-I. Yamasaki, Marcel Dekker, New York, New York, USA.

Bird, M. I., A. R. Chivas, and J. Head (1996), A latitudinal gradient in carbon turnover times in forest soils, *Nature*, *381*(6578), 143-146.

Bowling, D. R., D. E. Pataki, and J. T. Randerson (2008), Carbon isotopes in terrestrial ecosystem pools and CO2 fluxes, *New Phytologist*, *178*(1), 24-40.

Chimner, R. A. (2004), Soil respiration rates of tropical peatlands in Micronesia and Hawaii, *Wetlands*, *24*(1), 51-56.

Dawson, T. E., S. Mambelli, A. H. Plamboeck, P. H. Templer, and K. P. Tu (2002), Stable isotopes in plant ecology, *Annual Review of Ecology and Systematics*, *33*, 507-559.

Diochon, A., and L. Kellman (2008), Natural abundance measurements of ^{13}C indicate increased deep soil carbon mineralization after forest disturbance, *Geophysical Research Letters*, *35*(14), L14402.

Drewitt, G. B., T. A. Black, Z. Nesic, E. R. Humphreys, E. M. Jork, R. Swanson, G. J. Ethier, T. Griffis, and K. Morgenstern (2002), Measuring forest floor CO_2 fluxes in a Douglas-fir forest, *Agricultural and Forest Meteorology*, *110*, 299-317.

Dungait, J. A. J., D. W. Hopkins, A. S. Gregory, and A. P. Whitmore (2012), Soil organic matter turnover is governed by accessibility not recalcitrance, *Global Change Biology*, *18*(6), 1781-1796.

Ehleringer, J. R., N. Buchmann, and L. B. Flanagan (2000), Carbon isotope ratios in belowground carbon cycle processes, *Ecological Applications*, *10*(2), 412-422.

Ehleringer, J. R., D. R. Bowling, L. B. Flanagan, J. Fessenden, B. Helliker, L. A. Martinelli, and J. P. Ometto (2002), Stable isotopes and carbon cycle processes in forests and grasslands, *Plant Biology*, *4*(2), 181-189.

Ehrenfeld, J. G. (1995), Microtopography and vegetation in Atlantic white cedar swamps: the effects of natural disturbances, *Canadian Journal of Botany*, *73*(3), 474-484.

Formánek, P., and P. Ambus (2004), Assessing the use of $\delta^{13}C$ natural abundance in separation of root and microbial respiration in a Danish beech (*Fagus sylvatica L.*) forest, *Rapid Commun. Mass Spectrom.*, *18*(8), 897-902.

Frei, S., K. H. Knorr, S. Peiffer, and J. H. Fleckenstein (2012), Surface micro-topography causes hot spots of biogeochemical activity in wetland systems: A virtual modeling experiment, *Journal of Geophysical Research: Biogeosciences*, *117*(G4), G00N12.

Fung, I., et al. (1997), Carbon 13 exchanges between the atmosphere and biosphere, *Global Biogeochemical Cycles*, *11*(4), 507-533.

Garten Jr, C. T. (2006), Relationships among forest soil C isotopic composition, partitioning, and turnover times, *Canadian Journal of Forest Research*, *36*(9), 2157-2167.

Gaudinski, J., S. Trumbore, E. Davidson, and S. Zheng (2000), Soil carbon cycling in a temperate forest: radiocarbon-based estimates of residence times, sequestration rates and partitioning of fluxes, *Biogeochemistry*, *51*(1), 33-69.

Gaumont-Guay, D., T. A. Black, T. J. Griffis, A. G. Barr, R. S. Jassal, and Z. Nesic (2006), Interpreting the dependence of soil respiration on soil temperature and water content in a

boreal aspen stand, *Agricultural and Forest Meteorology*, *140*(1–4), 220-235.

Gibson, D. J. (1988), The relationship of sheep grazing and soil heterogeneity to plant spatial patterns in dune grassland, *Journal of Ecology*, *76*(1), 233-252.

GLOBALVIEW-CO2C13 (2009), Cooperative Atmospheric Data Integration Project - $\delta^{13}C$ of Carbon Dioxide. CD-ROM, NOAA ESRL, Boulder, Colorado [Also available on Internet via anonymous FTP to ftp.cmdl.noaa.gov, Path: ccg/co2c13/GLOBALVIEW].

Goulden, M. L., et al. (1998), Sensitivity of boreal forest carbon balance to soil thaw, *Science*, *279*(5348), 214-217.

Hanson, P. J., N. T. Edwards, C. T. Garten, and J. A. Andrews (2000), Separating root and soil microbial contributions to soil respiration: A review of methods and observations, *Biogeochemistry*, *48*(1), 115-146.

Hardin, E. D., and W. A. Wistendahl (1983), The effects of floodplain trees on herbaceous vegetation patterns, microtopography and litter, *Bulletin of the Torrey Botanical Club*, *110*(1), 23-30.

Ise, T., A. L. Dunn, S. C. Wofsy, and P. R. Moorcroft (2008), High sensitivity of peat decomposition to climate change through water-table feedback, *Nature Geoscience*, *1*, 763-766.

Jones, R. H., B. G. Lockaby, and G. L. Somers (1996), Effects of microtopography and disturbance on fine-root dynamics in wetland forests of low-order stream floodplains, *American Midland Naturalist*, *136*(1), 57-71.

Keeling, C. D. (1958), The concentration and isotopic abundances of atmospheric carbon dioxide in rural areas, *Geochim. et Cosmochim. Acta*, *13*, 322-334.

Knorr, W., I. C. Prentice, J. I. House, and E. A. Holland (2005), Long-term sensitivity of soil carbon turnover to warming, *Nature*, *433*(7023), 298-301.

Kodama, N., et al. (2008), Temporal dynamics of the carbon isotope composition in a Pinus sylvestris stand: from newly assimilated organic carbon to respired carbon dioxide, *Oecologia*, *156*(4), 737-750.

Kuptz, D., R. Matyssek, and T. E. E. Grams (2011), Seasonal dynamics in the stable carbon isotope composition ($\delta^{13}C$) from non-leafy branch, trunk and coarse root CO_2 efflux of adult deciduous (*Fagus sylvatica*) and evergreen (*Picea abies*) trees, *Plant, Cell & Environment*, *34*(3), 363-373.

Kuzyakov, Y. (2006), Sources of CO_2 efflux from soil and review of partitioning methods, *Soil Biology and Biochemistry*, *38*(3), 425-448.

Ladyman, S. J., and D. D. Harkness (1980), Carbon isotope measurement as an index of soil development, *Radiocarbon*, *22*(3), 885-891.

Lin, G., J. R. Ehleringer, P. T. Rygiewicz, Mark G. Johnson, and David T. Tingey (1999), Elevated CO_2 and temperature impacts on different components of soil CO_2 efflux in Douglas-fir terracosms, *Global Change Biology*, *5*(2), 157-168.

Liski, J., H. Ilvesniemi, A. Mäkelä, and C. J. Westman (1999), CO_2 emissions from soil in response to climatic warming are overestimated: The decomposition of old soil organic matter is tolerant of temperature, *Ambio*, *28*(2), 171-174.

Lugo, A. E., S. Brown, and M. Brinson (1990), *Forested wetlands*, Elsevier, Amsterdam, Netherlands.

Marron, N., C. Plain, B. Longdoz, and D. Epron (2009), Seasonal and daily time course of the 13C composition in soil CO_2 efflux recorded with a tunable diode laser spectrophotometer (TDLS), *Plant Soil*, *318*(1-2), 137-151.

Maunoury-Danger, F., et al. (2013), Carbon isotopic signature of CO_2 emitted by plant compartments and soil in two temperate deciduous forests, *Annals of Forest Science*, *70*(2), 173-183.

McFarlane, K., M. Torn, P. Hanson, R. Porras, C. Swanston, M. Callaham, Jr., and T. Guilderson (2013), Comparison of soil organic matter dynamics at five temperate deciduous forests with physical fractionation and radiocarbon measurements, *Biogeochemistry*, *112*(1-3), 457-476.

Miao, G., A. Noormets, J.-C. Domec, C. Trettin, S. G. McNulty, G. Sun, and J. S. King (in review), The effect of water table fluctuation on soil respiration in a lower coastal plain forested wetland in southeastern USA, *Journal of Geophysical Research: Biogeosciences*.

Millard, P., A. J. Midwood, J. E. Hunt, M. M. Barbour, and D. Whitehead (2010), Quantifying the contribution of soil organic matter turnover to forest soil respiration, using natural abundance $\delta^{13}C$, *Soil Biology and Biochemistry*, *42*(6), 935-943.

Morén, A.-S., and A. Lindroth (2000), CO_2 exchange at the floor of a boreal forest, *Agricultural and Forest Meteorology*, *101*, 1-14.

Natelhoffer, K. J., and B. Fry (1988), Controls on natural nitrogen-15 and carbon-13 abundances in forest soil organic matter, *Soil Sci. Soc. Am. J.*, *52*(6), 1633-1640.

Nickerson, N., and D. Risk (2009), Keeling plots are non-linear in non-steady state diffusive environments, *Geophysical Research Letters*, *36*(8), L08401.

Norby, R. J., et al. (2002), Net primary productivity of a CO_2-enriched deciduous forest and the implications for carbon storage, *Ecological Applications*, *12*(5), 1261-1266.

Parker, M. M., and D. H. Van Lear (1996), Soil heterogeneity and root distribution of mature loblolly pine stands in piedmont soils, *Soil Sci. Soc. Am. J.*, *60*(6), 1920-1925.

Pataki, D. E., J. R. Ehleringer, L. B. Flanagan, D. Yakir, D. R. Bowling, C. J. Still, N. Buchmann, J. O. Kaplan, and J. A. Berry (2003), The application and interpretation of Keeling plots in terrestrial carbon cycle research, *Global Biogeochemical Cycles*, *17*(1), 1022.

Pendall, E., et al. (2004), Below-ground process responses to elevated CO_2 and temperature: a discussion of observations, measurement methods, and models, *New Phytologist*, *162*(2),

311-322.

Phillips, C. L., N. Nickerson, D. Risk, Z. E. Kayler, C. Andersen, A. Mix, and B. J. Bond (2010), Soil moisture effects on the carbon isotope composition of soil respiration, *Rapid Commun. Mass Spectrom., 24*(9), 1271-1280.

Phillips, D. L., and J. W. Gregg (2001), Uncertainty in source partitioning using stable isotopes, *Oecologia, 127*(2), 171-179.

Phillips, S. C., R. K. Varner, S. Frolking, J. W. Munger, J. L. Bubier, S. C. Wofsy, and P. M. Crill (2010), Interannual, seasonal, and diel variation in soil respiration relative to ecosystem respiration at a wetland to upland slope at Harvard Forest, *Journal of Geophysical Research-Biogeosciences, 115*, G02019.

Prescott, C. (2010), Litter decomposition: what controls it and how can we alter it to sequester more carbon in forest soils?, *Biogeochemistry, 101*(1-3), 133-149.

Raich, J. W., and W. H. Schlesinger (1992), The global carbon dioxide flux in soil respiration and its relationship to vegetation and climate, *Tellus B, 44*(2), 81-99.

Richards, P. L., M. D. Norris, and B. B. Lin (2012), The hydrologic implications of old field succession: depression storage and leaf litter, *Ecohydrology*, n/a-n/a.

Risk, D., N. Nickerson, C. L. Phillips, L. Kellman, and M. Moroni (2012), Drought alters respired $\delta^{13}CO_2$ from autotrophic, but not heterotrophic soil respiration, *Soil Biology & Biochemistry, 50*, 26-32.

Schuur, E. A. G., J. G. Vogel, K. G. Crummer, H. Lee, J. O. Sickman, and T. E. Osterkamp (2009), The effect of permafrost thaw on old carbon release and net carbon exchange from tundra, *Nature, 459*(7246), 556-559.

Søe, A. B., A. Giesemann, T.-H. Anderson, H.-J. Weigel, and N. Buchmann (2004), Soil respiration under elevated CO_2 and its partitioning into recently assimilated and older carbon sources, *Plant Soil, 262*(1-2), 85-94.

Staddon, P. L. (2004), Carbon isotopes in functional soil ecology, *Trends in Ecology & Evolution*, *19*(3), 148-154.

Sullivan, P., S. T. Arens, R. Chimner, and J. Welker (2008), Temperature and microtopography interact to control carbon cycling in a high Arctic fen, *Ecosystems*, *11*(1), 61-76.

Taneva, L., and M. A. Gonzalez-Meler (2011), Distinct patterns in the diurnal and seasonal variability in four components of soil respiration in a temperate forest under free-air CO2 enrichment, *Biogeosciences*, *8*(10), 3077-3092.

Trumbore, S. (2000), Age of soil organic matter and soil respiration: Radiocarbon constraints on belowground carbon dynamics, *Ecological Applications*, *10*(2), 399-411.

Van der Ploeg, M. J., W. M. Appels, D. G. Cirkel, M. R. Oosterwoud, J.-P. M. Witte, and S. E. A. T. M. van der Zee (2012), Microtopography as a driving mechanism for ecohydrological processes in shallow groundwater systems, *Vadose Zone Journal*, *11*(3), DOI: 10.2136/vzj2011.0098.

Vargas, R., and M. F. Allen (2008), Environmental controls and the influence of vegetation type, fine roots and rhizomorphs on diel and seasonal variation in soil respiration, *New Phytologist*, *179*(2), 460-471.

Werth, M., and Y. Kuzyakov (2010), ^{13}C fractionation at the root–microorganisms–soil interface: A review and outlook for partitioning studies, *Soil Biology and Biochemistry*, *42*(9), 1372-1384.

Tables and Figures

Table 4-1 ^{13}C composition ($\delta^{13}C$) of soil-respired CO_2 ($\delta^{13}C_{Rs}$), $\delta^{13}C$ and content of three density fractions of soil organic carbon (SOC, $\delta^{13}C_{SOC}$ and C_{SOC}) in a coastal plain forested wetland in North Carolina, USA.

	mean±SD	Range
$\delta^{13}C_{R_s}$ **(‰)**		
Non-flooded	-27.8±1.5	-30.6 to -25.9
Flooded	-24.0±2.8	-28.2 to -22.8
δ^{13}Csoc (‰)		
Mean value*	-29.1±0.8	-30.1 to -27.7
F1 (density<1.0 g cm^{-3})	-29.6±0.3	
F2 (1.0<density<1.6 g cm^{-3})	-29.5±0.3	
F3 (density>1.6 g cm^{-3})	-28.2±0.5	
Csoc (%)		
Mean value*	19.4±18.0	0.2 to 57.8
F1**	34.4±13.3	
F2**	26.9±13.8	
F3**	0.8±0.5	

*: The mean value is the arithmetic mean of fraction, not the value for bulk soil.
**: F1: The fraction of the density (d) < 1.0 g cm^{-3}; F2: the fraction of 1.0<d<1.6 g cm^{-3}; F3: the fraction of d>1.6 g cm^{-3}.

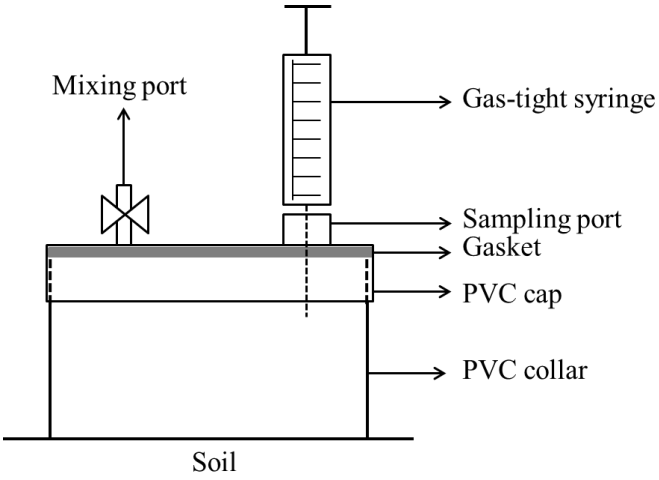

Figure 4-1 The sketch of the gas-sampling system used to collect soil-respired CO_2 on a monthly basis in a lower coastal plain forested wetland in North Carolina, USA, from 2010 to 2011. Gas was sampled at t = 0.5, 5.5, 11 and 16.5 minute after sealing the PVC collar. Every time before sampling with gas-tight syringe, the air was gently mixed for 0.5 minute with a syringe attached to the PVC cap (mixing port) in order to reduce the influence by the diffusion of air stored in the soil.

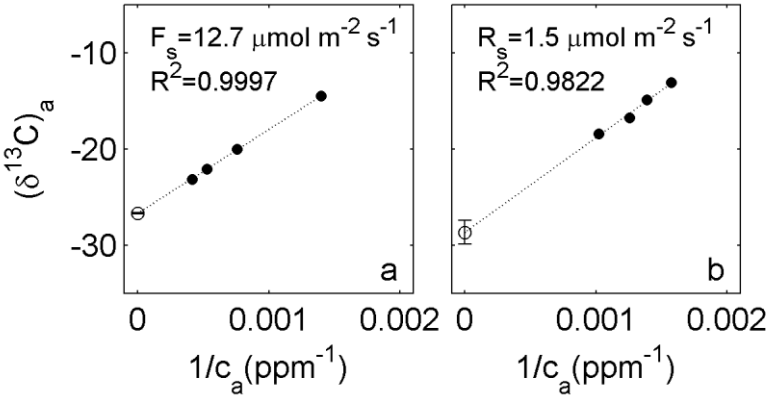

Figure 4-2 Examples of the Keeling plot method which assumes a linear relationship between the $\delta^{13}C$ of atmospheric CO_2 (y axis) and the reciprocal of atmospheric CO_2 concentration (x axis). Black solid dots represent the real data points. Open circles represent the regressed intercept, i.e. the $\delta^{13}C_{Rs}$, with the bar for standard error. (a) High data quality with high efflux and regression $R^2>0.99$. The intercept was -26.7±0.1‰. (b) Low data quality with low efflux and the regression $R^2<0.99$. The intercept was 28.7±1.2‰. Low quality data were excluded from data analysis.

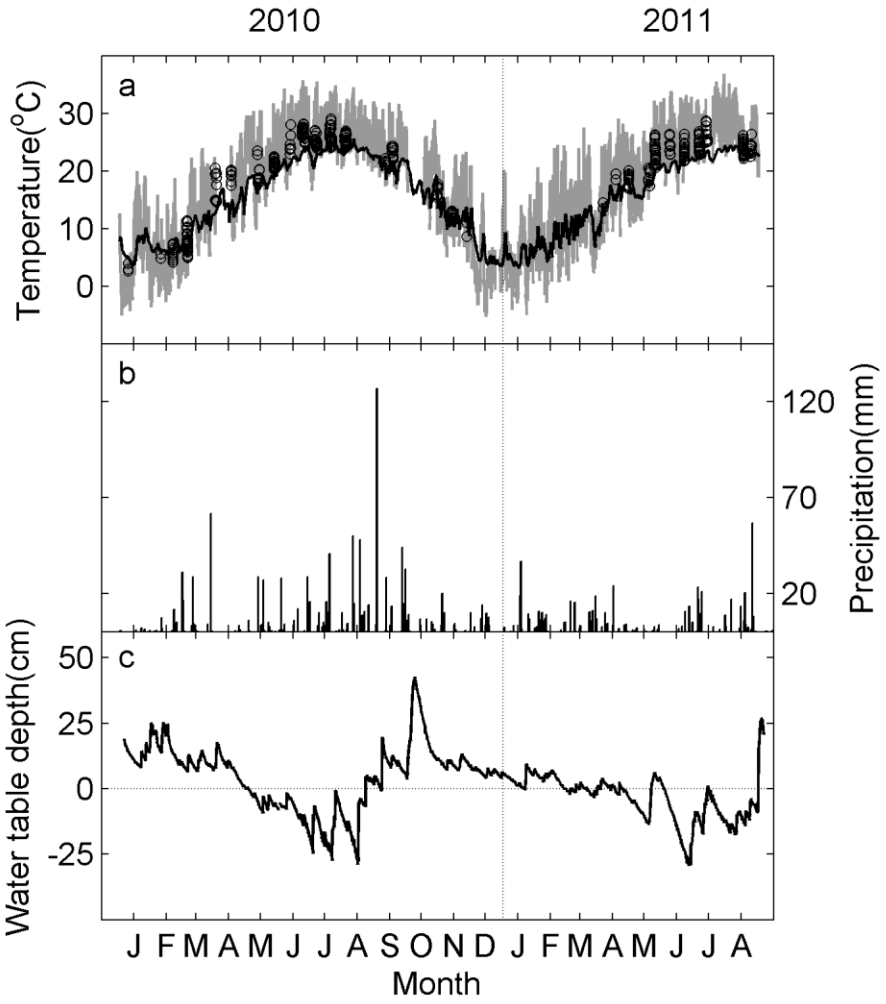

Figure 4-3 Time series of (a) air temperature (grey line) and soil temperature, (b) Precipitation, (c) Water table depth, in a lower coastal plain forested wetland from Jan. 2010 to Aug. 2011. In (a), open circles represent the soil temperature at the survey microsites. The spatial difference in soil temperature was small in this forested wetland.

(a)

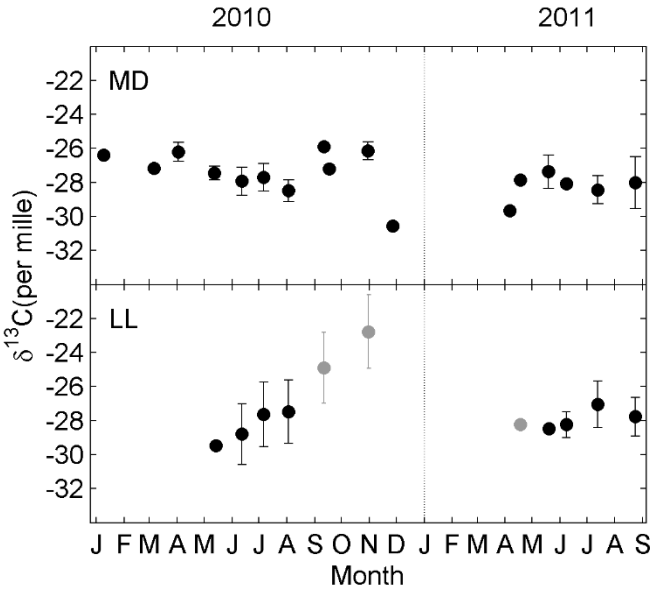

(b)

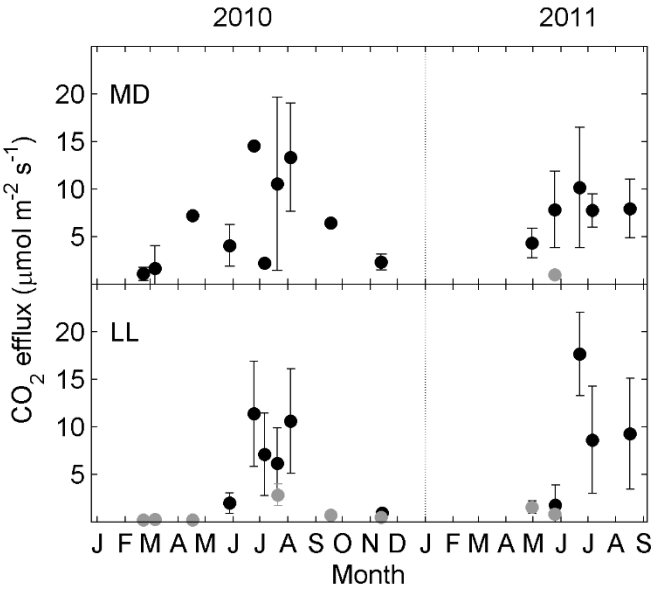

Figure 4-4 Seasonal variation of (a) ^{13}C composition of soil-respired CO_2 ($\delta^{13}C_{Rs}$), and (b) soil CO_2 efflux (R_s) from Jan. 2010 to Aug. 2010 at HIGH and LOW microsites in a lower coastal plain forested wetland. Black dots represent the mean values under non-flooded conditions and grey dots represent flooded conditions. The bar is the standard deviation demonstrating the spatial variation.

(a)

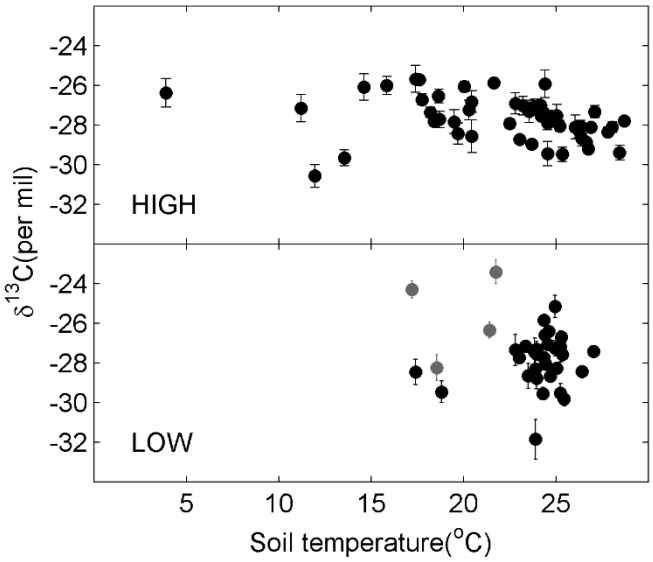

(b)

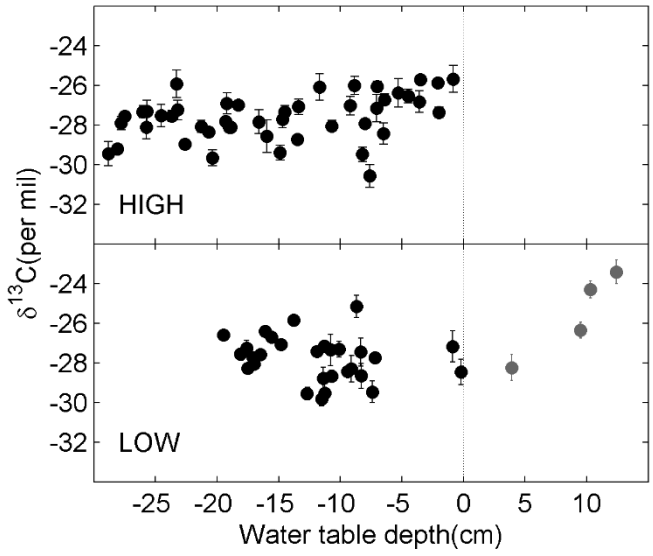

Figure 4-5 (a) Soil temperature and (b) water table depth effects on the ^{13}C composition of soil-respired CO_2 ($\delta^{13}C_{Rs}$) at HIGH and LOW microsites in a lower coastal plain forested wetland. Black dots represent the mean $\delta^{13}C_{Rs}$ under non-flooded conditions and grey dots represent flooded conditions. The bar is the standard error of $\delta^{13}C_{Rs}$.

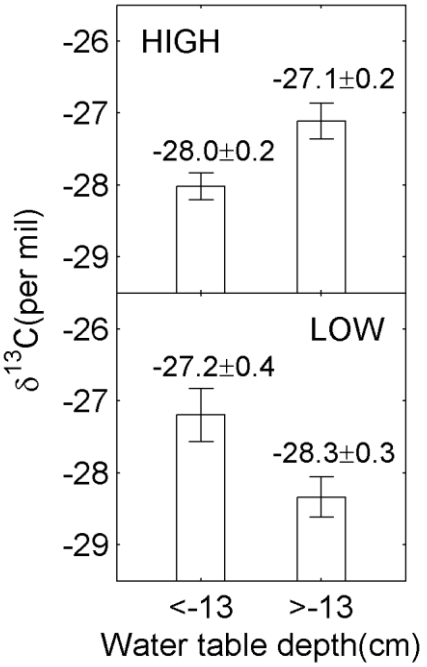

Figure 4-6 Comparison of the water table depth effects on the ^{13}C composition of soil-respired CO_2 ($\delta^{13}C_{Rs}$, mean±SD) between HIGH and LOW microsites under non-flooded conditions in a lower coastal plain forested wetland. The sample size was 31, 18, 16 and 19 for WTD<-13 cm at HIGH microsites, -13<WTD<0 cm at HIGH microsites, WTD<-13 cm at LOW microsites, and -13<WTD<0 cm at LOW microsites, respectively.

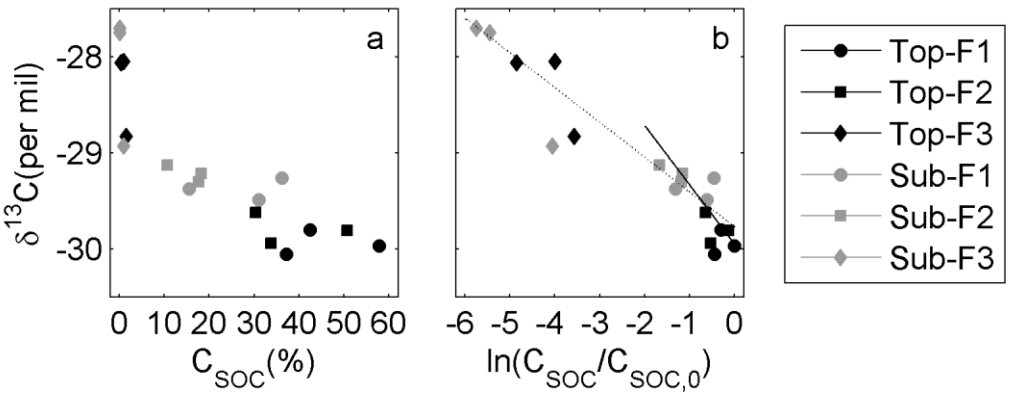

Figure 4-7 Relationship (a) between the soil organic carbon content (C_{SOC}) and the ^{13}C composition of soil organic carbon ($\delta^{13}C_{SOC}$), and (b) $\ln(C_{SOC}/C_{SOC,0})$ and $\delta^{13}C_{SOC}$ (see Equation 3) in a lower coastal plain forested wetland. The dotted line in (b) is the regression from all the three soil fractions (F1, F2 and F3) in top- and sub-layers, and the solid line is the regression from the lighter two fractions (F1 and F2). The regression equation was y = -0.4x-29.8 (R^2=0.83, p<0.0001) for the dotted line and y = -0.6x-30.0 (R^2=0.61, p<0.0001) for the solid line.

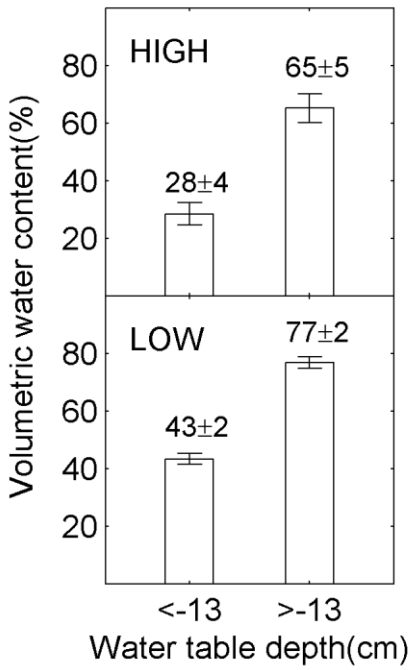

Figure 4-8 Comparison of soil volumetric water content (mean±SD) between HIGH and LOW microsites under non-flooded conditions in a lower coastal plain forested wetland.

CHAPTER 5. CONCLUSIONS AND RECOMMENDATIONS

Concerns over the role of wetlands in climate change and associated threats to coastal wetlands led to this research on carbon dynamics in a lower coastal plain forested wetland in Southeast USA. Comprehensive measurements were conducted for three growing seasons (2009-2011) to quantify carbon storage and parameterize carbon flow processes in this ecosystem. This dissertation focused on the process of respiration. Responses of respiratory components to environmental drivers were investigated, especially the responses to hydrologic regime. Models were developed to quantify three components, ecosystem respiration (R_e), soil respiration (R_s) and decomposition of coarse woody debris (R_{CWD}), using soil temperature (T_s) and water table depth (WTD) as predictor variables. Seasonal variation of ^{13}C composition ($\delta^{13}C$) of soil-respired CO_2 ($\delta^{13}C_{Rs}$) was also investigated to understand partition of R_s among components in soil.

1. Hydrologic and microtopographic effects on respiratory processes

Hydrologic regime (flooded or non-flooded conditions) determines the aerobic and anaerobic status of soil and fundamentally affects plant and microbial activities. As a result, the seasonal and inter-annual variations of CO_2 emission are closely related to the frequency and duration of flooding in wetlands. In the forested wetland of the current study, respiration during non-flooded periods contributed large proportion of total CO_2 emissions. In 2009, a wet year with 57% of non-flooded days in the growing season (Apr.-Oct.), R_s of non-flooded periods released 75% of the total 593 (95% CI: 503-702) g CO_2-C m^{-2} yr^{-1}; R_e of non-flooded periods released 62% of the total 1331 (1256-1406) g CO_2-C m^{-2} yr^{-1}. In 2010, a relatively dry year with 72% of non-flooded days in the growing season, the contribution of non-

flooded periods was 93% and 78% for R_s and R_e, respectively, with the respective total CO_2 emissions of 1015 (960-1103) and 1560 (1471-1650) g CO_2-C m^{-2} yr^{-1}, respectively. Contribution of non-flooded periods to R_e was lower than R_s because plants were tolerant to flooding and continued respiring during flooding period, whereas R_s decreased instantaneously and significantly (Chapter 2 and 3).

Respiratory components under non-flooded conditions responded to temperature in this forested wetland similarly to upland ecosystems, in an exponential pattern with comparable temperature sensitivities. Hydrology had additional effects on R_s and R_e, with the relationship resembling the saturating pattern of Michaelis-Menten (M-M) reaction, i.e. the rate increased with water table drawdown and was nearly constant at deeper WTD. To simulate R_s and R_e, I developed nested models using traditional Q_{10} model as the base and modifying the basal respiration rate with the M-M equation. These models accounting for water table depth effects provided better fits with observations compared to traditional models (Chapter 2 and 3), proving more appropriate for application to wetlands with fluctuating WTD.

Remarkable microtopographic effects existed in this forested wetland, and were reflected by both total soil CO_2 efflux and the $\delta^{13}C_{Rs}$. Physically, low-lying microsites were flooded more frequently and for longer time periods than mound microsites. The annual CO_2 emission was correspondingly lower at low-lying microsites than at mounds. In 2010, soil released total 1325 (95% CI: 1291-1365) g CO_2-C m^{-2} yr^{-1} at a HIGH microsite, and released 621 (555-710) and 430 (319-694) g CO_2-C m^{-2} yr^{-1} at a MID and a LOW microsite, respectively. Biologically, the difference in microtopography appears to result in the

difference in plant distribution and associated contributions from root respiration, litter and soil organic carbon decomposition. We did not test this hypothesis directly by quantifying the carbon storage in each component and the respective carbon fluxes, so this remains a challenge for future study of partitioning soil respiration. However, the difference in $\delta^{13}C_{Rs}$ between these two types of microsites supports the hypothesis indirectly. The relative contribution of root respiration to R_s was higher at mound microsites than at low-lying microsites, whereas the contribution from heterotrophic respiration (i.e. litter and soil organic carbon decomposition) to R_s was relatively higher at low-lying microsites (Chapter 4).

2. Carbon budget of the study wetland

The carbon budget for this forested wetland in 2010 was partially estimated (Figure 5-1), of which carbon storage terms need refinement in future studies. In general, soil stores more carbon than vegetation at this site, similar to other forested wetlands. While the absolute amount of carbon stocks seems lower than literature values, carbon fluxes through respiratory components were comparatively high relative to values reported for wetlands and similar to the CO_2 emissions from many upland forests (Chapter 2).

The annual average R_s:R_e ratio was to some degree similar between this forested wetland and upland forests, but the seasonal variation of R_s:R_e ratio and its response to hydrologic regime were unique to this intermittently flooded wetland. The R_s:R_e ratio linearly increased along with the drawdown of water table, implying the overwhelming contribution of R_s to R_e under drier conditions. The ratio rapidly decreased when the hydrologic regime transited from non-flooded to flooded condition, and remained nearly constant at low values during

flooding, demonstrating the contribution of the dominant plant respiration under near-saturated and saturated conditions (Chapter 3).

3. Implications and suggestions for future work

3.1 Spatial variation in microtopography

Spatial variation of R_s is related with a number of biotic and abiotic factors and its quantification is important to upscaling from single-location measurements to the ecosystem scale. In wetlands, microtopography plays a fundamental role in spatial variation of hydrology and associated CO_2 emissions. Therefore, **stratification of experiment locations in terms of microtopography** is necessary, e.g. the HIGH and LOW microsites in this study. Instead of randomly selecting microsites to investigate spatial variation, microtopography stratification can be a simplified approach to quantify the spatial variation of R_s and help reduce upscaling uncertainties.

Results from the $\delta^{13}C_{Rs}$ study suggest a common pattern within a given type of microsites, that is, similar relative contribution from respiratory components to total respiration (Chapter 4). The consistency between automated and survey measurements illustrates the utility of microtopographic stratification to account for spatial variation in R_s (Chapter 3). Although stratification alone is not sufficient to quantify the difference in absolute magnitude of R_s, associated uncertainty is likely decreased by characterizing the relationship between microtopography and R_s.

Microtopography is of importance not only for upscaling R_s, but also for partitioning unmeasurable components. Difference in R_s between the two types of microsites may result

from the difference in quantity and biochemical quality of carbon sources, with the assumption that the dynamics of each carbon source are spatially homogeneous within microsite type. By quantifying the quantity of carbon sources (e.g. roots, microbial biomass, soil organic carbon) and the difference in R_s and $\delta^{13}C_{Rs}$ between microsites, it is possible to partition the components of R_s noninvasively (Chapter 4). Furthermore, this approach may also be used to derive specific respiration rates for each carbon source under natural conditions, which are key parameters in ecosystem carbon cycle models but usually parameterized from lab incubation or by oversimplified assumptions.

3.2 Water table depth and substrate availability

Like most other wetland studies on R_s, my study also indicated that using water table depth (WTD) to substitute for soil water content improves simulation of R_s based on the model structure developed for upland ecosystems. Water table depth affects not only soil water content, but also the availability of substrate including oxygen, nutrients, extra-cellular enzymes and soil microbial communities, which are all affected by WTD, leading to its use as a good predictor of R_s.

To understand the mechanisms of WTD effects, further studies on the interaction between WTD, soil water content and substrate availability are necessary. Due to the continuous change of WTD in natural conditions in such systems, research is needed to analyze **the soil profile of these variables**. This necessity also applies to the above suggestions on microtopographic stratification, i.e. profiles of these variables need to be analyzed at each type of microsites.

Figures

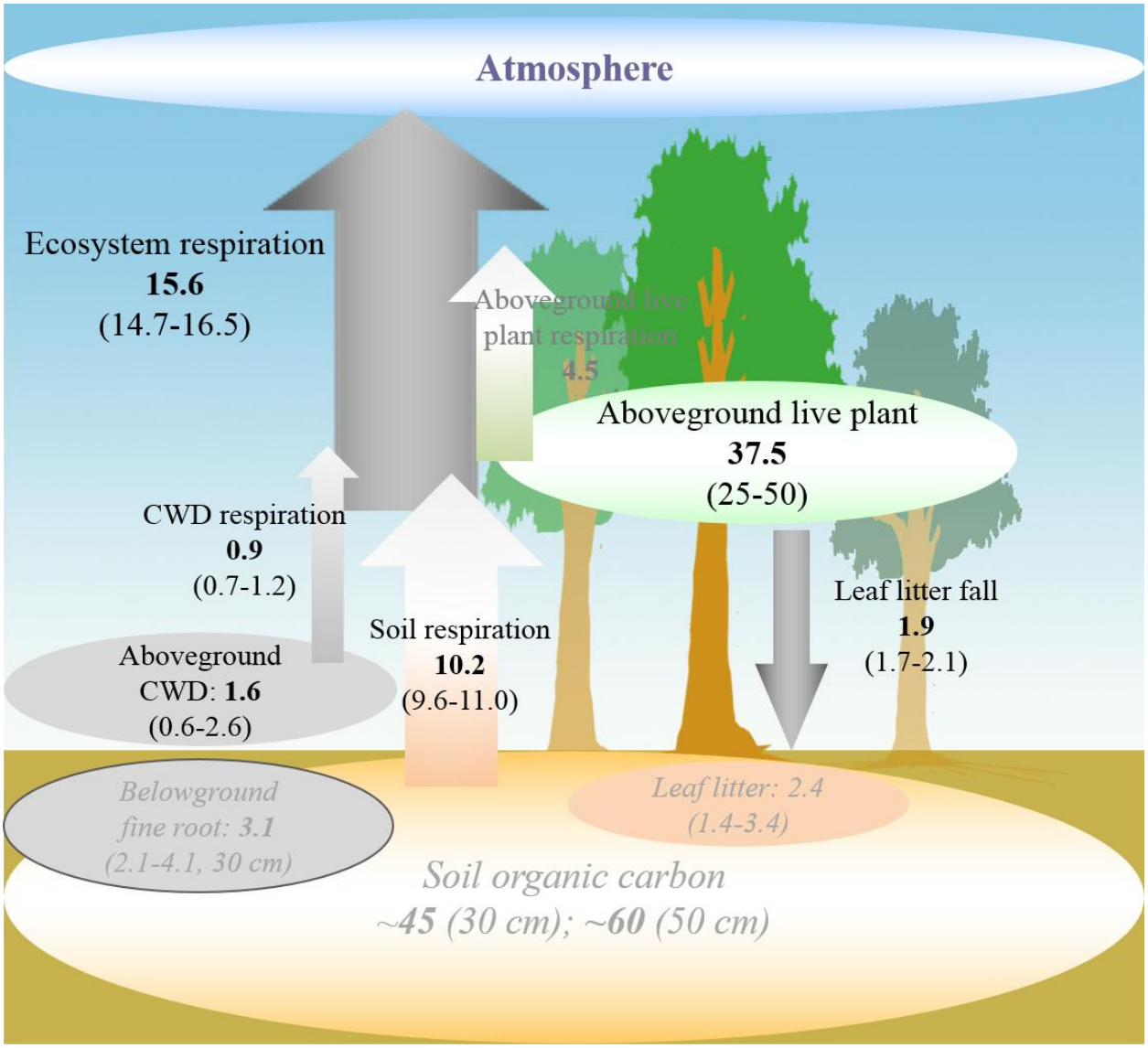

Figure 5-1 Partial of carbon budget in the lower coastal plain forested wetland studied at Alligator River National Wildlife Refuge in eastern North Carolina, USA. The pools and fluxes in black text were estimated by models or measurements (see Chapter 2 and 3) across a full year. The aboveground live plant respiration was calculated as the difference between ecosystem respiration and the sum of soil respiration and CWD respiration. The belowground pools in grey and italics were rough estimates based on only few samples collected at random time.

APPENDICES

Appendix A. Microtopography calibration

Microtopography was measured for three purposes:

(1) Quantify microtopography distribution across the study area for upscaling.

(2) Stratify survey microsites based on microtopography.

(3) Quantify the WTD at each microsite during each survey measurement.

To upscale studies from single location to ecosystem scale, especially the water table depth effect on respiration processes, elevation data for microtopography distribution or survey microsites needed to be calibrated to a reference location. In this study, we used the ground water probe location at ground meteorological station (MET-probe) as the reference location. The ground water probe location at each survey plot (PLOT-probes) was also used in the calibration. Although the soil height varied with the change in WTD, we assumed the bias of soil height change is insignificant compared to the change in WTD.

Relative elevation between MET-probe and PLOT-probe locations

The relative elevation difference between MET-probe and PLOT-probe locations was derived based on the WTD readings at each probe when the study site was severely flooded (at very high WTD). We hypothesized that during a short period of flooding immediately after a heavy rain event (e.g. after Hurricane Irene in 2011) the water surface across the study area was uniform. Therefore, the difference in WTD readings between probes would be the relative elevation between probe locations.

The WTD data from all five probes (i.e. MET-probe and 4 PLOT-probes) were sorted out during the period of 9/2/2011 00:00-9/4/2011 23:30 (Figure A-1b). The consistent difference

between the WTD readings from all probes supported the above hypothesis. The relative elevations of PLOT-probes to MET-probe were then calculated from the WTD differences (Table A-1).

Microtopography calibration

The schematic strategy of microtopography calibration is shown in Figure A-2. The original elevation measurements (h_{i,w_0}) were referred to the water surface at each survey plot at the measurement period, then converted relative to the LOCAL-probe location surface ($h_{i,P}$, Equation A1), and eventually converted relative to the MET-probe location surface ($h_{i,M}$, Equation A2). Positive values of these terms mean the elevation of a specific microsite is higher than the reference surface. The subscripts 'P, w_0, M' represent the reference surface, i.e. PLOT-probe, water surface at microtopography measurement date, and MET-probe, respectively. The subscript 'i' represents a specific microsite 'i'.

$$h_{i,P} = h_{i,w_0} + w_P \quad \text{(A1)}$$

$$h_{i,M} = h_{i,P} + \Delta h_M \quad \text{(A2)}$$

in which the meaning and values of Δh_M and w_P are described in Table A-1 and A-2. Because most of the PLOT-probes were installed after the survey dates, w_P was estimated from Figure A-1a based on the WTD records at MET-probe at the measurement periods (i.e. w_M in Table A-2).

Table A-1 Relative elevation of PLOT-probe locations to MET-probe location. Negative numbers represent the PLOT-probe location is lower than the MET-probe location, and positive represents higher.

Probe	Symbol	MET (PLOT 7)	PLOT 4	PLOT 5	Plot 9	Plot 10
Elevation (cm)	Δh_M	0	-2.6±0.2	7.6±0.2	-5.7±0.2	-9.5±0.1

Table A-2 Water table depth at probe location during microtopography survey measurements

	Symbol	MET (PLOT 7)	PLOT 4	PLOT 5	PLOT 9	PLOT 10
WTD at MET-probe	w_M	1.6	4	3.4	2.1	9.5
WTD at PLOT-probe	w_P	1.6	7.8	1.3	4.5	16.2
Survey year		2011	2011	2011	2011	2010
Survey date		4/17	2/16	2/16	4/3	9/19
Probe installation time		3/2009	5/2011	11/2010	5/2011	11/2010

Table A-3 Microtopography of all survey microsites relative to water table probes

Micro-site ID	Δh_M	Microtopo. survey date	w_M	w_P	2010			2011		
					h_{i,w_0}	$h_{i,P}$	$h_{i,M}$	h_{i,w_0}	$h_{i,P}$	$h_{i,M}$
Plot 4	-2.6	2/16/2011	3.8	7.4						
1					0.5	7.9	5.3	6.0	13.4	10.8
2					3.0	10.4	7.8	12.5	19.9	17.3
3					1.0	8.4	5.8	1.0	8.4	5.8
4					-0.5	6.9	4.3	6.5	13.9	11.3
5					0.5	7.9	5.3	-4.0	3.4	0.8
6					0.5	7.9	5.3	13.0	20.4	17.8
Plot 5	7.6	2/17/2011	3.3	1.3						
1					6.8	8.1	15.7	-0.5	0.8	8.4
2					n.a.	n.a.	n.a.	10.0	11.3	18.9
3					n.a.	n.a.	n.a.	1.0	2.3	9.9
4					-4.5	-3.2	4.4	1.5	2.8	10.4
5					-4.0	-2.7	4.9	12.5	13.8	21.4
6					n.a.	n.a.	n.a.	4.5	5.8	13.4
C1					16.0	17.3	24.9			
Plot 7	0	2/15/2011	4.4	4.4						
1					14.0	18.4	18.4	8.5	12.9	12.9
2					-4.0	0.4	0.4	-3.5	0.9	0.9
3					-3.0	1.4	1.4	-7.5	-3.1	-3.1
4					-3.5	0.9	0.9	11.0	15.4	15.4
5					0.0	4.4	4.4	17.0	21.4	21.4
6					-8.5	-4.1	-4.1	-6.5	-2.1	-2.1
C3					6.0	10.4	10.4			
C4					12.5	16.9	16.9			
Plot 9	-5.7	2/27/2011	-1.0	3.0						
1					-0.5	2.5	-3.2	-0.5	2.5	-3.2
2					1.0	4.0	-1.7	0.5	3.5	-2.2
3					-1.5	1.5	-4.2	-3.5	-0.5	-6.2
4					2.0	5.0	-0.7	-1.0	2.0	-3.7
5					5.0	8.0	2.3	23.5	26.5	20.8
6					n.a.	n.a.	n.a.	3.0	6.0	0.3
C5					3.0	6.0	0.3			

Table A-3 Continued

Micro -site ID	Δh_M	Microtopo. survey date	w_M	w_P	2010			2011		
					h_{i,w_0}	$h_{i,P}$	$h_{i,M}$	h_{i,w_0}	$h_{i,P}$	$h_{i,M}$
Plot 10	-9.5	2/15/2011	4.3	12.3						
1					-10.5	1.8	-7.7	-8.5	3.8	-5.7
2					-4.5	7.8	-1.7	7.5	19.8	10.3
3					-13	-0.7	-10.2	-10.0	2.3	-7.2
4					-4.5	7.8	-1.7	-10.0	2.3	-7.2
5					-2.0	10.3	0.8	9.5	21.8	12.3
6					-3.5	8.8	-0.7	-4.5	7.8	-1.7
C4					8.0	20.3	10.8			
C5					13.0	25.3	15.8			

(a)

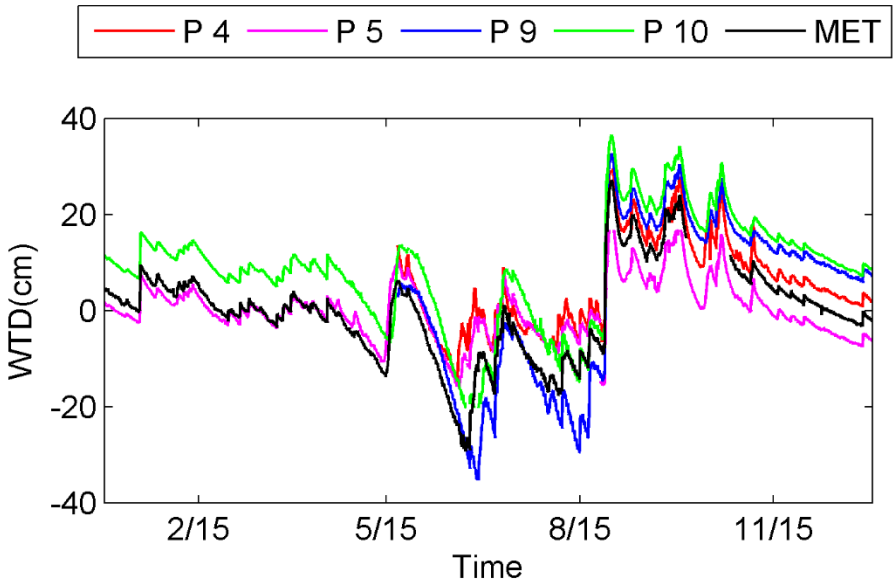

(b)

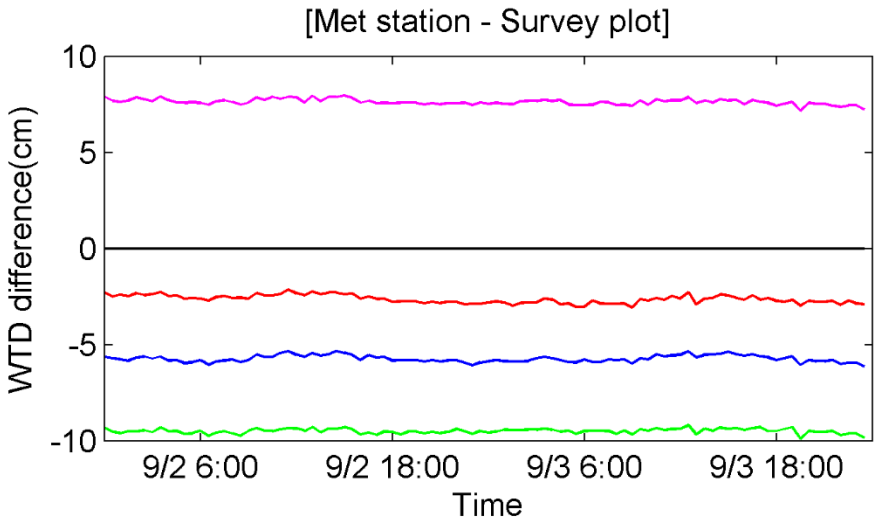

Figure A-1 (a) Time series of water table depth (WTD) from all water table probes in 2011; (b) Difference in WTD between the 5 probes during the period 9/2-9/3/2011 after hurricane Irene (using the same legend as (a)). All WTD values were calibrated relative to the WTD at MET-probe.

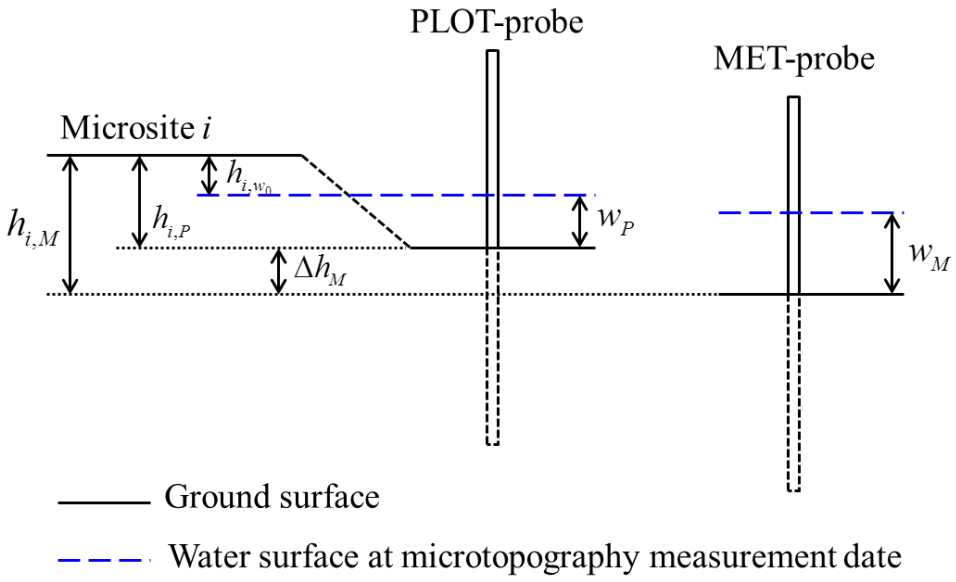

Figure A-2 Schematic chart showing the microtopography calibration for survey microsites.

Appendix B. Water table depth adjusting in survey data

Water table depth adjusting is more complicated due to its temporal variation than microtopography calibration. We used microtopography of each microsite and WTD readings from the PLOT-probes to adjust the WTD at each microsite for each survey measurements.

The MET-probe was installed in March 2009, while PLOT-probes were installed in November 2010 and May 2011 (Table A-2). The microtopography measurement of survey microsites was done in February 2011, and the respiration survey measurement was conducted from early 2010 to August 2011. Due to the asynchronous operation, the WTD in 2010 or data gaps in 2011 at the 4 remote survey plots were estimated through the following steps from the WTD reading at MET-probe which had the full WTD records from early 2009 to the end of 2011.

For the measurement dates when the WTD records of PLOT-probe ($w_{t,P}$) existed, the WTD of a specific microsite at a specific date was calculated by Equation B1. The meaning and calculation of $h_{i,P}$ was described in Appendix A (Equation A1).

$$w_{t,i} = w_{t,P} - h_{i,P} \quad \text{(B1)}$$

For the measurement dates when the WTD records of PLOT-probe did not exist, firstly I had to estimate the WTD of PLOT-probe at the specific measurement date from the WTD of MET-probe ($w_{t,M}$), and then calculated the WTD of a specific microsite relative to the PLOT-probe with equation B1.

Table B-1 Water table depth at survey plots during R_s survey measurements

Plot 4			Plot 5			Plot 7			Plot 9			Plot 10		
Date	$w_{t,M}$	$w_{t,P}$	Date	$w_{t,M}$	$w_{t,P}$	Date	$w_{t,M}$	$w_{t,P}$	Date	$w_{t,M}$	$w_{t,P}$	Date	$w_{t,M}$	$w_{t,P}$
2010														
----	----	----	2/21	9.9	3.7	2/21	9.6	9.6	----	----	----	----	----	----
3/7	9.4	10.9	3/7	9.3	2.8	3/6	9.9	9.9	----	----	----	3/6	9.8	19.7
----	----	----	----	----	----	4/17	5.6	5.6	4/17	5.8	14.2	----	----	----
5/29	-5.9	-1.4	5/28	n.a.	n.a.	5/28	n.a.	n.a.	5/28	n.a.	n.a.	5/29	-6.2	-3.5
6/26	-18.5	-10.0	6/24	-15.9	-9.6	6/25	-18.1	-18.1	6/25	-17.1	-13.5	6/25	-17.8	-8.0
----	----	----	----	----	----	7/6	-16.1	-16.1	7/8	-19.2	-15.5	7/8	-19.6	-10.0
7/22	-2.7	0.3	7/20	-11.4	-4.7	7/21	-1.5	-1.5	----	----	----	7/21	-1.0	8.6
8/5	-17.9	-9.6	8/4	-17.4	-10.6	8/5	-18.1	-18.1	8/4	-17.5	-13.5	8/5	-18.6	-8.6
----	----	----	----	----	----	9/18	10.4	10.4	9/18	10.6	18.0	----	----	----
11/14	7.3	10.0	11/14	7.3	2.0	11/14	7.2	7.2	----	----	----	11/13	7.6	18.0
2011														
4/30	-4.5	-0.9	----	----	----	4/30	-4.7	-4.7	4/30	-4.6	0.0	----	----	----
5/26	2.9	7.9	5/25	4.2	8.7	5/25	4.1	4.1	5/26	2.9	4.9	5/25	3.9	12.4
----	----	----	6/22	-26.8	-10.2	6/22	-27.7	-27.7	6/22	-27.2	-28.8	6/22	-27.5	-19.0
----	----	----	7/6	-9.3	-1.8	7/6	-9.2	-9.2	7/7	-5.4	-11.4	7/7	-5.5	-1.0
8/18	-10.9	-2.6	8/17	-10.4	-4.0	8/17	-10.5	-10.5	8/17	-10.5	-24.3	8/18	-11.0	-11.0

Table B-2 Water table depth at survey plots during ^{13}C gas sampling

	Plot 4			Plot 5			Plot 7			Plot 9			Plot 10	
Date	$w_{t,M}$	$w_{t,P}$	Date	$w_{t,M}$	$w_{t,P}$	Date	$w_{t,M}$	$w_{t,P}$	Date	$w_{t,M}$	$w_{t,P}$	Date	$w_{t,M}$	$w_{t,P}$
2010														
----	----	----	----	----	----	1/9	11.6	11.6	----	----	----	----	----	----
----	----	----	----	----	----	2/9	20.6	20.6	----	----	----	----	----	----
3/7	9.4	10.9	3/7	9.3	2.8	3/6	9.8	9.8	3/7	9.3	16.3	3/6	9.8	19.4
4/2	13.5	15.8	4/3	12.3	5.6	4/2	13.3	13.3	4/3	12.2	18.1	4/3	12.1	21.8
5/14	-4.4	-0.5	5/13	-3.2	2.6	5/12	-8.8	-8.8	5/14	-4.6	-11.6	5/13	-3.4	6.0
6/13	-8.2	-4.5	6/12	-7.3	-5.3	6/13	-8.6	-8.6	6/12	-7.6	-7.6	6/12	-7.8	1.6
7/8	-18.9	-10.2	7/7	-16.7	-10.2	7/6	-15.6	-15.6	7/7	-17.1	-13.1	7/7	-17.5	-7.3
8/5	-18.1	-9.6	8/4	-17.1	-10.8	8/3	-15.4	-15.4	8/4	-16.4	-12.3	8/5	-18.8	-8.8
9/11	8.6	11.2	9/17	9.0	2.8	9/11	8.3	8.3	9/11	8.2	15.5	9/17	8.9	16.1
10/31	9.2	10.9	10/30	9.7	3.5	10/30	9.6	9.6	10/31	9.1	16.3	10/31	8.9	18.9
----	----	----	11/28	7.4	2.0	----	----	----	11/28	7.1	14.8	11/27	7.6	17.7
2011														
----	----	----	----	----	----	4/6	1.0	1.0	4/18	0.9	9.9	----	----	----
5/20	5.9	13.4	5/19	5.2	9.3	5/19	5.4	5.4	5/20	6.0	3.3	----	----	----
6/9	-12.7	-7.4	6/8	-11.9	-7.5	----	----	----	6/8	-12.3	-7.2	6/9	-13.0	-2.0
7/13	-4.0	-0.3	7/14	-2.9	3.1	7/14	-3.2	-3.2	7/13	-4.6	-5.9	7/13	-4.1	6.9
8/25	-8.2	-2.9	8/24	-7.4	-2.2	8/24	-7.4	-7.4	8/25	-8.1	-13.5	8/25	-8.3	-4.9

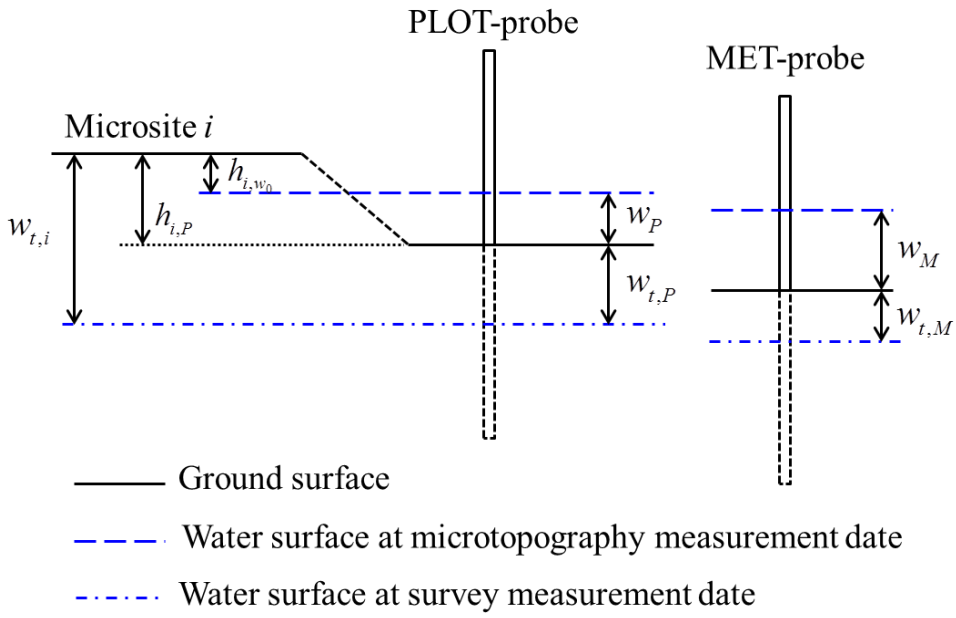

Figure B-1 Schematic chart showing the water table depth adjustment at each measurement.

Appendix C. Records in the field

Data tell stories behind woods, pictures tell stories behind data.

Top-left: A chamber under non-flooded conditions. **Top-middle:** A chamber under normal flooded conditions. **Bottom:** Chambers were submerged after Hurricane Ida in 2009. **Right:** Legs are attached onto chambers to help them stand firmly in water.

Left: Tower built in early 2009, retired at the end of 2012. **Right:** Tower built at the end of 2012, on duty from early 2013.

Top: Boardwalk built in summer, 2008. **Bottom:** Boardwalk built at late 2012 and early 2013.

Change of water table level.
Top: During a normal rain, Sep. 10, 2009. **Bottom:** After Hurricane Ida, Nov. 15, 2009.

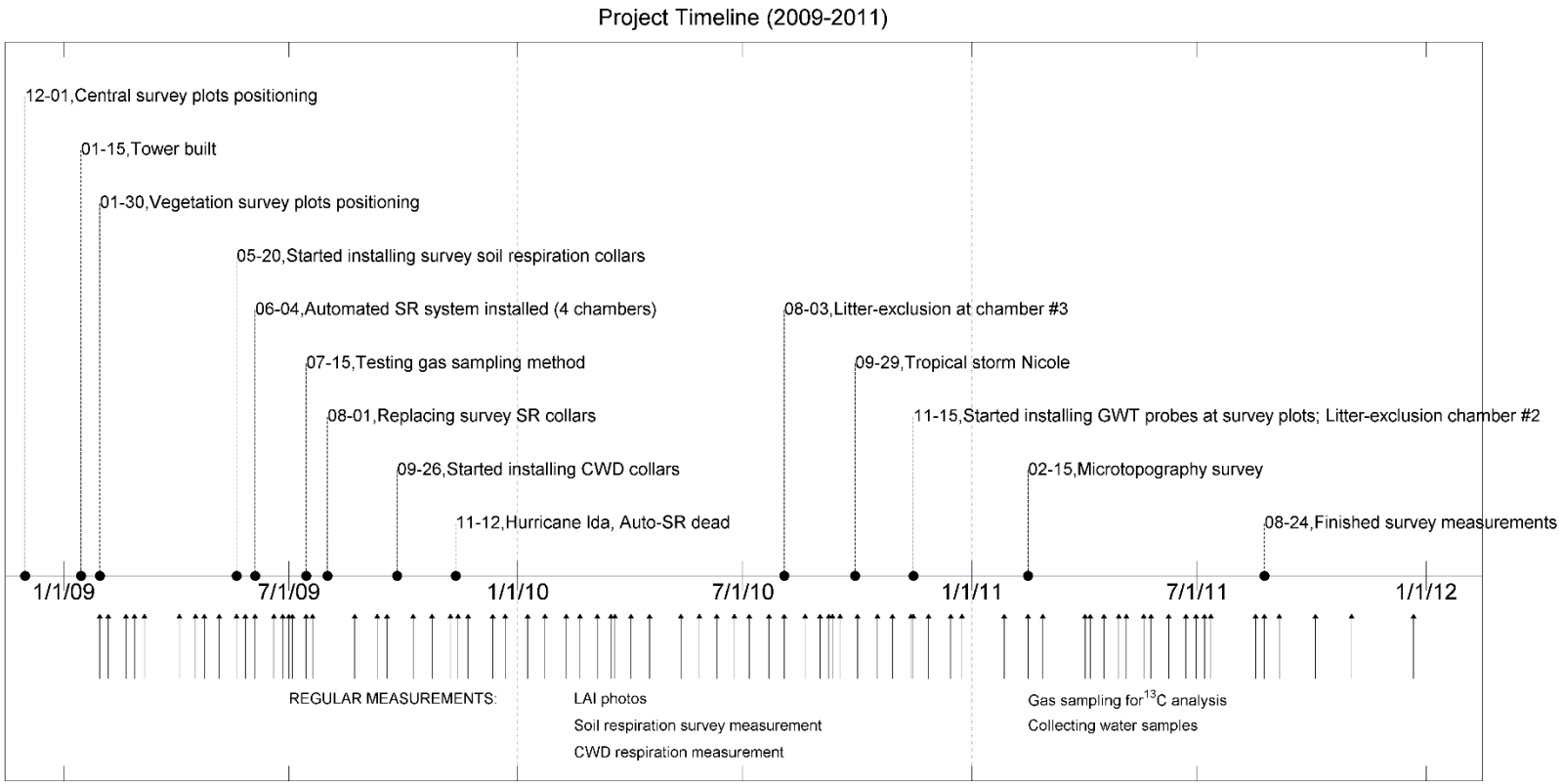

Timeline of the project at the Alligator River National Wildlife Refuge (ARNWR) from 2009 to 2011.
Arrows: Regular field trips from 2009 to 2011. In total, 78 trips, 390 miles per trip, driving a pick-up truck most of the time.
The total CO_2 emissions during the field trips were estimated approximately 21 tons of CO_2, with an average of 7 tons of CO_2 per year (calculated by the carbon footprint calculator of the Nature Conservancy). For comparison, soil respiration in ARNWR in 2010 released 2.2 tons of CO_2 (roughly estimated by multiplying the site average CO_2 flux with the refuge area).